

# **The Institute of Paper Science and Technology**

**Atlanta, Georgia**

**Doctoral Dissertation  
Reprint**

**A MATHEMATICAL MODEL OF HIGH INTENSITY PAPER DRYING**

**A thesis submitted by**

**Joseph R. Pounder**

**B.S. 1979, Philadelphia College of Textiles and Science**

**M.S. 1982, Lawrence University**

**in partial fulfillment of the requirements  
of The Institute of Paper Chemistry  
for the degree of Doctor of Philosophy  
from Lawrence University,  
Appleton, Wisconsin**

**Publication Rights Reserved by  
The Institute of Paper Chemistry**

**January, 1986**

## TABLE OF CONTENTS

	Page
ABSTRACT	1
INTRODUCTION	3
OBJECTIVE	6
EXPERIMENTAL BACKGROUND	7
Introduction	7
Experimental Results	8
Bulk Vapor Flow	11
Liquid Displacement	12
Mechanical Dewatering	13
Zone Development	14
Summary	14
MOVING BOUNDARY MODELS	15
Introduction	15
Temperature-Based Models	15
Enthalpy-Based Models	16
Position-Based Models	17
Drying Models	17
Summary	19
THE MATHEMATICAL MODEL	20
Introduction	20
Elementary Models	21
Description of the Advanced Model	26
Assumptions	26
Advanced Model Equations	31

Zone Continuity and Momentum Equations	32
Zone Thermal Energy Equation	36
Convective-Diffusion Equations	38
Interface Equations	44
Heatup and Transition Regimes	45
Linear Regime	50
Supplementary Relationships	55
Applied Mechanical Pressure	55
Physical Properties	56
Latent Heat Correction Factor	56
Thermal Conductivity	57
Contact Coefficient	57
Compressibility	58
Permeability	61
Model Validation	63
Summary	64
PARAMETRIC STUDY	65
Input Parameters	65
Output Variables	65
Design of Parametric Study	66
Results and Discussion	66
Base Case	67
Comparisons of Drying Behavior	76
Sensitivity Analysis	83
Summary	85
EXPERIMENTAL COMPARISONS	86
Purpose	86

Experimental Conditions	86
Ramp-And-Hold Pressure Pulse	87
Short Duration (Impulse) Pressure Pulse	103
Summary	109
SUMMARY	110
RECOMMENDATIONS	111
ACKNOWLEDGMENTS	112
NOMENCLATURE	113
LITERATURE CITED	118
APPENDIX 1: HIDRYER1 Program and Documentation	125

## ABSTRACT

High intensity paper drying is defined as any drying process in which the web is at or above the thermodynamic saturation temperature corresponding to the ambient pressure. Rapid generation of vapor under these circumstances causes the drying process to be driven by a gradient of total pressure and not by a gradient of partial vapor pressure. Therefore, the generated vapor leaves the web by a bulk (convective) flow mechanism rather than a slower diffusion mechanism. The vapor pressure build-up in the web also offers the opportunity for removal of moisture in liquid form, since the fast flowing vapor can displace and/or entrain liquid as it moves through the web. This can result in significantly lower energy usage relative to conventional drying, since only a fraction of the moisture has to be evaporated.

The thesis objective is a mathematical model simple enough to be easily modified or expanded but comprehensive enough to be applicable to a wide variety of process conditions and sheet variables.

Early experiments suggested that the high intensity drying process could be described effectively by a discrete "zone" model. The process is idealized by picturing the sheet as composed of different zones which contain various amounts of fiber, liquid water, and water vapor. The model is based on sets of equations which account for the heat and moisture transfer within and among the zones during three regimes: heatup, transition, and quasi-static. Once the hot surface temperature, boiling point temperature, basis weight, Canadian Standard Freeness, initial moisture ratio, and mechanical pressure pulse are specified, the equations may be solved to predict the moisture content as a function of time.

Comparisons between experimental data and the model's predictions demonstrate that the model qualitatively and quantitatively describes high intensity drying

behavior and provide indirect evidence that the mechanisms on which the model is based actually are in effect under high intensity conditions. An exploratory parametric study shows that the predicted drying behavior is most sensitive to changes in hot surface temperature and sheet basis weight. Peak pressure and freeness have a more moderate effect, and initial moisture ratio has almost no effect. Comparisons to laboratory data show that the model tends to overpredict the extent of liquid moisture removal and underpredict the heat flux. Changing the values of constants in the model modifies the predictions and suggests that a mathematical optimization of all constants, constrained by experimental data, would improve the predictive capability of the model.

## INTRODUCTION

Low heat transfer rates, low drying rates, and low mechanical pressures characterize conventional can drying of paper. Moisture removal is dominated by a vapor diffusion mechanism, and average sheet temperatures are well below the boiling point.

In contrast, high intensity drying occurs at high surface temperatures and high mechanical pressures. Heat transfer rates and drying rates are orders of magnitude above those in the conventional process (see Fig. 1 and 2). Moisture removal is dominated by bulk (convective) vapor flow and liquid displacement or entrainment, and sheet temperatures frequently exceed the boiling point.

Mathematical modeling provides a convenient and comprehensive means for exploring the effects of temperature, pressure, freeness, and other factors on high intensity drying behavior. Mathematical modeling complements experimental study by identifying incomplete areas in knowledge of the physical system and suggesting areas for further research. Finally, mathematical modeling offers the opportunity for blending and balancing theoretical and empirical relationships to provide a fast, low-cost investigative tool.

Early experiments indicated that high intensity drying could be described effectively by a discrete "zone" model, since the drying behavior is consistent with other examples of phase change problems involving the development of zones. Initially, two zones of different moisture content were assumed to be present. As more information became available, additional zones were added to the model. Fundamental mass and energy balances for the zones are linked by the boundary conditions and the conditions at the interfaces between the zones. Solving the system of equations allows a prediction of the temperature distribution within



the sheet, the positions and rates of advance of the interfaces, and the moisture content of the sheet as functions of time.

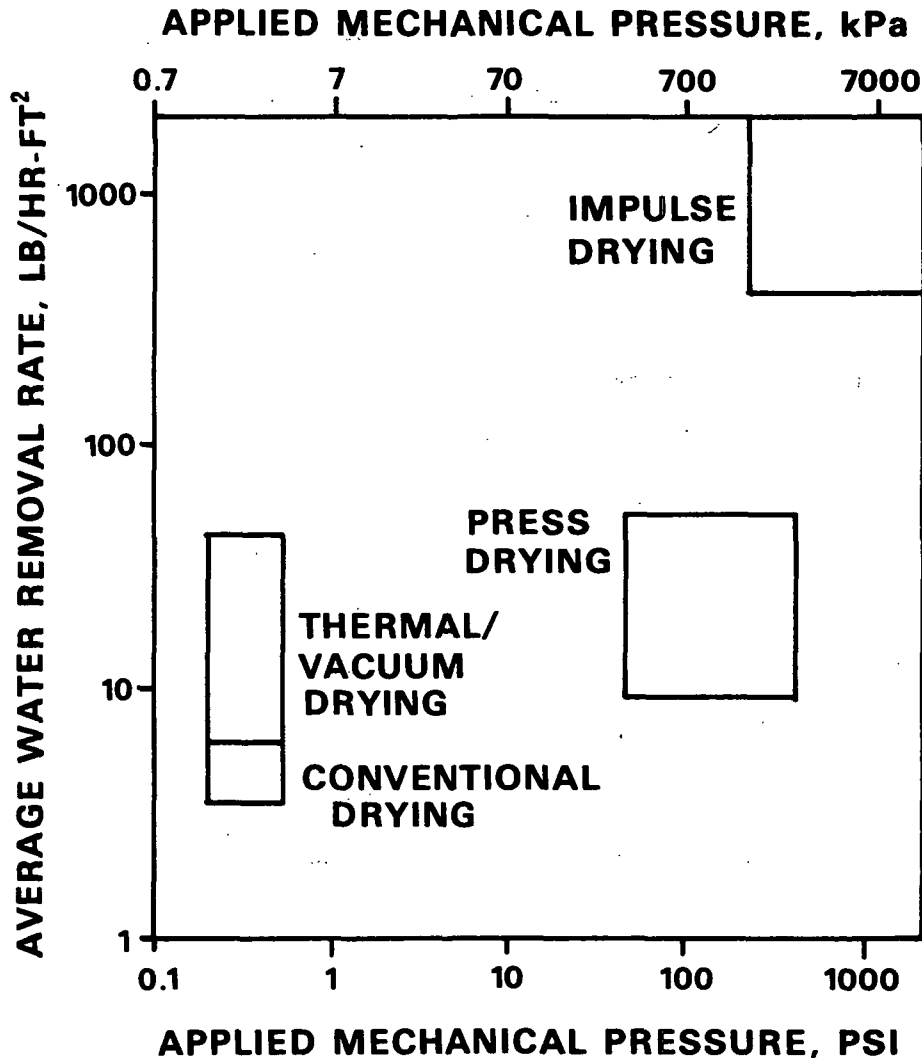


Figure 1. Water removal rates at different applied mechanical pressures for various drying methods.

This thesis presents the objective, experimental background, theoretical background, assumptions, and equations of the model. A parametric study details changes in the model's predictions resulting from changes in process variables. A sensitivity analysis shows the effects of varying certain model constants, and direct comparisons to experimental data demonstrate that the model qualitatively and quantitatively describes high intensity drying behavior.

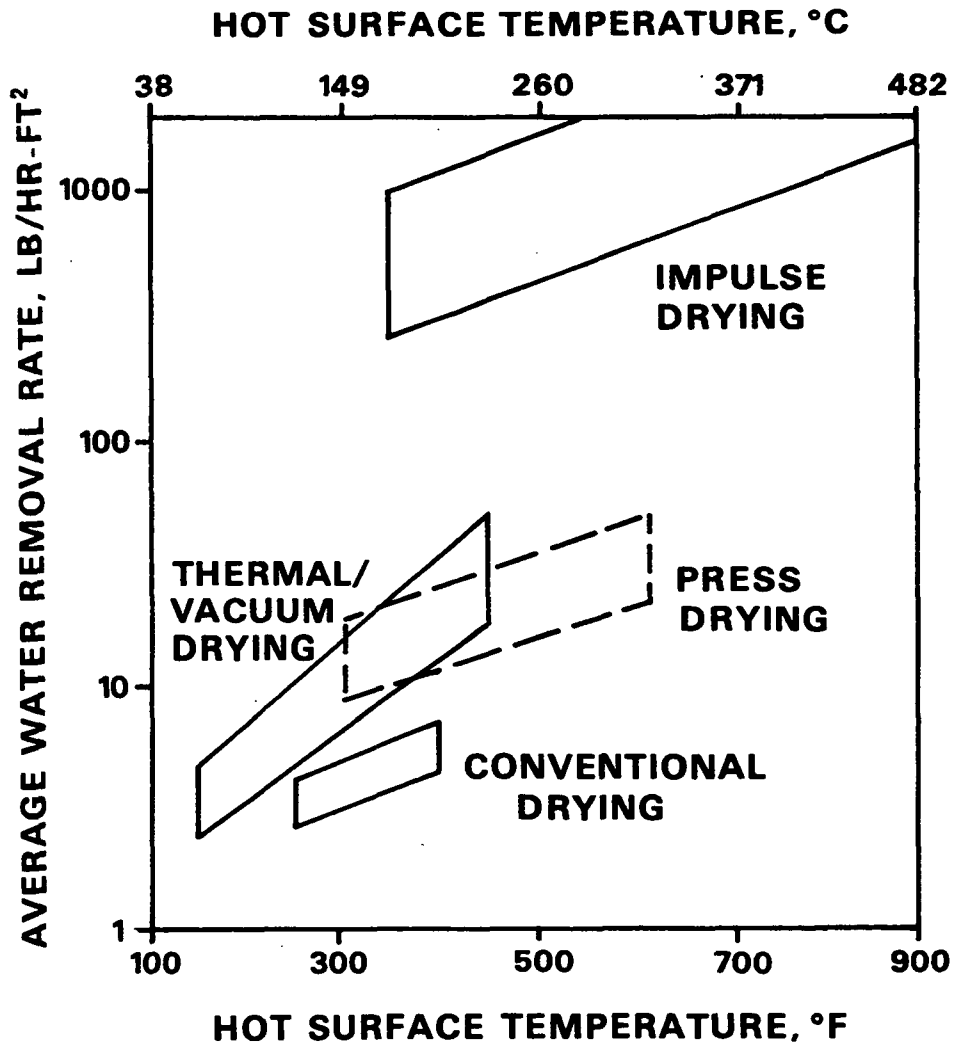


Figure 2. Water removal rates at different hot surface temperatures for various drying methods.

## OBJECTIVE

The objective of this thesis is the creation of a mathematical model of high intensity drying simple enough to be easily modified or expanded but comprehensive enough to be applicable to a wide variety of process conditions and sheet variables. The mechanisms of bulk vapor flow and liquid displacement are analyzed within the framework of a moving boundary model, and comparisons to experimental data are used to verify that the model describes high intensity drying behavior.

## EXPERIMENTAL BACKGROUND

### INTRODUCTION

High intensity paper drying occurs when the web is at or above the thermodynamic saturation temperature corresponding to the ambient pressure. This definition encompasses press drying,<sup>1</sup> where the web is heated from both sides symmetrically, and the "one-sided" drying methods: thermal/vacuum drying,<sup>2</sup> where the web is dried in a reduced pressure environment; impulse drying,<sup>3</sup> where the web is dried in a heated press nip; and one-sided drying where temperatures and mechanical pressures are elevated above conventional conditions.<sup>4</sup> The conventional conditions are a reference state of surface temperatures from about 127 to 171°C (260 to 340°F) and mechanical pressures from 1.2 to 7 kPa (0.17 to 1 psi). High intensity conditions are on the order of 177 to 399°C (350 to 750°F) and 7 to 4826 kPa (1 to 700 psi).

Experimental investigations into high intensity drying are extensions of the mechanistic studies of conventional paper drying. Within the range of conventional operating conditions, increases in surface temperature and/or mechanical pressure lead to increases in drying rate. Recent publications<sup>4,5</sup> cite several references in this area, provide data at higher temperatures and pressures, and cite an example of press drying work at very high temperatures and pressures that shows the trend of increasing drying rate continues well beyond conventional conditions. It is clear that a dramatic increase in the drying rate is observed whenever the sheet temperature can be brought to or above the boiling point.

## EXPERIMENTAL RESULTS

Figure 3 shows the configuration for the high intensity drying process modeled in this thesis. The paper contacts an impermeable heated surface directly. A felt, wire, or other highly porous material provides an escape path for the vapor and liquid to be removed from the paper, and another impermeable surface is used to exert mechanical pressure on the system. This arrangement causes one-sided heating of the paper. The overall heat and mass transfer are one-dimensional in the direction away from the hot surface. For experimental purposes, thermocouples are placed at various locations in the sheet so that the temperature distribution can be monitored throughout the course of drying.

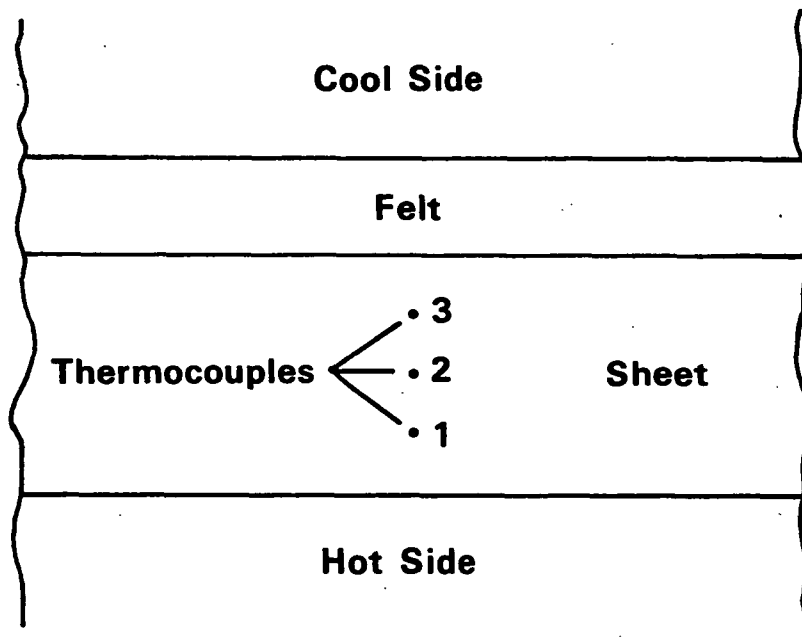


Figure 3. Configuration for one-sided high intensity drying.

Figure 4 depicts a typical sheet temperature history from several types of high intensity drying experiments.<sup>6-8</sup> It is important to note that all thermocouples reach a plateau value equal to or above the boiling point at approximately the same time and that this time is much shorter than the time needed to

simply conduct heat to the far thermocouples. The square roots of the times when the temperatures begin to rise above their plateaus are proportional to the distances of the thermocouples from the hot surface. When the temperature exceeds the boiling point, the vapor pressure exceeds the ambient pressure. The extent of the rise is related to the flow resistance of the sheet. The peak pressure is much higher in the high flow resistance cases than in the low flow resistance cases.<sup>9</sup>

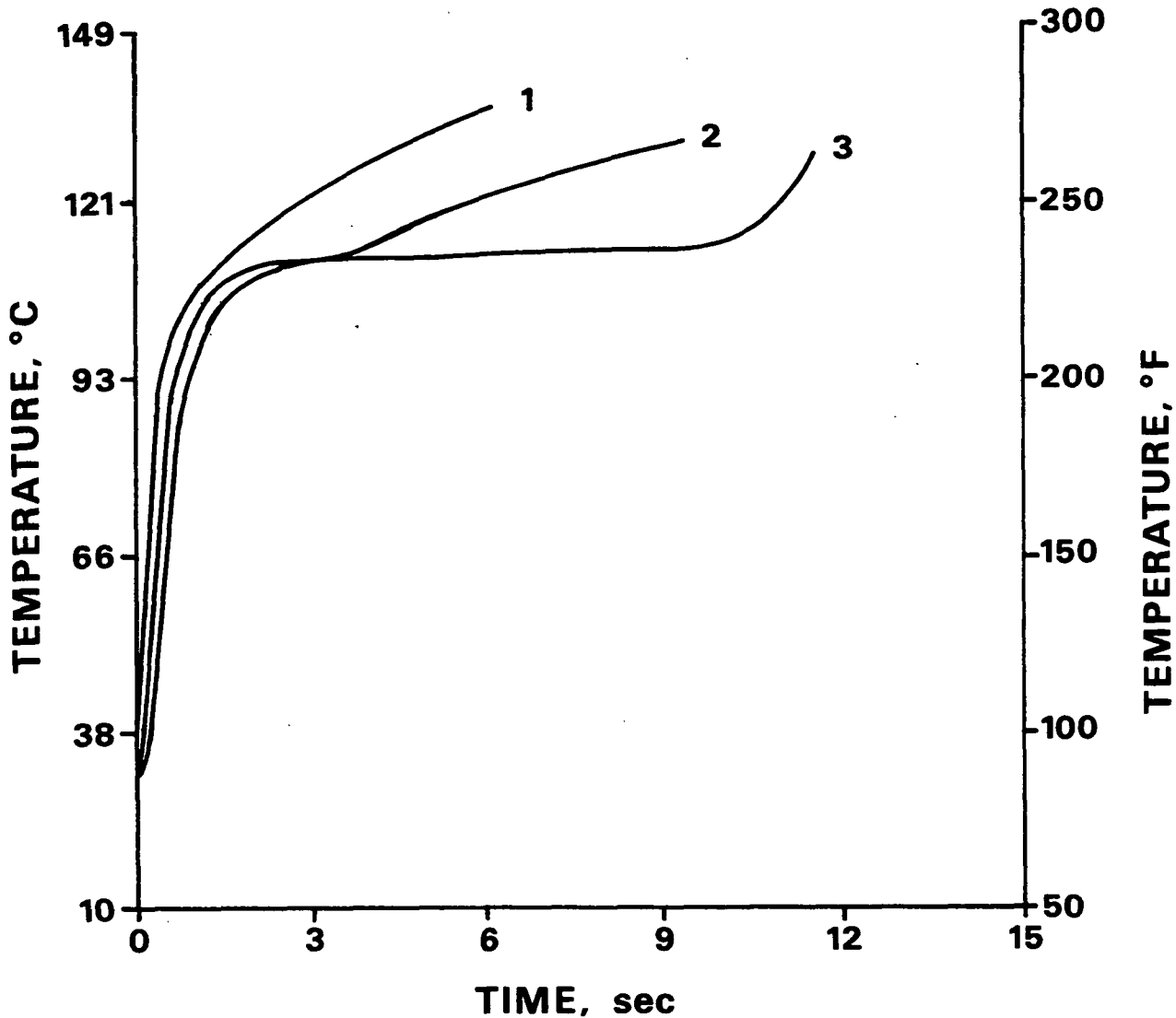


Figure 4. Internal sheet temperatures during high intensity drying.

Figure 5 shows a qualitative comparison between drying rates for conventional and high intensity drying. Four outstanding features differentiate the processes. In high intensity drying the peak drying rate is much greater than in conventional drying. In high intensity drying the peak rate is achieved (almost) instantaneously, but there is a significant heatup time required in conventional drying. The high intensity drying time is much shorter than the conventional drying time, and most importantly from a mechanistic point of view, high intensity drying does not exhibit a "constant rate" period as conventional drying does.

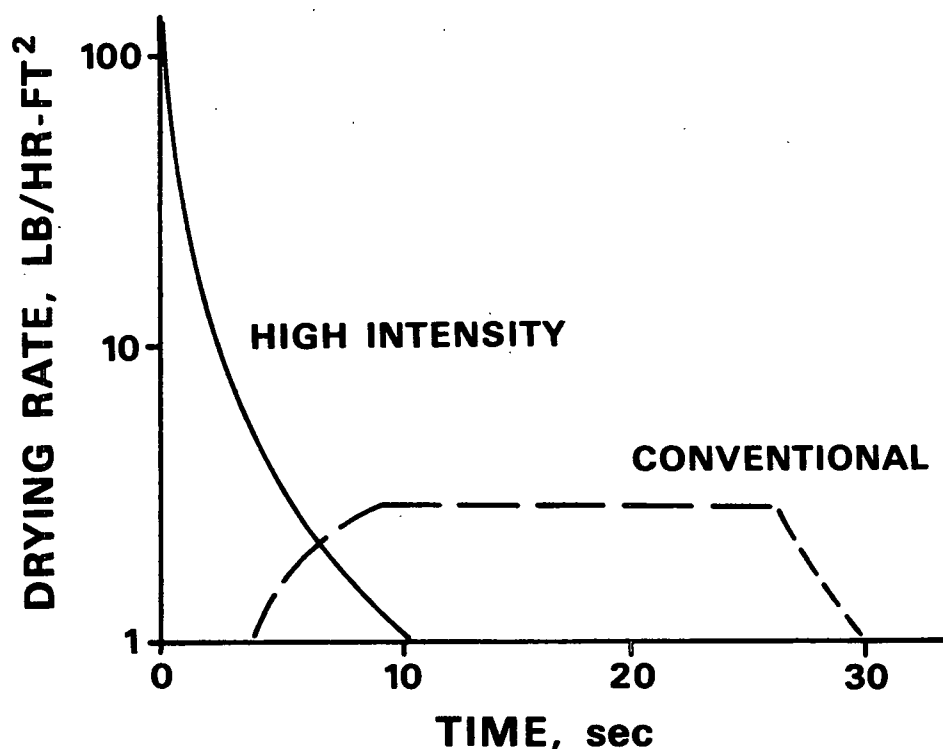


Figure 5. Comparison of high intensity and conventional drying rates.

Figure 6 depicts the results of a study designed to track the liquid distribution in the sheet.<sup>8</sup> A nonvolatile LiCl tracer is incorporated into the sheet during formation. This tracer moves with liquid water movement. After drying,

a cross section of the sheet is analyzed with the EDAX electron microscope technique to determine the location of the tracer. For conventional drying, most of the tracer is found near the side of the sheet which was adjacent to the hot surface. High intensity drying shows an opposite tracer distribution.

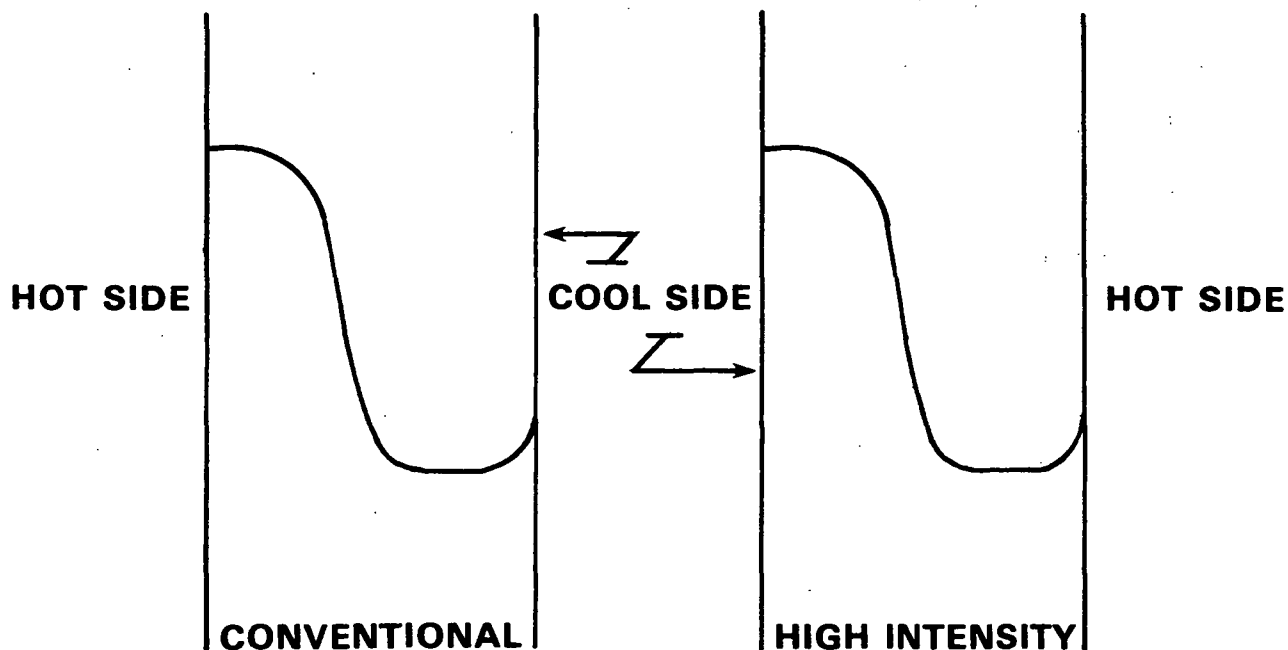


Figure 6. Comparison of tracer distributions for high intensity and conventional drying.

The experimental results lead to the postulation of three dominant mechanisms operative during high intensity drying: bulk vapor flow, liquid displacement and/or entrainment, and the development of zones within the sheet.

#### BULK VAPOR FLOW

Simple visual observation of a high intensity drying experiment is enough to suggest convective vapor flow. Vapor is forcibly ejected from the sheet. Even under impulse conditions where the nip residence time is as short as 0.005 second, a vapor pulse exiting the sheet is clearly visible. The rapid temperature rise



of thermocouples far from the hot surface supports this mechanism (see Fig. 4). The drying rate is insensitive to ambient air flow rate,<sup>4</sup> and this would not be true if diffusion were dominant since a diffusion mechanism would depend on convective transport external to the sheet. Finally, direct experimental evidence of vapor flow under a vapor-pressure-gradient driving force comes from a study of steady state heat transfer in a granular porous medium<sup>10</sup> and work involving heat pipes.<sup>11</sup> Darcy's law can be used to model the vapor flow in these cases, and while they are not examples of "drying," the fundamental transport mechanisms are identical.

#### LIQUID DISPLACEMENT

Liquid in the larger pores of a fibrous material can be displaced by a flowing gas. Devices for dewatering paper by passing air through the wet web were described in a patent filed for in March, 1963 and granted November 8, 1966.<sup>12</sup> Extensions of this concept<sup>13-20</sup> have shown that pressure differentials across the sheet on the order of 7 to 210 kPa (1 to 30 psi) can raise solids content from the 10 to 30% range up to the 40 to 45% range. For textile materials, steam pressurized at up to 700 kPa (100 psi) can be used to preheat the web, displace liquid, and raise solids content from around 20% to nearly 80%.<sup>21</sup>

High intensity drying achieves its pressure driving force by vaporizing some liquid in the vicinity of the hot surface. As the vapor tries to escape, it pushes or entrains interfiber liquid out of the sheet. Figure 6 indicates the flow of liquid away from the hot surface. Heat flux determinations reveal that the actual thermal energy input can be on the order of 50% or less than the energy which would be required to raise the sheet to the boiling point and then evaporate all the liquid at that temperature.<sup>8</sup>

Therefore, water has to be removed in liquid form. High intensity, vapor-induced expulsion of liquid droplets has been observed for other porous materials as well.<sup>22</sup> Note that since the necessary condition for liquid displacement is a vapor pressure differential across the web, the symmetrical heating of the press drying process precludes this mechanism.

#### Mechanical Dewatering

High-pressure, short-duration mechanical pressing of paper is a fundamental water removal method used prior to conventional drying. The extent of the dewatering is controlled by the relationship between the applied pressure and time and by either the flow resistance or compressibility of the sheet (or both). In addition to bulk vapor flow and vapor-induced liquid displacement, the temperature and pressure levels in impulse drying encourage effects similar to those found from pressing at higher than normal temperatures.

Pressing at up to 90°C (194°F) can take a sheet at ingoing solids content of 38% and raise it to nearly 50%, depending on temperature, basis weight, and freeness.<sup>23,24</sup> Additionally, hot pressing offers the possibility for moisture profile control.<sup>25</sup> Hot pressing and impulse drying use temperature to decrease the viscosity and surface tension of the water and to decrease the sheet compression resistance. Lower viscosity allows the liquid to flow more easily; this factor should be of key importance in a flow controlled situation. Lower compression resistance allows the sheet to be deformed more easily and should therefore be of key importance in a compression controlled case, particularly when a high percentage of lignin is present. Lower surface tension should benefit both cases by reducing capillary pressure and the possibility of rewetting.

## ZONE DEVELOPMENT

Figure 6 indicates the presence of two main zones within the sheet at the end of drying: a zone of lower moisture content close to the hot surface and a zone of higher moisture content, created by liquid flow, far from the hot surface. This in itself is no guarantee of a uniform moving front that progresses through the sheet, but when there is no constant rate drying period (see Fig. 5) and the external boundary layer does not affect the drying,<sup>4</sup> then a simple approach to modeling the phenomenon is with a moving boundary or zone model.<sup>26</sup> The proportionality of the square roots of plateau rise times to thermocouple distances in Fig. 4 is compatible with the classical moving boundary problem called the Neumann problem<sup>27</sup> and suggests that an elementary model of high intensity drying might be based on a Neumann-like analysis.

## SUMMARY

There is experimental evidence to indicate that high intensity drying might be conveniently described by a moving boundary or zone model based on the bulk vapor flow and liquid displacement mechanisms. In the case of impulse drying, the additional effects of high temperature pressing may contribute to the overall moisture loss by changing the physical properties of the liquid water and/or the sheet compressibility. The similarities between high intensity drying behavior and a classical moving boundary problem suggest a logical starting point for the mathematical modeling.

## MOVING BOUNDARY MODELS

### INTRODUCTION

Muehlbauer and Sunderland<sup>28</sup> present a brief summary of the Neumann problem and an excellent review of the mathematical investigations of moving boundary problems up until 1965. Substantial work in this area since then has centered on obtaining solutions to moving boundary problems with boundary and/or initial conditions or assumptions about key thermal properties which are different than those in the original and early analyses. Generally, the problems deal with one-dimensional heat transfer through one phase of a material to the interface with a different phase of the same material. The models usually treat melting or solidification problems, and mass transfer is not considered except in rare cases of convection in the liquid phase. The models either calculate the temperature or enthalpy distribution and position of the interface within the material or track the positions of isotherms that progress through the material.

### TEMPERATURE-BASED MODELS

The original temperature-based model was formulated by Neumann. Details of the model are in.<sup>27</sup> Heat conduction equations for each phase or "zone" coupled with appropriate initial, boundary, and interface conditions allow a prediction of the temperature distribution and interface position within a semi-infinite medium. Extensions of this model allow for phase transitions over a range of temperatures<sup>29,30</sup> and a modified rate of interface advance due to the different densities of the two phases.<sup>31</sup> Simple dependence of thermal conductivity on temperature is treated analytically,<sup>32</sup> and clever numerical schemes handle more complicated dependencies of conductivity and density.<sup>33,34</sup>

The primary problems with these methods, with reference to drying, are that they deal only with semi-infinite media and that they deal only with the presence of a one-component (multiphase) system. Paper behaves as a finite medium with regard to heat transfer during drying and contains two or more components (fiber, water, air, etc.). Integral transform methods have been applied to solve the problem in finite media of various geometries and with boundary conditions of the first, second, and third kinds,<sup>35</sup> but the problem of multiple components remains.

#### ENTHALPY-BASED MODELS

When knowledge of the exact position of a phase change interface is not required, modeling the system in terms of an enthalpy equation often leads to greatly simplified (numerical) solution methods.<sup>36</sup> In elementary cases, the solution of the enthalpy-based analysis is identical to that of the analytical temperature-based problem. In this method, the temperature-based model is formulated and then converted to an enthalpy-based model by using a relationship between temperature and enthalpy.<sup>37,38</sup> This relationship describes the latent heat effect as a large jump in heat capacity over a very narrow temperature range. The advantages of this approach are: there are no conditions to be satisfied at the phase change boundary; there is no need to track the position of the phase change boundary accurately; there is no need to consider the regions on either side of the boundary separately; and it is possible to vary the range of temperatures over which the transition takes place.<sup>38</sup> It is also relatively easy to extend this technique to more than one dimension.<sup>39</sup>

The disadvantage of this method is that it can lead to problems when convective effects need to be considered. In a model of high intensity drying,

convection of vapor and liquid is a key mechanism, and so an enthalpy-based method is not directly applicable.

#### POSITION-BASED MODELS

The Isotherm Migration Method (IMM) and its modifications are alternatives to the temperature- and enthalpy-based approaches. IMM tracks the position of a given isotherm within the medium, and distance replaces temperature as the dependent variable.<sup>40,41</sup> It is another attempt to avoid calculating the exact position of the phase change front.

While IMM is flexible and capable of handling more than one moving front, it is limited because it requires some analytical solution to "start" the process. This analytical solution is an exact solution for very short times, places all isotherms in the slab, and sets an initial temperature profile to start the finite difference numerical scheme. Thus, IMM is somewhat limited in that an analytical solution may not exist to start the process. The lack of an analytical starting solution, however, is a relatively minor shortcoming compared to its inability to handle convective aspects of problem.

#### DRYING MODELS

Drying differs significantly from simple moving boundary problems, since drying involves simultaneous heat and mass transfer. Furthermore, drying takes place within a matrix of solid material from which a volatile component is evaporated. The strong coupling of heat and mass transfer in drying thus requires a careful extension of the general concepts of moving boundary problems.

An exact solution of an evaporation problem in porous media has been known since 1975.<sup>42</sup> This is the most elementary case involving constant surface

temperature, constant evaporation temperature, and a semi-infinite medium. Penetrating front models for finite media have evolved, generally for freeze drying applications.<sup>43-47</sup> The geometry of the models is such that the medium is heated either symmetrically or with one face perfectly insulated and impermeable. The heat and mass transfer occur in opposite directions, and therefore these models are directly applicable only to press drying or to drying in which the heated surface is permeable.

Most models do not account for the hygroscopic nature of the matrix, but models for drying of wood<sup>48-50</sup> and other materials<sup>51</sup> do include this factor. However, these also involve opposite heat and mass transfer.

Models which calculate the pressure rise inside the porous medium are not applicable because they either use a diffusion mechanism for vapor transport<sup>52</sup> or they assume a constant evaporation temperature but calculate the vapor flux based on a total pressure gradient.<sup>53,54</sup> These are also opposite heat and mass transfer cases.

Strek and Nastaj have used the moving boundary concept to model the falling rate period in vacuum drying of a bed of granular material.<sup>55</sup> Heat and mass transfer are in the same direction, but the experimental conditions are drastically different than those in high intensity paper drying. Mild temperature gradients and large bed thicknesses lead to very long drying times. The nature of the granular material is unlike that of cellulose papermaking fibers; the bed is not compressible and thickness is not sensitive to changes in moisture content.

Baines used a moving boundary concept to model a conventional drying process,<sup>56</sup> and Ahrens used the concept in modeling high intensity drying.<sup>9,57</sup> The Ahrens model is highly simplified and based on descriptions of the physical

processes dominant in high intensity conditions. The model is mathematically identical to an elementary analysis of the one-dimensional freezing of water.<sup>58</sup> The Ahrens model gives reasonable agreement with experimental data and serves as the starting point from which this thesis has been developed.

#### SUMMARY

Moving boundary models in general prove unsatisfactory for the description of high intensity drying because: they deal with only one component; they assume a constant phase transition temperature equal to the normal phase transition temperature of the one component; they model processes with heat and mass transfer in opposite directions; they usually deal only with boundary conditions of the first kind; they do not account for vapor-pressure-induced liquid convection; and/or they present analytical solutions only for semi-infinite media.

Of the drying models, an elementary one possesses the required characteristics to be used as a starting point for further development. The Ahrens model, which is mathematically identical to a simplified analysis of a freezing water problem, is the starting point of this thesis.



## THE MATHEMATICAL MODEL

### INTRODUCTION

For modeling purposes, the high intensity process is pictured as a series of linked mechanisms. As the sheet is brought into contact with the hot surface, heat flow into the sheet through a finite contact resistance raises its temperature in a "heatup" regime. The contact resistance depends on the mechanical pressure and on the degree of saturation of the sheet next to the hot surface. Because of the high thermal diffusivity of the (metal) hot surface, its temperature does not change much in reality and remains constant in the mathematical model.

If the sheet surface temperature adjacent to the hot surface becomes incrementally greater than the thermodynamic saturation temperature corresponding to the ambient pressure, then the vapor pressure difference across the sheet is assumed to cause slug flow of the interfiber liquid and air. The position of this slug flow interface defines the limit of linear temperature gradients and thermodynamic saturation so that no vapor flows into the outer zone until the temperature gradient there becomes linear due to heat transfer by conduction and liquid convection within the sheet.

If the sheet becomes saturated before the inner surface temperature exceeds the boiling point, liquid water starts to be mechanically expressed from the sheet and vapor induced liquid flow does not begin until the inner surface temperature exceeds the thermodynamic saturation temperature corresponding to the hydraulic pressure at the inner surface.

Once vapor induced liquid flow starts, the sheet is in the "transition" regime where zones of different moisture content develop inside the sheet. A dry zone is created by evaporation. A zone with water trapped inside the fibers is created

when interfiber water is pushed ahead and the evaporative front has not yet reached the trapped water. If the heat transfer is such that the sheet's outer surface temperature exceeds the boiling point, then a second evaporative front can move into the sheet if the rate of liquid flow toward the cool side is less than the rate of evaporation there.

The "linear" or quasi-static regime begins when all temperature gradients become linear due to heat transfer or when they become linear because all interfiber water has been removed (and the interface defining the limit of linear gradients no longer exists).

#### ELEMENTARY MODELS

The Ahrens model is formulated to describe macroscopic trends and is based on a few of the physical processes judged to be controlling under high intensity conditions. Figure 7 diagrams the configuration considered.

The paper is divided into a dry zone (devoid of liquid water) adjacent to the hot surface and a wet zone with stagnant liquid adjacent to the dry zone.  $\delta$  is the time-varying dry zone thickness and  $\delta_T$  is the total thickness of the fully dry sheet. The wet zone is assumed to be at the boiling point temperature (TB) that corresponds to the ambient pressure. Thus, there is no heatup or transition regime.

The process is considered to be controlled by the rate of heat transfer from the hot surface (at constant temperature  $T_H$ ) to the paper. The vapor generated at the dry-wet interface flows through the partially saturated wet zone and out of the sheet. The flow resistance of the wet zone is considered to be negligible so that the vapor is generated essentially at TB. (In any case, the difference between the interface temperature and TB would be much less than the

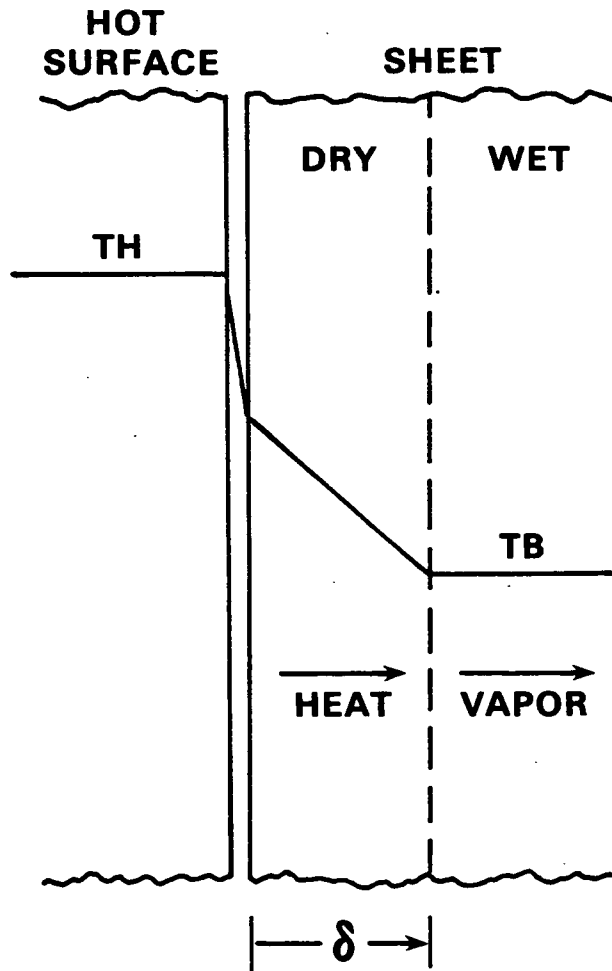


Figure 7. Configuration for Ahrens two zone model.

difference between  $T_H$  and  $T_B$ ). The state of the system is described by an equation for heat flux

$$Q = U*(T_H - T_B) \quad (1)$$

where  $Q$  is the heat flux and  $U$  is the overall heat transfer coefficient. As a consequence of assuming a linear temperature gradient in the dry zone,  $U$  is defined by

$$\frac{1}{U} = \frac{1}{H_c} + \frac{\delta}{K_d} \quad (2)$$

where  $H_c$  is the thermal contact coefficient between the hot surface and the sheet and  $K_d$  is the thermal conductivity of the dry zone (both assumed constant). The interface energy balance is

$$Q = \epsilon * S * \rho_w * \Delta h * \frac{d\delta}{dt} \quad (3)$$

where  $\epsilon$  and  $S$  are the porosity and saturation of the wet zone,  $\rho_w$  is the density of water,  $\Delta h$  is the latent heat (all assumed constant), and  $t$  is time; and the relative mass of water removed is

$$MREL = \frac{\delta}{\delta_T} \quad (4)$$

Equations (1) through (3) can be combined to solve for  $\delta$  as a function of time by separating the variables and using the initial condition that  $\delta = 0$  at time = 0. The moisture removal (drying curve) is then given by:

$$MREL = \sqrt{\frac{1}{BI^2} + \tau} - \frac{1}{BI} \quad (5)$$

where  $BI$  is the dimensionless Biot number defined by:

$$BI = \frac{H_c * \delta_T}{K_d} \quad (6)$$

and  $\tau$ , a dimensionless time variable, is defined by:

$$\tau = \frac{2 * K_d * (T_H - T_B) * t}{\Delta h * M_o * \delta_T} \quad (7)$$

where  $M_o$  is the initial mass of water present per unit area.

The limiting case of "perfect" thermal contact between the sheet and hot surface ( $BI = \infty$ ) reduces to a zone model with the interface location being directly proportional to the square root of time. Figure 8 graphs the results and<sup>9</sup> gives some comparisons to experimental data.

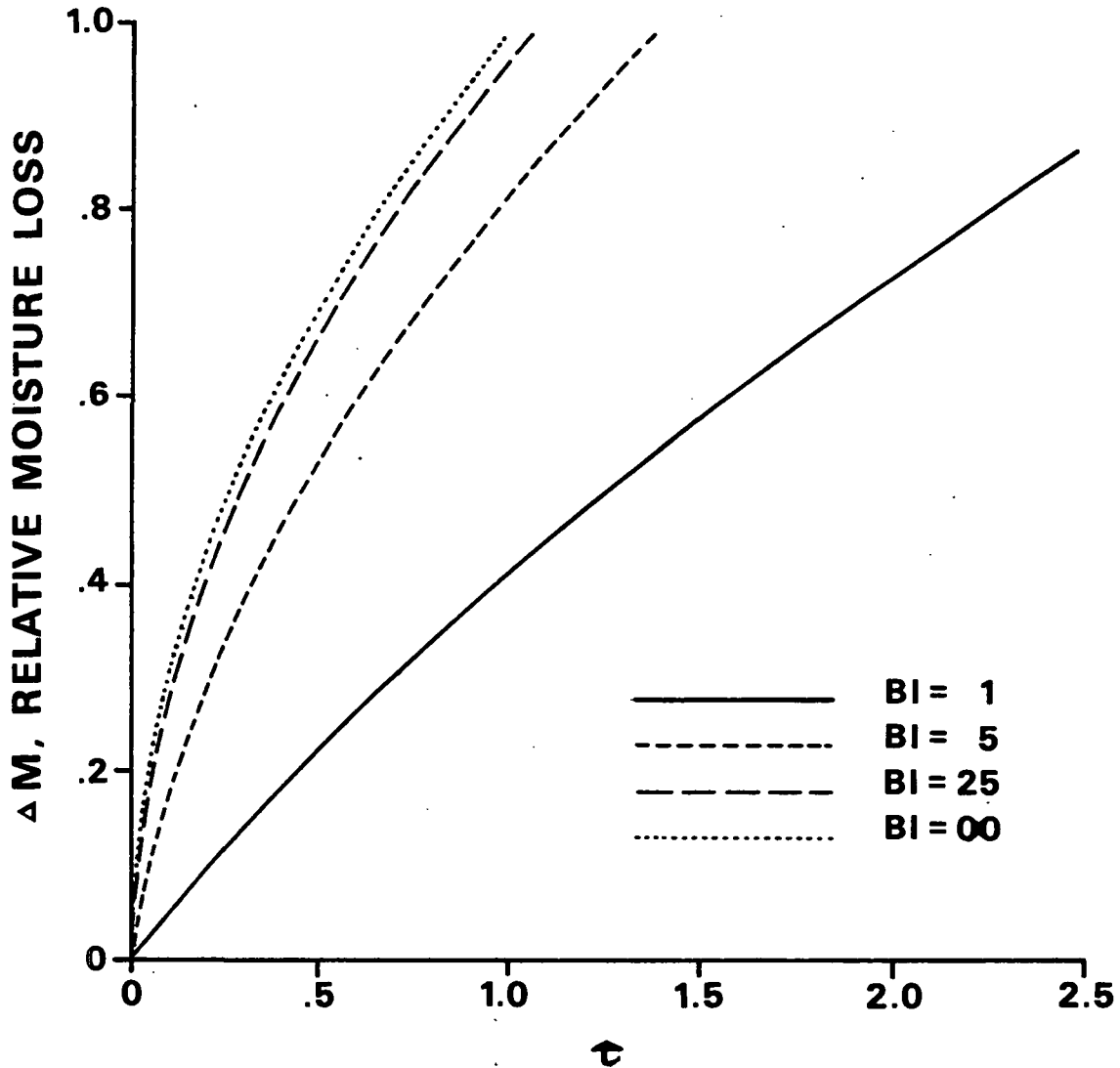


Figure 8. Moisture removal as a function of dimensionless time with Biot number as a parameter for the Ahrens model.

If the permeability of the wet zone were zero, heat transferred by conduction would cause an evaporative front to move into the sheet from the cool side

toward the hot side. Making the same assumptions as in the Ahrens model (stagnant liquid, constant properties, etc.) allows a calculation of moisture loss from:

$$MREL = 1 + \frac{1}{BI} - \sqrt{1 + \frac{2}{BI} + \frac{1}{BI^2} - \tau} \quad (8)$$

where  $BI$  and  $\tau$  are calculated based on the wet zone thermal conductivity and  $\delta_T$  is the initial sheet thickness. Figure 9 shows the drying curves for this model.

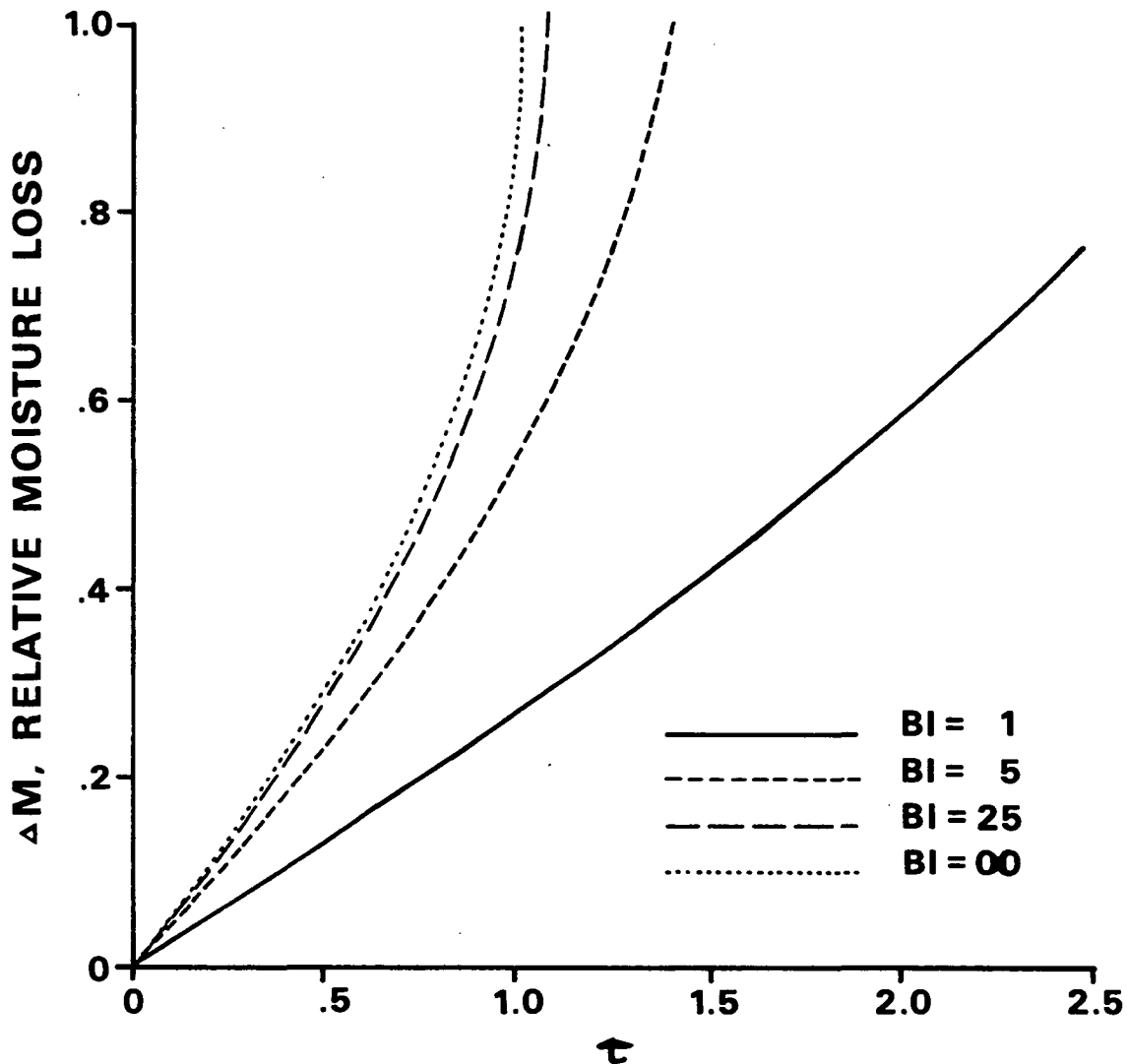


Figure 9. Moisture removal as a function of dimensionless time with Biot number as a parameter for the second limiting case.

## DESCRIPTION OF THE ADVANCED MODEL

This thesis is developed from the Ahrens model of high intensity drying. The elementary analysis is extended by accounting for flowing liquid, elevated phase transition temperatures resulting from sheet flow resistance, and hygroscopic effects on latent heat at zone interfaces. The advanced model idealizes the high intensity paper drying process by picturing the sheet as composed of different zones which contain various amounts of fiber, liquid water, and water vapor. The model is based on sets of equations which account for the heat and moisture transfer within and among the zones during three regimes: heatup, transition, and quasi-static. Once the hot surface temperature, boiling point temperature, basis weight, Canadian Standard Freeness (CSF), initial moisture ratio, and mechanical pressure pulse are specified, the equations may be solved to predict the moisture content as a function of time.

The heat and mass balance equations are combined with supplementary equations that describe the nature of the pressure pulse; the liquid and vapor physical properties; and the thermal, compression, and permeability properties of the sheet. The complete model is converted to a FORTRAN program called HIDRYER1.

The program is used to run simulations of various drying conditions by calculating the rates of interface advance, multiplying the rates by a small time increment, and adding to the old values to obtain updated estimates of interface position, zone basis weight, and sheet moisture content.

## ASSUMPTIONS

The fundamental assumptions of the model are listed in this section. Other assumptions are listed as they are invoked.

- A1. Heat is transferred to the sheet from the hot surface by conduction only.
- A2. The hot surface is an impermeable boundary.
- A3. There is no conductive heat flux from the sheet to the felt.
- A4. The vapor pressure at the sheet-felt interface is equal to the ambient pressure because of the negligible felt flow resistance.
- A5. Heat and mass transfer occur only in one dimension.
- A6. In the continuity equation, vapor and liquid storage terms within a zone are negligible.
- A7. Change of phase occurs only at the zone interfaces.
- A8. Porosity, saturation, and physical properties are uniform within a zone, but can differ from one zone to another and vary with time.
- A9. Darcy's law is sufficient to describe liquid and vapor flow.
- A10. The fiber flow can be described by a compression equation such that the fiber velocity at any point in a zone is linearly related to the velocities of the interfaces bounding the zone.
- A11. Potential and kinetic energy contributions to the energy equation are negligible compared to thermal energy transfer.
- A12. Conversion of mechanical energy to thermal energy is negligible.
- A13. In energy calculations, the density, thermal conductivity, and specific heat of water vapor are negligible compared to those quantities for liquid water and fiber.
- A14. Local thermal equilibrium exists at all points.
- A15. Gravity effects are negligible.
- A16. A representative value for the vapor and liquid physical properties of a zone may be obtained by calculating the values of



these properties at the temperatures of the interfaces bounding the zone and averaging the results.

- A17. There is no net capillary force on a zone and there is no capillary pressure gradient within a zone.
- A18. Fibers have a zero lumen volume and, in zones where water is present, a constant apparent cell wall density equal to 1.0 g/cc.<sup>59</sup>
- A19. Hygroscopic effects on vapor pressure reduction and moisture distribution in the zones are neglected.
- A20. As the inner zones develop, air is pushed ahead of the progressing interfaces so that the gas in zones with linear temperature gradients is composed of vapor only.

Assumptions A1 through A4 are the overall boundary conditions on the sheet. A1 simply states that radiation heat transfer to the sheet from the hot surface is negligible. Paper emissivity is low and the hot surface-to-sheet temperature difference declines rapidly after contact. A2 means that the hot surface is solid, not porous, and no mass is transferred through it. A3 indicates that the thermal contact from the sheet to the felt is minimal compared to the contact between the hot surface and sheet. A4 means that there is no substantial pressure differential across the felt. Note that this is a condition on the pressure at the outer surface, not a condition on the temperature there.

A5 is an approximation to the overall direction of heat and mass transfer because the thickness of the sheet is much less than the lateral dimensions.

A6 through A8 pertain to the continuity equations for the model. A6 is an assumption of slug flow to simplify the transport calculations. A7 and A8 allow each zone to be characterized by its own unique value of moisture content and

state that this moisture content is not altered by vapor condensing within the zone.

A9 and A10 are for the momentum equations. Darcy's law is the momentum equation for flowing liquid and vapor. Calculations show that the Reynolds number is well within the appropriate regime for suitable application of Darcy's law.<sup>60</sup> A10 allows the momentum equation for the deforming fiber bed to be replaced by a simple compression equation and states that each zone undergoes its own uniform compression.

Assumptions A11 through A15 pertain to the energy equation. All are standard assumptions used in drying models.<sup>61,62</sup>

A16 is made so that unique values can characterize a zone's vapor and liquid properties and variations with position in the zone can be neglected.

A17 might appear to be the most questionable approximation. The capillary pressure is typically calculated with the Laplace equation

$$P_{cap} = \frac{2 * \gamma * \cos \theta}{r} \quad (9)$$

where  $P_{cap}$  is the capillary pressure,  $\gamma$  is the liquid surface tension,  $\theta$  is the contact angle, and  $r$  is the pore radius. First, this applies to pores of circular cross section and therefore should NOT apply to paper since it has irregularly shaped pores. Second, at high drying temperatures the surface tension of water is drastically reduced and this serves to decrease  $P_{cap}$ . Third, even at elevated mechanical pressure there are still many pores in the sheet with large radii.<sup>63</sup> Fourth, the equation applies to a SATURATED pore, and it requires very

large mechanical pressures to achieve interfiber saturation. Therefore, at least in the initial stages of drying, the larger pores remain unsaturated.

When the sheet does become saturated, then a significant capillary pressure might be expected. However, it is exactly in this regime (wet pressing) that moisture loss by liquid expression dominates water removal and so the "drying" (evaporative) aspect becomes a secondary process. Thus, A17 may not be as bad an approximation as it would first appear to be. The net result is that the liquid pressure (and its gradient) is identical to the vapor pressure (and its gradient).

A18 is a means of trapping a certain fraction of liquid inside the fibers, thereby making it unavailable for vapor-induced displacement. Since the actual density of cellulose is about 1.55 g/cc, an apparent cell wall density of 1.0 g/cc means that roughly one-third of the fiber volume can contain liquid. Given the density of water and a "typical" fiber cross-sectional area, it is possible to determine the moisture ratio at which the fibers just become saturated.

Furthermore, by holding the apparent cell wall density fixed, a limit is placed on the minimum porosity attainable. Compressing the sheet is equivalent to moving the fibers closer together. The porosity of the zone can be no lower than the fiber wall porosity (about 0.33). In dry zones, A18 allows the porosity to go to zero by removing the apparent cell wall density restriction. Since there is no water there to occupy the space, the fiber wall can collapse.

A19 is made so that the moisture distribution in a zone can be treated as uniform and so that the vapor pressure is simply a function of the temperature. However, the hygroscopic effect on the heat of desorption is accounted for, since it strongly influences heat transfer calculations. This is detailed later in the thesis.

A20 is a convenience to simplify the mass and energy equations in zones of linear temperature gradient (zones where vapor flow is handled by Darcy's law) and to eliminate the need for a detailed gas continuity equation in the outer zone during the transition regime.

#### ADVANCED MODEL EQUATIONS

Continuity and energy equations determine the temperatures and rates of change of position of the interfaces and describe the heat and mass transfer within each zone. The interfaces separate zones of different moisture content. Figure 10 shows each kind of zone that may be present and the terminology for the zones, interfaces, and temperatures. Interface 1 separates zone 1 (no liquid moisture), which is adjacent to the hot surface, from zone 2 (liquid moisture only inside the fibers). Interface 2 separates zone 2 from zone 3 (liquid moisture inside and outside the fibers), or zone 2 from zone 4 (no liquid moisture), which can develop if heat is transferred to the far side of the sheet faster than interfiber liquid can flow there. Interface 3 separates zone 3 from zone 4. If zone 3 does not exist, either because there is initially not enough moisture present to saturate the fibers or because all the interfiber liquid is pushed out or evaporated, H1DRYER1 places interface 3 at  $\delta_T$ .

The reasonable assumption of linear temperature gradients in zones 1 and 2 because of the low moisture contents and the porosities, and because of the low specific heat of cellulose, introduces a considerable simplification to the required calculations. For example, the energy equations for these zones are converted from partial differential equations to algebraic ones (which are easily solved provided the interface temperatures can be determined). Thus, the zone concept is a means of simplifying a more "continuous" type of model by limiting the regions over which detailed calculations have to be performed.

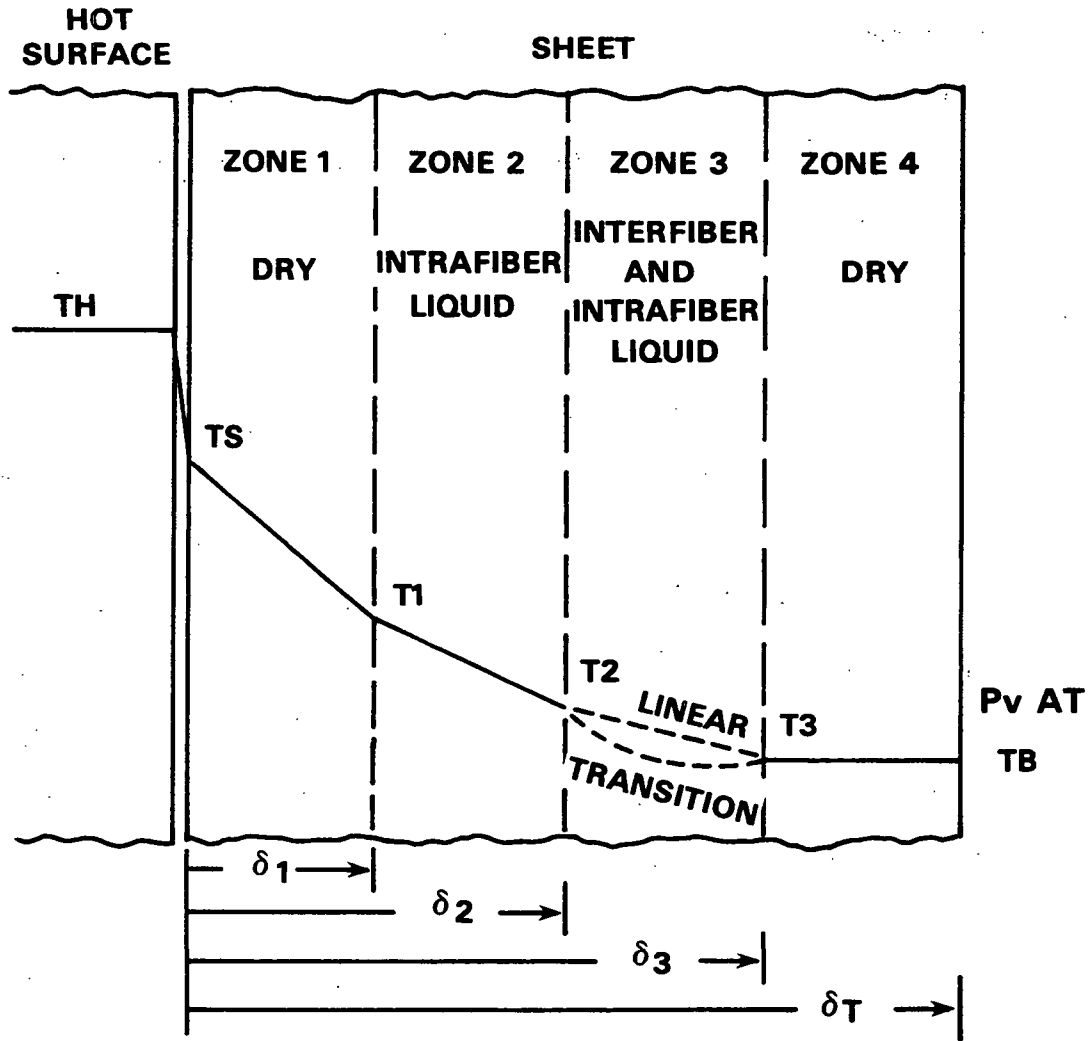


Figure 10. Zone, interface, and temperature designations for advanced model equations.

#### Zone Continuity and Momentum Equations

Consider the one-dimensional flow of a mixture of fibers, liquid water, and a gas composed of water vapor. Consider further that a certain fraction of the liquid water is trapped within the fibers and moves at the fiber velocity. The continuity equation is:

$$\begin{aligned}
 \frac{\partial}{\partial t} (\rho_F * (1-\epsilon) + \rho_W * (1-a) * \epsilon * S + \rho_W * a * \epsilon * S + \rho_V * \epsilon * (1-S)) = \\
 - \frac{\partial}{\partial z} (\rho_F * (1-\epsilon) * V_f + \rho_W * (1-a) * \epsilon * S * V_f \\
 + \rho_W * a * \epsilon * S * V_{\text{water}} + \rho_V * \epsilon * (1-S) * V_{\text{gas}})
 \end{aligned} \quad (10)$$

where  $\rho_F$ ,  $\rho_W$ , and  $\rho_V$  are the fiber, water, and vapor densities;  $a$  is the fraction of liquid water external to the fibers;  $V_f$ ,  $V_{water}$ , and  $V_{gas}$  are the fiber, water, and vapor velocities relative to the fixed origin;  $z$  is the position coordinate and  $t$  is time.

Darcy's law, the momentum equation for the flowing gas and liquid, is used to describe the velocities of the flowing gas and liquid relative to the moving fibers.<sup>64</sup>

$$V_v = \epsilon * (1-S) * (V_{gas}-V_f) = - \frac{K_a * K_v}{\mu_v} * \frac{\partial P_v}{\partial z} \quad (11)$$

$$V_w = a * \epsilon * S * (V_{water}-V_f) = - \frac{K_a * K_w}{\mu_w} * \frac{\partial P_w}{\partial z} \quad (12)$$

where  $V_v$  and  $V_w$  are the vapor and liquid superficial velocities relative to the moving fibers;  $K_a$  is the absolute permeability;  $K_v$  and  $K_w$  are the vapor and liquid relative permeabilities;  $P_v$  and  $P_w$  are the vapor and liquid pressures; and  $\mu_v$  and  $\mu_w$  are the vapor and liquid viscosities.

With these definitions, the continuity equation can be written as:

$$\frac{\partial D}{\partial t} = - \frac{\partial}{\partial z} (D * V_f + \rho_w * V_w + \rho_v * V_v) \quad (13)$$

where

$$D = \rho_F * (1-\epsilon) + \rho_w * \epsilon * S + \rho_v * \epsilon * (1-S) \quad (14)$$

However,  $\rho_v \ll \rho_w < \rho_F$ , and with

$$S = \frac{(1-\epsilon) * M_R * \rho_F}{\rho_w * \epsilon} \quad (15)$$

then

$$D = \rho_F * (1-\epsilon) * (1+MR) \quad (16)$$

where MR is the moisture ratio.

The momentum equation for each zone of the fiber matrix is replaced by a power law compression equation:

$$C = M * P^N \quad (17)$$

where C is the dry fiber concentration (mass/total volume), and where each zone has its own compression constants (M and N) and effective mechanical pressure (P); the assumption of uniform zone compressibility gives

$$V_f = \frac{\bar{L}}{L} * \frac{\partial L}{\partial t} + V_f' \quad (18)$$

where  $\bar{L}$  is the distance inside the zone measured from the zone's interface closer to the origin, L is the zone thickness,  $\partial L / \partial t$  is the "compression velocity" or change in zone thickness caused by P, and  $V_f'$  is the compression velocity of the zone interface closer to the origin with respect to that (fixed) origin.

For an unsaturated medium during the heatup regime, make the approximation that  $V_{water} = V_f$  so that  $V_w = 0$ . (This is a compression model, not a wet pressing model.) For this case, and for an unsaturated or saturated zone in the transition or linear regimes, use assumption A6 so that the continuity equation becomes

$$\frac{\partial D}{\partial t} = - \frac{\partial}{\partial z} (D * V_f) \quad (19)$$

If the sheet becomes saturated during heatup, its compression is significantly affected by the buildup of a substantial internal hydraulic pressure. The overall continuity equation can be separated into its fiber and water components and combined with Darcy's law to produce:

$$\frac{\partial MR}{\partial t} = \frac{\rho_w * Ka * Kw}{(1-\epsilon) * \rho_F * \mu_w} * \frac{\partial^2 P_w}{\partial z^2} \quad (20)$$

Write  $\partial MR/\partial t$  as  $(\partial MR/\partial L) * (\partial L/\partial t)$  and when  $S = 1$ ,  $\partial MR/\partial L = \rho_w/BW$  where  $BW$  is the sheet basis weight. With  $BW/L = (1-\epsilon) * \rho_F$  and  $Kw = 1$  when  $S = 1$ , Eq. (20) becomes

$$\frac{1}{L} * \frac{\partial L}{\partial t} = \frac{Ka}{\mu_w} * \frac{\partial^2 P_w}{\partial z^2} \quad (21)$$

Let

$$P_w = A_1 + A_2 * z + A_3 * z^2 \quad (22)$$

so that

$$\frac{\partial P_w}{\partial z} = A_2 + 2 * A_3 * z \quad (23)$$

and

$$\frac{\partial^2 P_w}{\partial z^2} = 2 * A_3 \quad (24)$$

At  $z = 0$ ,  $\partial P_w/\partial z = 0$  and therefore  $A_2 = 0$ . Integrating Eq. (22) from  $z = 0$  to  $z = L$  and noting that at  $z = L$   $\partial P_w/\partial z = 2 * A_3 * L$  and  $P_w = P_{atm}$  (the ambient pressure) allows a calculation of  $A_1$  and  $A_3$  to yield:

$$P_w = P_{atm} + \frac{\mu_w * (z^2 - L^2)}{2 * Ka * L} * \frac{\partial L}{\partial t} \quad (25)$$



For simplicity, define an integral-average hydraulic pressure such that

$$\overline{P_w} = P_{atm} - \frac{\mu_w * L}{3 * K_a} * \frac{\partial L}{\partial t} \quad (26)$$

and use  $P = P_{mech} - \overline{P_w}$  in the compression equation, where  $P_{mech}$  is the absolute applied mechanical pressure. The applied mechanical pressure is the sum of  $P_{mechg}$  (the gage mechanical pressure) and ambient pressure and therefore

$$P = P_{mechg} + \frac{\mu_w * L}{3 * K_a} * \frac{\partial L}{\partial t} \quad (27)$$

With  $C = M * P^N = BW/L$  and  $K_a = 1/(R * C)$  then

$$\frac{\partial L}{\partial t} = \frac{3 * ((C/M)^{1/N} - P_{mechg})}{\mu_w * BW * R} \quad (28)$$

$R$ , the specific filtration resistance, is a function of  $P_{mechg}$ ;  $P_{mechg}$  is a prescribed function of time, so Eq. (28) is an initial value problem solvable by standard numerical techniques once  $L$  at  $t = 0$  is specified.

#### Zone Thermal Energy Equation

Consider a one-dimensional energy equation where energy is transferred only by conduction or convection. Using the same kinds of manipulation as in the continuity equation gives:

$$\begin{aligned} \frac{\partial}{\partial t} (D_c * T) = & - \frac{\partial}{\partial z} (-K * \frac{\partial T}{\partial z} \\ & + (D_c * V_f + \rho_w * C_{pw} * V_w + \rho_v * C_{pv} * V_v) * T \end{aligned} \quad (29)$$

where  $T$  is temperature,  $K$  is thermal conductivity,  $C_{pw}$  and  $C_{pv}$  are the constant pressure specific heats of water and vapor, and where

$$Dc = \rho_F * (1-\epsilon) * Cpf + \rho_w * \epsilon * S * Cpw + \rho_v * \epsilon * (1-S) * Cpv \quad (30)$$

Cpf is the constant pressure specific heat of cellulose and with Eq. (15)

$$Dc = \rho_F * (1-\epsilon) * (Cpf + MR * Cpw) \quad (31)$$

Observe that  $Dc = b * D$  where

$$b = \frac{(Cpf + MR * Cpw)}{(1 + MR)} \quad (32)$$

Expand and rearrange Eq. (29) noting that  $b$  is independent of  $z$  within a given zone and use continuity Eq. (13) to simplify; divide by  $b * D$  to obtain

$$\begin{aligned} \frac{\partial T}{\partial t} + \frac{T}{b} * \frac{\partial b}{\partial t} + \frac{T}{D} * \frac{\partial}{\partial z} \left( \left( \frac{Cpw}{b} - 1 \right) * \rho_w * Vw + \left( \frac{Cpv}{b} - 1 \right) * \rho_v * Vv \right) = \\ \frac{K}{b * D} * \frac{\partial^2 T}{\partial z^2} - \left( Vf + \frac{\rho_w * Cpw * Vw}{b * D} + \frac{\rho_v * Cpv * Vv}{b * D} \right) * \frac{\partial T}{\partial z} \end{aligned} \quad (33)$$

For a nonsaturated medium  $\partial b / \partial t = 0$  ( $Cpf$  and  $Cpw$  held constant). Using the slug flow assumption and the approximation  $\rho_v * Cpv / (b * D) = 0$  gives

$$\frac{\partial T}{\partial t} = \frac{K}{b * D} * \frac{\partial^2 T}{\partial z^2} - Vf * \frac{\partial T}{\partial z} \quad (34)$$

for the nonsaturated heatup regime (with  $Vw = 0$  as before) and

$$\frac{\partial T}{\partial t} = \frac{K}{b * D} * \frac{\partial^2 T}{\partial z^2} - \left( Vf + \frac{\rho_w * Cpw * Vw}{b * D} \right) * \frac{\partial T}{\partial z} \quad (35)$$

for the saturated heatup regime and the saturated or nonsaturated outer zone during the transition regime. Equations (34) and (35) must be solved to yield the temperature profiles.

For the inner zone during transition and all zones during the quasi-static regime no energy equation is required, since all temperature gradients are assumed linear.

### Convective-Diffusion Equations

Two general methods available for the solution of Eq. (34) and (35) are transformation of variables and numerical solution. Transform Eq. (34) by defining  $x = z/L$  and  $t' = t$  so that  $\partial x / \partial z = 1/L$ ,  $\partial x / \partial t = -(z/L^2) * \partial L / \partial t$ ,  $\partial t' / \partial z = 0$ , and  $\partial t' / \partial t = 1$ . Thus,  $\partial T / \partial z = (1/L) * \partial T / \partial x$ ,  $\partial^2 T / \partial z^2 = (1/L^2) * \partial^2 T / \partial x^2$ , and  $\partial T / \partial t = \partial T / \partial t' - (z/L^2) * \partial L / \partial t * \partial T / \partial x$ . Since  $V_f = (z/L) * \partial L / \partial t$ , substitution converts Eq. (34) to

$$\frac{\partial T}{\partial t'} = \psi * \frac{\partial^2 T}{\partial x^2} \quad (36)$$

where

$$\psi = \frac{K}{b * D * L} \quad (37)$$

The initial condition is  $T = T_I$  at  $t' = 0$  for all  $x$ . The boundary conditions are:  $BI * (T_H - T) = -\partial T / \partial x$  at  $x = 0$  and  $\partial T / \partial x = 0$  at  $x = 1$ . The first BC is a statement of the imperfect thermal contact between the hot surface and sheet with  $BI = H_c * L / K$ . The second BC is the assumption of no conductive heat flux from the sheet to the felt.

Equation (35) requires different transformations depending on its application to the saturated heatup or saturated or nonsaturated transition regimes. For the saturated heatup regime continuity demands  $V_w = -(z/L) * \partial L / \partial t$ . The same transformation of variables as for Eq. (34) gives

$$\frac{\partial T}{\partial t'} = \psi * \frac{\partial^2 T}{\partial x^2} + \phi * \frac{\partial T}{\partial x} \quad (38)$$

with  $\psi$  as in Eq. (37) and

$$\phi = - \frac{\rho_w * C_{pw} * x}{b * D * L} * \frac{\partial L}{\partial t'} \quad (39)$$

The initial and boundary conditions are the same as before.

The application of Eq. (35) to the outer zone during transition requires a different transformation. The outer zone is designated as zone 3 and is bounded by interfaces 1 and 3 or 2 and 3. Define  $x = (z - L_2 - L_1)/L_3$  and  $t' = t$  so that  $\partial x / \partial z = 1/L_3$ ,  $\partial x / \partial t = -(\partial L_1 / \partial t + \partial L_2 / \partial t + x * \partial L_3 / \partial t) / L_3$ , and again  $\partial t' / \partial z = 0$  and  $\partial t' / \partial t = 1$ .  $L_1$ ,  $L_2$ , and  $L_3$  are the thicknesses of zones 1, 2, and 3. Substitution into Eq. (35) yields an equation of the form of Eq. (38) with

$$\psi = \frac{K}{b * D * L_3} \quad (40)$$

and

$$\phi = \frac{\rho_w * C_{pw} * V_w}{b * D * L_3} \quad (41)$$

The value of  $V_w$  is uniform in zone 3 by the slug flow assumption and is calculated using Darcy's law (with the pressure gradient given by the vapor pressure drop across zone 3). The initial condition for this case is the temperature distribution just after the heatup regime. The boundary conditions are that the heat conducted to interface 1 or 2 is just balanced by the sum of the heat conducted into zone 3 and a "source" or "sink" term composed of the latent heat and the net condensation or evaporation at interface 1 or 2. The other boundary condition is that there is no net conductive heat flux past interface 3.

A numerical scheme is needed to solve Eq. (38). A stable, high-order accuracy, finite difference method is available which uses weighted finite differences to overcome calculational instabilities.<sup>65</sup> This method also removes some severe restrictions on the time step-grid spacing combination typical of other convective-diffusion numerical solutions. The second spatial derivative is treated as a central difference:

$$\frac{\partial^2 T}{\partial x^2} = \frac{T(i+1,j) - 2 * T(i,j) + T(i-1,j)}{\Delta x^2} \quad (42)$$

where  $\Delta x$  is the grid spacing,  $i$  is the grid number ( $i = 1$  to  $i = k$ ), and  $j$  is the time increment number. The time derivative is treated as a forward difference:

$$\frac{\partial T}{\partial t'} = \frac{T(i,j+1) - T(i,j)}{\Delta t} \quad (43)$$

where  $\Delta t$  is the time increment. The temperature gradient is treated as an upstream weighted difference. Since  $\phi > 0$  for the outer zone cases considered in this thesis,

$$\frac{\partial T}{\partial x} = \frac{2 * T(i+1,j) + 3 * T(i,j) - 6 * T(i-1,j) + T(i-2,j)}{6 * \Delta x} \quad (44)$$

Equations 42 through 44 are combined to give

$$\begin{aligned} T(i,j+1) = & (A - B/3) * T(i+1,j) + (1 - 2 * A - B/2) * T(i,j) \\ & + (A + B) * T(i-1,j) - (B/6) * T(i-2,j) \end{aligned} \quad (45)$$

where

$$A = \frac{\psi * \Delta t}{\Delta x^2} \quad (46)$$

and

$$B = \frac{\phi * \Delta t}{\Delta x} \quad (47)$$

and HIDRYER1 maintains

$$\Delta t < \frac{\Delta x}{2 * \psi / \Delta x + \phi / 2} \quad (48)$$

Equation 45 applies from  $i = 3$  to  $i = k-1$ . At  $i = 2$ , a central difference operator is used for  $\partial T / \partial x$  to give

$$\begin{aligned} T(2,j+1) &= (A - B/2) * T(3,j) + (1 - 2 * A) * T(2,j) \\ &+ (A + B/2) * T(1,j) \end{aligned} \quad (49)$$

At the boundaries  $i = 1$  and  $i = k$  the operative equation is derived by integrating the energy equation over a half interval.<sup>66</sup> At  $x = 0$ , integrate from 0 to  $\Delta x/2$  to obtain:

$$\frac{\Delta x}{2} * \frac{\partial T}{\partial t'(avg)} = \psi * \left. \frac{\partial T}{\partial x} \right|_0^{\Delta x/2} - \bar{\phi} * T \Big|_0^{\Delta x/2} \quad (50)$$

$\bar{\phi}$  and  $\partial T / \partial t'(avg)$  are averages over the half interval such that

$$\bar{\phi} = \frac{\phi(\Delta x/2) + \phi(0)}{2} \quad (51)$$

and

$$\frac{\partial T}{\partial t'(avg)} = \frac{1}{2} * \left( \frac{\partial T}{\partial t'(\Delta x/2)} + \frac{\partial T}{\partial t'(0)} \right) \quad (52)$$

Let

$$\frac{\partial T}{\partial t'(\Delta x/2)} = \frac{1}{2} * \left( \frac{\partial T}{\partial t'(\Delta x)} + \frac{\partial T}{\partial t'(0)} \right) \quad (53)$$

so that

$$\frac{\partial T}{\partial t'(\text{avg})} = \frac{1}{4} * \left( \frac{\partial T}{\partial t'(\Delta x)} + 3 * \frac{\partial T}{\partial t'(0)} \right) \quad (54)$$

and Eq. (33) can be used to find the time derivatives at  $x = \Delta x$  and  $x = 0$ .

Let

$$\frac{\partial T}{\partial x(\Delta x/2)} = \frac{1}{2} * \left( \frac{\partial T}{\partial x(\Delta x)} + \frac{\partial T}{\partial x(0)} \right) \quad (55)$$

Apply the boundary condition  $BI*(TH - T(1,j)) = -\partial T/\partial x(0)$  and

$$\frac{\partial T}{\partial x(0)} = \frac{2}{\Delta x} * T \Big|_0^{\Delta x/2} \quad (56)$$

to get  $T(\Delta x/2)$ . Let

$$\frac{\partial T}{\partial x(\Delta x)} = \frac{-2 * T(1,j) - 3 * T(2,j) + 6 * T(3,j) - T(4,j)}{6 * \Delta x} \quad (57)$$

to get

$$\begin{aligned} T(1,j+1) = & T(1,j) - (T(2,j+1) - T(2,j))/3 \\ & + 4 * B * BI * \Delta x * (TH - T(1,j))/3 + (2 * A/9) * (6 * BI * \Delta x \\ & * (TH - T(1,j)) - 2 * T(1,j) - 3 * T(2,j) + 6 * T(3,j) - T(4,j)) \end{aligned} \quad (58)$$

At the cold side, integrate from  $x = 1 - \Delta x/2$  to  $x = 1$ . Apply the boundary condition  $\partial T/\partial x(1) = 0$  and use similar averaging techniques to get

$$\begin{aligned} T(k,j+1) = & T(k,j) - (T(k-1,j+1) - T(k-1,j))/3 \\ & - (2*A/9) * (2 * T(k,j) + 3 * T(k-1,j) - 6 * T(k-2,j) + T(k-3,j)) \end{aligned} \quad (59)$$

Observe that when  $\phi = 0$  Eq. (45), (49), (58), and (59) are solutions of Eq. (36) and so all cases are covered.

As  $\delta_2$  and  $\delta_3$  move into the sheet, a modification of the numerical method is employed. The first grid point in the transition zone is designated as  $i'$ . The last grid point of the transition zone is designated as  $i''$ .  $\delta'$  and  $\delta''$  are the distances of these points from the origin. Because the distance between these special grid points and the interfaces closest to them may not correspond to the usual grid point spacing, temperatures at  $i'$ ,  $i''$ , and the grid points adjacent to them must be calculated based on uncentered finite differences.

Taylor series expansions for the temperatures at the grid points around the one in question can be added, subtracted, and combined to give

$$\begin{aligned} T(i', j + 1) = & T(i', j) - \phi * \Delta t * (T(i' + 1, j) - T_x) / (\Delta x + \text{DIFF}') \\ & + 2 * \psi * \Delta t * (T(i' + 1, j) / (\Delta x * (\Delta x + \text{DIFF}')) \\ & - T(i', j) / (\Delta x * \text{DIFF}') + T_x / (\text{DIFF}' * (\Delta x + \text{DIFF}')) \end{aligned} \quad (60)$$

where  $T_x$  is either  $T_1$  or  $T_2$  depending on which interface is involved. The model treats the transition zone as if it were part of one large zone undergoing heating and compression. Instead of applying boundary conditions and calculating new temperatures for all the grid points, the model simply calculates the bounding interface temperatures from the interface equations and applies these temperatures directly. In terms of the relative (dimensionless) distance  $\Delta x$

$$\text{DIFF}' = \frac{BW_3 * (1 + BW_4/BW)}{BW} - \Delta x * (1 - i' + i'') \quad (61)$$

At the other end

$$\begin{aligned} T(i'', j + 1) = & T(i'', j) - \phi * \Delta t * (T_x - T(i'' - 1, j)) / (\Delta x + \text{DIFF}'') \\ & + 2 * \psi * \Delta t * (T_x / (\text{DIFF}'' * (\Delta x + \text{DIFF}'')) \\ & - T(i'', j) / (\Delta x * \text{DIFF}'') \\ & + T(i'' - 1, j) / (\Delta x * (\Delta x + \text{DIFF}'')) \end{aligned} \quad (62)$$



where

$$\text{DIFF}'' = \Delta x - \frac{\text{BW3} * \text{BW4}}{\text{BW}} \quad (63)$$

and  $T_x$  is either  $T_2$  or  $T_3$ . The new temperature at  $i'+1$  is found from Eq. (49). If  $\text{DIFF}'$  is equal to  $\Delta x$  or if the interface advances across a grid point, then Eq. (49) is also used at  $i'$  and Eq. (60) is bypassed. All other interior points are calculated with Eq. (45), but the temperature at  $i''$  is found with Eq. (62) if  $\text{DIFF}''$  is less than  $\Delta x$  and the interface does not cross a grid point.

### Interface Equations

During the high intensity drying process zones of different moisture content develop inside the sheet. These zones are bounded by interfaces at various temperatures. The temperatures determine the rates of heat transfer and rates of change of interface position; since the interfaces separate zones of different moisture content, their positions are directly related to the overall sheet moisture content. Refer to Fig. 10 for the zones that may be present and the terminology for the zones, interfaces, and temperatures.

The "dry" zones contain water vapor. Zone 2 contains liquid water only inside the fibers. Zone 3 contains liquid water inside and outside the fibers.

Consider a "general" interface. Heat, liquid, and gas (vapor only) flow toward the interface on the (-) side close to the hot surface and flow away from the interface on the (+) side toward the felt. The net mass flux results in a change in interface position and is calculated from

$$(\rho_w * V_w(+)) - \rho_w * V_w(-)) + (\rho_v * V_v(+)) - \rho_v * V_v(-)) = \epsilon * S * \rho_w * d\delta/dt \quad (64)$$

for interfaces 1 and 2 and

$$\rho_w * Vw(-) - (\rho_v * Vv(+) - \rho_v * Vv(-)) = \epsilon * S * \rho_w * d\delta/dt \quad (65)$$

at interface 3. There is no liquid flow on the (+) side of interface 3 (unless  $\delta_3 = \delta_T$ ) because any flow past  $\delta_3$  would be absorbed by the dry fibers in zone 4.

An energy balance gives

$$Q(-) = Q(+) + (\rho_v * Vv(+) - \rho_v * Vv(-)) * (\Delta h + \Delta h^*) \quad (66)$$

at interfaces 1 and 2; at interface 3 the energy balance gives

$$Q(-) = (\rho_v * Vv(+) - \rho_v * Vv(-)) * (\Delta h + \Delta h^*) \quad (67)$$

where  $\Delta h^*$  is the average heat of desorption at the interface.

#### Heatup and Transition Regimes

During the heatup regime there is only one zone (2 or 3) present, since the sheet starts and stays at uniform saturation. Interface 1 is at  $z = 0$ . Interface 2 is at  $\delta_T$  if zone 2 is present and at  $z = 0$  if zone 3 is present. Interface 3 is at  $\delta_T$ . It is assumed that no evaporation takes place during heatup.

When TS is raised incrementally above the saturation temperature corresponding to the hydraulic pressure at  $z = 0$ , the liquid in the pores of the sheet sees the apparent pressure gradient corresponding to the vapor pressures at TS and TB. The liquid is assumed to flow in slug flow, and  $\delta_2$  defines the limit of thermodynamic saturation (and linear temperature gradient) so that no vapor flows past  $\delta_2$  in transition. For the first time increment the only nonzero term of Eq. (64) is  $\rho_w * Vw(+)$ . By assumption, the vapor and liquid pressures are identical and Darcy's law for the flowing liquid is

$$Vw = - \frac{Ka3 * Kw}{\mu_w} * \frac{\partial Pv}{\partial z} \quad (68)$$

where  $Ka3$  is the absolute permeability of zone 3. To link the mass and energy balance equations write  $\partial Pv/\partial z$  as  $(\partial Pv/\partial T) * (\partial T/\partial z)$ . The correct expression for  $\partial T/\partial z$  is  $(TB - TS)/\delta_T$ , the virtual gradient that the liquid experiences. Then, from Eq. (64) and (68)

$$\rho_w * KAKW * \frac{\partial Pv}{\partial T} * \frac{(TS - TB)}{(\mu_w * \delta_T)} = \epsilon' * S' * \rho_w * D2 \quad (69)$$

where  $KAKW = Ka3 * Kw$ ,  $\epsilon'$  and  $S'$  are the interfiber porosity and saturation (since only interfiber water flows), and  $D2$  is the rate of change of position of  $\delta_2$  due only to vapor-induced liquid flow. This rate multiplied by  $BW * \Delta t/\delta_T$  gives an increment in the basis weight of zone 2 and a corresponding decrement in the basis weight of zone 3. The increment or decrement is added to the old value of zone basis weight to get a new value at  $TIME(new) = TIME(old) + \Delta t$ . The liquid properties are evaluated at  $TS$ .

If no interfiber water exists, the transition regime is simply a continuation of the heatup regime calculation until the temperature at  $\delta_T$  is raised incrementally above  $TB$ . Then, a dry zone propagates into the sheet toward the hot surface. This case is treated later.

After the first time increment, two cases can occur:  $\delta_1$  and  $\delta_2$  are either equal or they are unequal. When  $\delta_1 = \delta_2$  the only nonzero term in Eq. (64) is  $\rho_w * Vw(+)$ . Since no vapor flows  $Q(-) = Q(+)$ , where  $Q(-) = U * (TH - T2)$  and  $Q(+) = K3 * (T2 - T')/(\delta' - \delta_2)$ .  $U$  is defined so that  $1/U = 1/Hc + \delta_2/K1$ .  $T'$  is the temperature at the first finite difference grid point in zone 3,  $\delta'$  is the distance of this grid point from the origin, and  $K1$  and  $K3$  are the thermal conductivities of zones 1 and 3. From the heat balance, a new value for  $T2$  is isolated as

$$T_2 = \frac{T_H + I * T'}{1 + I} \quad (70)$$

where

$$I = \left( \frac{1}{H_c} + \frac{\delta_2}{K_1} \right) * \left( \frac{K_3}{\delta_1 - \delta_2} \right) \quad (71)$$

Of course, when  $\delta_1 = \delta_2$ ,  $T_1 = T_2$ . The mass balance gives the rate of advance of interface 2 using Eq. (69) with the (virtual) temperature gradient  $(T_2 - T_3)/(\delta_3 - \delta_2)$ . If  $\delta_3 = \delta_T$  then  $T_B$  is used in place of  $T_3$ .

If  $\delta_1$  and  $\delta_2$  are not equal, then equations are needed at both interfaces. At  $\delta_1$ ,  $\rho_v * V_v(+)$  is the only nonzero mass flow term. Thus,

$$\rho_v * \frac{K a_2}{\mu_v} * \frac{\partial P_v}{\partial T} * \frac{(T_1 - T_2)}{(\delta_2 - \delta_1)} = \epsilon_2 * S_2 * \rho_w * D_4 \quad (72)$$

$D_4$  is the rate of advance of  $\delta_2$  due solely to evaporation.  $\epsilon_2$  and  $S_2$  are the porosity and saturation of zone 2. Vapor properties are evaluated at  $T_1$  and  $T_2$  and then averaged. In the heat balance,  $Q(-) = U * (T_H - T_1)$  and  $Q(+) = K_2 * (T_1 - T_2)/(\delta_2 - \delta_1)$ . Isolating for  $T_1$  gives

$$T_1 = \frac{T_H + I * T_2}{1 + I} \quad (73)$$

where

$$I = \left( \frac{1}{H_c} + \frac{\delta_1}{K_1} \right) * \frac{1}{(\delta_2 - \delta_1)} * \left( \frac{\rho_v * K a_2 * (\Delta h + \Delta h^*)}{\mu_v} * \frac{\partial P_v}{\partial T} + K_2 \right) \quad (74)$$

The vapor properties, except  $\Delta h$ , are averaged using  $T_1$  and  $T_2$ .  $\Delta h$  is evaluated at  $T_1$  only and  $\Delta h^*$  is the latent heat correction factor based on the moisture ratios of zones 1 and 2.

At  $\delta_2$ ,  $\rho_w * Vw(+)$  and  $\rho_v * Vv(-)$  are the mass flow terms.  $\rho_v * Vv(-)$  at  $\delta_2$  is just  $\rho_v * Vv(+)$  at  $\delta_1$ .  $\rho_w * Vw(+)$  is derived as for Eq. (68) and (69) so that

$$\frac{\rho_w * KAKW * (T2 - T3)}{\mu_w * (\delta_3 - \delta_2)} * \frac{\partial P_v}{\partial T} - \frac{\rho_v * Ka2 * (T1 - T2)}{\mu_v * (\delta_2 - \delta_1)} * \frac{\partial P_v}{\partial T} = \epsilon' * S' * \rho_w * D5 \quad (75)$$

D5 is the net rate of motion of  $\delta_2$ . Vapor and liquid properties are averaged with T2 and T3 or T1 and T2 as appropriate. In the heat balance, Q(-) is the same as Q(+) at  $\delta_1$ .  $Q(+) = K3 * (T2 - T') / (\delta' - \delta_2)$ , so that

$$T2 = \frac{II * T1 + T'}{1 + II} \quad (76)$$

where

$$II = \left( \frac{K2}{K3} + \frac{\rho_v * Ka2 * (\Delta h + \Delta h^*)}{\mu_v * K3} * \frac{\partial P_v}{\partial T} \right) * \frac{(\delta' - \delta_2)}{(\delta_2 - \delta_1)} \quad (77)$$

The vapor properties are evaluated in the usual way. Equations (73) and (76) then yield

$$T1 = \frac{(1 + II) * TH + I * T'}{1 + I + II} \quad (78)$$

$$T2 = \frac{II * TH + (1 + I) * T'}{1 + I + II} \quad (79)$$

HIDRYER1 calculates T' and then finds T1 and T2.

If  $\delta_3 = \delta_T$  and T3 is equal to TB then

$$\frac{K3}{\Delta h + \Delta h^*} * \frac{(T3 - T'')}{\Delta x} = \epsilon_3 * S3 * \rho_w * D6 \quad (80)$$

where  $T''$  is the temperature of the first finite difference grid point just toward the origin relative to  $\delta_3$ . If  $T_3$  is less than  $T_B$  then  $D_6 = 0$ .

The liquid mass flow to  $\delta_3$  is given by the first term of Eq. (75) so that

$$\epsilon' * S' * D_2 = \epsilon_3 * S_3 * D_7 \quad (81)$$

The net change in the position of  $\delta_3$  is determined by the sum of  $D_6$  and  $D_7$ . The new value of  $T_3$  comes from the finite difference temperature calculations.

If  $\delta_3$  is not equal to  $\delta_T$  then

$$\frac{\rho_v * Ka_4 * (T_3 - T_B)}{\mu_v * (\delta_T - \delta_3)} * \frac{\partial P_v}{\partial T} = - \epsilon_3 * S_3 * \rho_w * D_6 \quad (82)$$

and Eq. (81) still applies. The heat balance yields

$$T_3 = \frac{T'' + III * T_B}{(1 + III)} \quad (83)$$

where

$$III = \frac{\rho_v * Ka_4 * (\Delta h + \Delta h^*)}{\mu_v * K_3} * \frac{\partial P_v}{\partial T} * \frac{(\delta_3 - \delta'')}{(\delta_T - \delta_3)} \quad (84)$$

$\delta''$  is the distance of the  $T''$  grid point from the origin. HIDRYER1 calculates  $T''$  and then  $T_3$ .

Once the interface temperatures have been calculated, the change in interface position (zone basis weight) is performed. The rate of change of basis weights is found from:

$$DBW1DT = RATE1 * BW1/L1 \quad (85)$$

$$DBW2DT = RATE2 * BW3/L3 - DBW1DT \quad (86)$$

$$DBW3DT = (RATE3 - RATE2) * BW3/L3 \quad (87)$$

$$DBW4DT = -RATE3 * BW3/L3 \quad (88)$$

where RATE1 is either 0 or D4, RATE2 is either D2 or D5, and RATE3 is the sum of D6 and D7. These are multiplied by  $\Delta t$  and added to the old basis weight values to get new values. The temperatures at the new positions are calculated and the cycle continues.

If no interfiber water exists at the end of heatup, the transition regime is a continuation of heatup until the temperature at  $\delta_T$  is raised incrementally above TB.  $\delta_2$  moves into the sheet toward the hot surface. There is no liquid flow term and all evaporation occurs at  $\delta_2$ . Equation (82) is applicable with T3 replaced by T2,  $\delta_3$  by  $\delta_2$ , and  $\epsilon_3$  and S3 by  $\epsilon_2$  and S2. T2 is calculated by Eq. (83) with appropriate substitutions.

#### Linear Regime

The linear (quasi-static) regime begins when  $\delta_2 = \delta_3$  (if interfiber water is present) or when all the temperature gradients in the outer zone become linear due to heat transfer. Vapor can flow through all zones in this regime. Several possible cases exist. If  $\delta_1 = \delta_2$  and  $\delta_3$  is not equal to  $\delta_T$  then the heat balance gives:

$$T2 = \frac{(1 + I) * TH + II * TB}{1 + I + II} \quad (89)$$

$$T3 = \frac{I * TH + (1 + II) * TB}{1 + I + II} \quad (90)$$

where

$$I = \frac{\frac{K3}{\Delta h + \Delta h^*} + \frac{\rho_v * KAKV}{\mu_v} * \frac{Pv}{\partial T}}{\frac{\rho_v * Ka4}{\mu_v} * \frac{\partial Pv}{\partial T}} * \frac{(\delta_T - \delta_3)}{(\delta_3 - \delta_2)} \quad (91)$$

$$II = \left( \frac{1}{H_c} + \frac{\delta_2}{K1} \right) * \left( \frac{1}{\delta_3 - \delta_2} \right) * \left( K3 + \frac{\rho_v * KAKV * (\Delta h + \Delta h^*)}{\mu_v} \right) * \frac{\partial P_v}{\partial T} \quad (92)$$

and  $KAKV = Ka3 * Kv$ . The vapor properties in II and the numerator of I are evaluated using T2 and T3. The latent heat term in I is evaluated at T3 and corrected using the moisture ratios of zones 3 and 4. The latent heat term in II is evaluated at T2 and corrected using the moisture ratios of zones 1 and 3. The vapor properties in the denominator of I are evaluated using T3 and TB.

If  $\delta_1$  is not equal to  $\delta_2$  and  $\delta_3$  is not equal to  $\delta_T$  then

$$T1 = \frac{(1 + IV) * TH + I * TB}{1 + I + IV} \quad (93)$$

$$T2 = \frac{IV * TH + (1 + I) * TB}{1 + I + IV} \quad (94)$$

$$T3 = \frac{II * III * TH + (1 + I + II) * TB}{1 + I + IV} \quad (95)$$

where I is given by Eq. (74) and

$$II = \frac{\frac{K2}{\Delta h + \Delta h^*} + \frac{\rho_v * Ka2}{\mu_v} * \frac{\partial P_v}{\partial T}}{\frac{K3}{\Delta h + \Delta h^*} + \frac{\rho_v * KAKV}{\mu_v} * \frac{\partial P_v}{\partial T}} * \frac{(\delta_3 - \delta_2)}{(\delta_2 - \delta_1)} \quad (96)$$

$$III = \frac{\frac{K3}{\Delta h + \Delta h^*} + \frac{\rho_v * KAKV}{\mu_v} * \frac{\partial P_v}{\partial T}}{\frac{\rho_v * Ka4}{\mu_v} * \frac{\partial P_v}{\partial T}} * \frac{(\delta_T - \delta_3)}{(\delta_3 - \delta_2)} \quad (97)$$



and  $IV = II * (1 + III)$ . Vapor properties in the numerator of II are evaluated with  $T1$  and  $T2$ . The latent heat in II is at  $T2$  and the correction is made with the moisture ratios of zones 2 and 3. The vapor properties in the denominator of II and the numerator of III are evaluated with  $T2$  and  $T3$ ; the denominator of III is evaluated with  $T3$  and  $TB$ . The latent heat term is at  $T3$  and corrected with the moisture ratios of zones 3 and 4.

If  $\delta_1$  is not equal to  $\delta_2$  and zone 3 does not exist, then

$$T1 = \frac{(1 + I) * TH + II * TB}{1 + I + II} \quad (98)$$

$$T2 = \frac{I * TH + (1 + II) * TB}{1 + I + II} \quad (99)$$

where

$$I = \frac{\frac{K2}{\Delta h + \Delta h^*} + \frac{\rho_v * Ka2}{\mu_v} * \frac{\partial P_v}{\partial T}}{\frac{\rho_v * Ka4}{\mu_v} * \frac{\partial P_v}{\partial T}} * \frac{(\delta_T - \delta_2)}{(\delta_2 - \delta_1)} \quad (100)$$

and II is given by Eq. (74). Vapor properties in the numerator of I are evaluated with  $T1$  and  $T2$ . The latent heat is at  $T2$  and corrected with the moisture ratios of zones 2 and 4. The vapor properties in the denominator of I are evaluated with  $T2$  and  $TB$ .

The mass transfer terms for the linear regime are similar to those previously outlined for the transition regime with the additional consideration that when  $\delta_1 = \delta_2$  there may be evaporation and flow of vapor. The mass transfer equations that apply when  $\delta_1 = \delta_2$  are

$$\rho_v * \frac{KAKV}{\mu_v} * \frac{\partial P_v}{\partial T} * \frac{(T_2 - T_3)}{(\delta_3 - \delta_2)} = \epsilon_3 * S_3 * \rho_w * D1 \quad (101)$$

$$\rho_w * \frac{KAKW}{\mu_w} * \frac{\partial P_v}{\partial T} * \frac{(T_2 - T_3)}{(\delta_3 - \delta_2)} = \epsilon' * S' * \rho_w * D2 \quad (102)$$

$$\rho_v * \frac{KAKV}{\mu_v} * \frac{\partial P_v}{\partial T} * \frac{(T_2 - T_3)}{(\delta_3 - \delta_2)} = \epsilon_2 * S_2 * \rho_w * D3 \quad (103)$$

where D1 represents the evaporation of interfiber and intrafiber water, D2 is the slug flow of interfiber water, and D3 is the evaporation of intrafiber water accompanying D2. HIDRYER1 selects the larger of D1 or D2 (or D1 if they are equal) as the rate of advance. If D1 is equal to or larger than D2,  $\delta_1$  and  $\delta_2$  move according to D1. If D2 is larger,  $\delta_2$  moves according to D2 and  $\delta_1$  moves according to D3.

When  $\delta_1$  is not equal to  $\delta_2$ , the mass balance gives

$$\rho_v * \frac{Ka2}{\mu_v} * \frac{\partial P_v}{\partial T} * \frac{(T_1 - T_2)}{(\delta_2 - \delta_1)} = \epsilon_2 * S_2 * \rho_w * D4 \quad (104)$$

which is the evaporation of intrafiber water at  $\delta_1$  and

$$\rho_v * \frac{KAKV}{\mu_v} * \frac{\partial P_v}{\partial T} * \frac{(T_2 - T_3)}{(\delta_3 - \delta_2)} = \epsilon' * S' * \rho_w * D5 \quad (105)$$

which is the evaporation of interfiber liquid at  $\delta_2$ . The expression for D2 also applies at  $\delta_2$  and HIDRYER1 selects the larger of D2 or D5 as the rate of advance of  $\delta_2$ .

At  $\delta_3$

$$\frac{-K3}{(\Delta h + \Delta h^*)} * \frac{(T2 - T3)}{(\delta_3 - \delta_2)} = \epsilon_3 * S3 * \rho_w * D6 \quad (106)$$

and Eq. (81) also applies. Note that if D1 or D5 is greater than D2 then D2 is set = 0 and so D7 = 0.  $\delta_3$  is advanced according to the sum of D6 and D7.

In the special case where zone 3 is not present, the expression for D4 is used to advance  $\delta_1$  and

$$\frac{-K2}{(\Delta h + \Delta h^*)} * \frac{(T1 - T2)}{(\delta_2 - \delta_1)} = \epsilon_2 * S2 * \rho_w * D8 \quad (107)$$

is used for  $\delta_2$ .

The size of the time increment used depends on the magnitudes of D1, D2, etc.  $\delta_1$  can never pass  $\delta_2$ , and  $\delta_2$  can never pass  $\delta_3$ . H1DRYER1 calculates the largest time increment which will not violate the interface position criterion or the finite difference stability criterion and compares it to DT0, the default time increment. The smaller of the two is chosen and used.

Because the interface temperature calculations involve vapor and liquid properties whose values depend on the temperatures, an iterative procedure is used such that a temperature is calculated and averaged with the previous temperature to obtain an updated value. The updated value is used for property calculations, and a new temperature is determined. The new temperature is averaged with the previously updated one and the cycle continues for a fixed number of iterations.

## SUPPLEMENTARY RELATIONSHIPS

The following relationships are in the form of correlations which yield the required quantity, given an original input parameter or a value calculated in a previous step of the program.

### Applied Mechanical Pressure

The nature of the applied mechanical pressure is specified in the form of input parameters. The peak pressure and time to achieve that pressure are required. HIDRYER1 offers the option of either a ramp-and-hold pressure pulse or a pulse that duplicates a press nip. The ramp-and-hold pulse rises linearly with time to the peak pressure value and maintains pressure at the peak value until drying is complete (at a final moisture content of 6%). An extremely short rise time mimics a step change in pressure.

The press-nip pulse uses a sinusoidal function to create a symmetrical pressure pulse that achieves its peak value at the input rise time. Thus, the "nip residence time" is twice the input rise time. HIDRYER1 terminates when the moisture content reaches its target value or when the nip residence time is exceeded.

The functional forms for the pressure options are:

$$P = A1 + A2 * \frac{TIME}{RISTIM} \quad (108)$$

and

$$P = A1 + \frac{A2}{2} * (1 + \sin(\frac{A3 * TIME}{RISTIM} + A4)) \quad (109)$$

where A1 is some small but finite pressure value (contact pressure at time zero) required for the compressibility equation; A2 is the peak pressure, which is an

input parameter; A3 is the numerical constant  $\pi$  multiplied by 3600; and A4 is the numerical constant  $\pi$  multiplied by 1.5. The factor of 3600 is required since HIDRYER1 calculates TIME in hours and RISTIM, the time required to achieve the peak pressure, is specified in seconds.

Typical RISTIM values are on the order of 0.05 second. A1 is arbitrarily given the value of 0.7 kPa (0.1 psi), and A2 is specified in the input conditions.

### Physical Properties

The vapor and liquid physical properties are derived by modeling steam table data with a multiple regression analysis program over the range from 0 to 232°C (32 to 450°F).<sup>67</sup> The functional form for the properties is:

$$\text{PROP} = B1 + T * (B2 + T * (B3 + T * (B4 + T * B5))) \quad (110)$$

where PROP is the property to be determined (latent heat, specific volume, etc.) and T is the temperature.

### Latent Heat Correction Factor

The hygroscopic nature of cellulose requires that an additional quantity of energy above that of the latent heat (at a given temperature) be supplied during drying. This quantity is usually treated as a correction factor to the latent heat. Data on vapor pressure reduction in the presence of cellulose can be used to calculate the incremental heat of desorption at a given moisture ratio and temperature. Available data from<sup>68</sup> have been used to derive a functional relationship for the incremental heat of desorption over the range of 65 to 80°C (149 to 176°F) from moisture ratios of 0.01 up to 0.24.<sup>69</sup> Above moisture ratios of 0.24 the heat of desorption becomes infinitesimal relative to the latent heat.

The correlation has the form:

$$\Delta h' = C1 * \exp(C2 * MR) \quad (111)$$

where  $\Delta h'$  is the heat of desorption, C1 has a value of 1157.5 kJ/kg (497.63 BTU/lbm), and C2 has a value of -14.9522.

Because HIDRYER1 assumes a step change in moisture ratio from one zone to the next, an integral-average latent heat increment at each interface is used as the correction factor and is defined by integrating Eq. (111) from the moisture ratio of one zone to the moisture ratio of the adjacent zone so that:

$$\Delta h^* = D1 * \frac{\exp(D2 * MR_i) - \exp(D2 * MR_f)}{MR_f - MR_i} \quad (112)$$

where D1 has a value of 77.4 kJ/kg (33.28 BTU/lbm) and D2 has a value of -14.9522.

### Thermal Conductivity

The thermal conductivity is evaluated using the parallel conductor model<sup>61,70</sup> and neglecting the contribution of vapor conductivity. The thermal conductivity is given by:

$$K = E1 * (1-\epsilon) + E2 * \epsilon * S \quad (113)$$

where E1 and E2 are the thermal conductivities of cellulose and water, 0.24 W/m-K (0.14 BTU/ft-hr-°F) and 0.682 W/m-K (0.394 BTU/ft-hr-°F), and are assumed constant.

### Contact Coefficient

The relationship for the contact coefficient between the sheet and the hot surface has the form:

$$H_c = F_1 * (1-\epsilon) + F_2 * \epsilon * S \quad (114)$$

where  $F_1$  is the contact coefficient for dry cellulose, obtained from data in,<sup>71</sup> that depends on the mechanical pressure<sup>72</sup> and  $F_2$  is a value typical of a boiling heat transfer coefficient between water and a flat plate that is on the order of  $5678 \text{ W/m}^2\text{-K}$  ( $1000 \text{ BTU/ft}^2\text{-hr-}^\circ\text{F}$ ).

### Compressibility

Mathematical descriptions of saturated sheet compression originate in the modeling of wet pressing. The sheet is modeled in one of three ways: a power law model relating the concentration of fibers to the mechanical pressure; a Kelvin body model describing the sheet thickness in terms of the applied pressure and certain viscoelastic constants; and a combination model using a power law to describe fiber bending and a time dependent expression for fiber compression.

Strictly speaking, a power law model applies only to an equilibrium condition and not to a dynamic compression case. However, modification of the basic power law<sup>73,74</sup> to account for time dependent effects is possible.<sup>75</sup> A Kelvin body (spring and dashpot in parallel) exhibits a first order response to a step change in pressure and therefore only models flow-controlled pressing phenomena, which also exhibit a first order response.<sup>76</sup> The combination model treats fiber bending with a power law expression and models fiber compression as a rate process, since it is time dependent.<sup>77</sup> After short times (milliseconds), the rate of change of the fiber compression contribution is very small in comparison with the value of the bending contribution. Thus, it should be sufficient to describe the thickness in terms of just the bending term (power law) along with some slight correction which may amount to a nearly constant fraction of the bending term.

HIDRYER1 uses the power law compression model because it is the simplest and most easily modified model and because the most data are available for relating

its constants to commonly measured sheet properties such as freeness and basis weight. The form of the power law is:

$$C = M * p^N \quad (115)$$

The coefficients M and N vary with the degree of beating<sup>78,79</sup> and the moisture ratio of the sheet.<sup>79</sup> Data from,<sup>79</sup> although limited to pressures on the order of 7 kPa (1 psi), demonstrated that the power law describes the compression behavior of unsaturated sheets as well as saturated sheets. Using this information, expressions for evaluating M and N at different moisture ratios are obtained by multiple linear regression.<sup>80</sup> The form is:

$$COEFF = G1 + G2 * MR + \frac{G3}{MR + 1.5} + \frac{G4}{(MR + 1.5)^2} + \frac{G5}{MR + 1} + \frac{G6}{(MR + 1)^2} \quad (116)$$

where COEFF is either M or N and the values of G1 through G6 change depending on whether M or N is to be calculated and on the freeness of the pulp in the sheet.

To account for the dependence on refining, the values for the regression constants in Eq. (116) are determined for the same pulp at two available freeness levels<sup>79</sup> and fit to a parabola with an assumed minimum at a freeness of 100 CSF. (Below 100 CSF, M and N are held fixed at the 100 CSF values.) Thus, each constant in Eq. (116) is found from an expression of the form:

$$CONST = H1 + H2 * \frac{(CSF - H3)^2}{H4} \quad (117)$$

where CONST represents G1 through G6 and H1 through H4 change depending on which value of G is to be calculated.

The compressibility of a sheet is known to be highly temperature dependent. Data describing the overall gain in moisture removal by pressing at elevated



temperatures are available,<sup>23</sup> but no data are available on the specific changes in sheet compressibility constants. To account for this effect, the value of M calculated from Eq. (116) is (arbitrarily) multiplied by a function of the mean temperature of the zone such that:

$$M' = M * \left( \frac{TBAR}{TI} \right)^{I1} \quad (118)$$

where M' is the modified M value, TBAR is the average zone temperature, TI is the initial sheet temperature at which M and M' are identical, and I1 is an exponent less than unity (0.25 in HIDRYER1) so that the temperature effect moderates as TBAR increases.

A moist but unsaturated sheet can be brought to saturation if the mechanical pressure is high enough. To account for this observed behavior, the value of N is modified by making it a function of the effective mechanical pressure on the sheet. The effective mechanical pressure is the applied pressure minus the hydraulic pressure. Nsat, the value of N which would give a saturated sheet at a reference pressure equal to or greater than the peak pressure, is calculated and N becomes a function of this saturation value and the original value (Nref) calculated from Eq. (116) so that there is a smooth transition in the N value as effective pressure increases. N can never be greater than Nsat since the reference pressure is equal to or greater than the peak pressure. N can never be less than Nref since the pressure is never less than the A1 constant in the pressure function. The form is:

$$N = J1 + J2 * \left( \frac{P-J3}{J4} \right)^{J5} \quad (119)$$

where J1 and J2 depend on Nref and Nsat, and J3 and J4 depend on the value of the large reference pressure chosen. J5 is the reciprocal of an odd integer and

provides a smooth transition from  $N_{ref}$  to  $N_{sat}$  as effective mechanical pressure changes.<sup>81</sup>

### Permeability

The final supplementary relationship is that of permeability. Methods of characterizing permeability are based on theoretical or empirical relationships modeling permeability as a function of sheet porosity and/or fiber cross-sectional shape.<sup>63,82-85</sup> The empirical relationships are, of course, limited to the ranges of porosities and fiber types investigated. The theoretical approaches in this class are of limited applicability because the fiber is assumed to be of smooth (but not necessarily circular) cross sectional shape. Consequently, the theoretical relationships tend to predict permeabilities larger (by one or two orders of magnitude) than experimentally determined ones, except at high porosities and/or freenesses.

Paper fibers have many fibrils extending into the interfiber space. While the volume of the fibrils is generally small in comparison to the volume occupied by the bulk of the fiber, the effect of the fibrils on the flow properties is quite dramatic. The amount of fibrils depends on the extent to which the fiber has been physically degraded. Since Canadian Standard Freeness is a commonly performed test and gives a reasonable (but indirect) indication of the trend of the flow properties, it seems likely that a relationship between permeability and CSF would be both convenient and consistent with a model based on macroscopic trends.

An empirical linear relationship exists between  $\ln(\text{CSF})$  and the square root of specific filtration resistance<sup>86,87</sup> over a range of 100 to 700 CSF. The relationship has the form:

$$\ln(\text{CSF}) = K_1 + K_2 * \sqrt{R} \quad (120)$$

The calculated value of R is for a given pressure drop across the mat. Data at a variety of pressure drops on the order of 7 kPa (1 psi) and a broad range of freeness values define a family of curves of R vs. pressure drop whose shape is roughly independent of freeness.<sup>88</sup> Thus, by selecting some reference pressure (Pref) and the specific filtration resistance (Rref) at this pressure, a generalized relationship can be developed,<sup>72</sup> such as:

$$R = L_1 + L_2 * P + L_3 * \sqrt{P} \quad (121)$$

where L1 depends on Rref, and L2 and L3 depend on Rref and Pref. The pressure drop in a saturated flow experiment is equivalent to the effective mechanical pressure exerted on the mat, and the permeability is related to R by:

$$K_a = \frac{1}{R * C} \quad (122)$$

Therefore, there is a direct link between mechanical pressure and permeability (for a given CSF).

The permeability determined in saturated flow experiments is the absolute permeability; this is the permeability in the presence of only one flowing species. To adjust for the presence of two or more flowing species, the absolute permeability is generally multiplied by a correction factor called the relative permeability. Relative permeabilities vary between zero and unity and typical relationships are:<sup>89</sup>

$$K_w = S' M_1 \quad (123)$$

and

$$K_v = (1 + N_1 * S') * (1 - S')^{N_2} \quad (124)$$

where M1 is on the order of 4 and N1 and N2 are each on the order of 3. These relationships were developed for granular media. To be consistent with the

saturation concept for which they were developed, they are based here on the interfiber saturation of the paper, since it is the interfiber liquid (or intergranular liquid) that impedes the flow of vapor. This also makes them consistent with measurements of liquid relative permeability for paper at very low moisture ratios because below a critical but finite moisture ratio the liquid relative permeability becomes infinitesimally small.<sup>90</sup>

HIDRYER1 is organized so that the values for constants used in the supplementary relationships are grouped in DATA statements and/or COMMON statements. Therefore, modification of the model by changing the numerical value of a constant is a simple procedure. Most supplementary relationships are implemented in either the form of a SUBROUTINE or a FUNCTION so that changing the functional form also becomes simple. Refer to Appendix 1 for a detailed program listing.

#### MODEL VALIDATION

HIDRYER1 is the culmination of a series of drying models that began with a numerical implementation of the Ahrens model. First, the analytical solution to the Ahrens model was programmed to provide a reference for future comparisons. Next, the equations of the Ahrens model were programmed and solved numerically to duplicate the analytical result.<sup>91</sup> This numerical model was expanded by accounting for effects such as heat conduction into the outer zone, the influence of permeability on interface temperature, vapor-pressure-induced liquid flow, and an initial heatup period. At each stage of development, the model's predictions were compared to the previous version of the model to demonstrate that the advanced case reduced to the simpler case if conditions consistent with the less stringent assumptions were introduced into the advanced model.

The result was a model called HIDRYER that assumed zones of constant permeability and porosity. It was based primarily on low mechanical pressure cases

where the thickness did not change much as drying progressed, but gave good agreement with experimental data even in higher pressure cases,<sup>92</sup> since any values for porosity, thickness, heat transfer coefficient, and permeability could be specified as inputs and held fixed through the drying simulation.

The final step was to convert HIDRYER to HIDRYER1 by specifying the required supplementary relationships that determine how porosity, etc., vary with pressure, temperature, moisture ratio, and freeness. Each relationship was tested separately before being incorporated into HIDRYER and then tested again after incorporation to verify that it had been implemented correctly. Thus, the model was validated at each stage of development so that the predictions of HIDRYER1 are a result of the model and its assumptions and not a result of problems in the FORTRAN coding of the equations.

#### SUMMARY

Fundamental heat and mass transfer relationships, with supplementary property equations, have been assembled into a model of high intensity paper drying. The model has been converted into a FORTRAN program called HIDRYER1.

The following sections describe simulations involving an exploratory or "parametric" study to determine the basic behavior of the model and direct comparisons to laboratory data to check on the values of constants used in the model.

## PARAMETRIC STUDY

### INPUT PARAMETERS

HIDRYER1 requires the user to provide values for hot surface temperature (TH), boiling point temperature (TB), basis weight (BW), Canadian Standard Freeness (CSF), initial moisture ratio (MRO), default time increment (DTO), peak mechanical pressure (PMAX), and pressure rise time (RISTIM). Additionally, the user must specify choices for the following options: ramp-and-hold or sinusoidal pressure pulse; English or SI units; and two options for a packaged subroutine used to calculate sheet thickness when the sheet becomes saturated during the heatup regime. These last two options select either a variable-order Adams predictor-corrector method or Gear's method for solving a differential equation and specify how the Jacobian matrix is to be calculated (analytically, by finite differences, etc.).

### OUTPUT VARIABLES

HIDRYER1 produces two types of output: printed output and output stored on magnetic disk. The printed output consists of the input parameters and the following calculated values: time (SEC), amount of moisture removed relative to the initial amount present (MREL), sheet surface temperature (TS), temperatures at the various interfaces in the sheet (T1, T2, T3), positions of the interfaces relative to total sheet thickness (RATIO1, RATIO2, RATIO3), total sheet thickness (DELTAT), instantaneous heat flux (Q), overall heat transfer coefficient (OHTC), and the gage vapor pressure corresponding to T1 (PGAUGE). The disk output does not include the input parameters, but contains all the calculated values of the printed output plus the temperature at a point midway through the basis weight of the sheet (TMID). Other variables calculated in the program can be obtained by modifying the WRITE statements in the output subroutine.

## DESIGN OF PARAMETRIC STUDY

The effect of various input parameters on drying behavior is determined by running the program at different sets of conditions for each of the two pressure pulse options. Table 1 lists the parameters and the values investigated. The center column gives the values for the base case. Results from all other cases are compared against this base case and are generated by varying the value of an individual parameter from its base value while maintaining all other parameters at their base case values. The pressure option is designated as either RAMP or SINE.

Table 1. Input parameter values for parametric study.

<u>Parameter</u>	<u>Minimum</u>	<u>BASE</u>	<u>Maximum</u>
TH, °C(°F)	148.9(300)	204.4(400)	260.0(500)
MRO	1.00	1.25	1.50
BW, g/m <sup>2</sup> (lbm/ft <sup>2</sup> )	50.25(0.0105)	102.50(0.0210)	205.00(0.0420)
CSF	300	450	600
PMAX, kPa(lbf/in <sup>2</sup> )	2068(300)	3447(500)	4826(700)
RISTIM, s	0.005	0.010	0.050

## RESULTS AND DISCUSSION

The HIDRYER1 program was allowed to run to completion or for one hour of CPU time, whichever was shorter. In general, the SINE cases took about 20 seconds to run. The exception is the SINE case with 0.050 second RISTIM, which took about 18 minutes of CPU time. The RAMP cases averaged around 30 minutes of CPU time, and no case took longer than 38 minutes.

### Base Case

Figures 11 through 18 show the results of the base case with the RAMP pressure option. Figure 11 is the drying curve for this experiment. Two points on the curve are significant. The first point, at about 0.04 second, signals the onset of drying. Examination of the numerical output reveals that the transition regime actually started at about 0.02 second, but it takes several time increments of the transition regime before noticeable (on the graph) drying occurs. The second point, at about 0.13 second, signals the end of the transition regime and the onset of the linear regime. The steep slope of the drying curve in the transition regime indicates that the drying is dominated by liquid dewatering in this period. The abrupt change in slope at the start of the linear regime indicates a shift to an evaporation and bulk vapor flow dewatering mechanism.

Figure 12 traces the sheet thickness history. The rapid pressure rise during the heatup period causes a rapid sheet compression early in the process. As the pressure levels off and as the transition regime begins, the hydraulic pressure in the sheet builds and reduces the rate of compression. As more and more liquid is removed from the sheet, it becomes easier to compress and the rate of compression increases until all the interfiber liquid is removed (which coincides with the onset of the linear regime in this case). Once the interfiber liquid is removed, the permeability of the sheet increases and results in low hydraulic (vapor) pressure. The rate of compression slows as the moisture removal becomes dominated by an evaporation mechanism and the sheet approaches its final (zero moisture content) thickness.

Figure 13 tracks the relative position of the various interfaces in the sheet. Interfaces 1 and 2 move together from the start of the transition regime for a short time. In this period, the heat transfer rate is able to keep up



with the liquid flow rate. At about 0.05 second the liquid dewatering rate becomes greater than the heat transfer (evaporation) rate and interface 2 progresses into the sheet faster than interface 1. When interface 2 reaches the cool side of the sheet, the linear regime begins and heat transferred to the cool side causes evaporation. Interface 2 then recedes back toward the hot side. As interface 2 reaches the far side of the sheet the inflection and change in slope of the curve for  $RATIO1$  signals the shift from liquid dewatering and internal sheet evaporation to an evaporation-only mechanism. Interface 3 is held at  $DELTAT$  because evaporation at the outer surface does not occur until all interfiber water is removed.

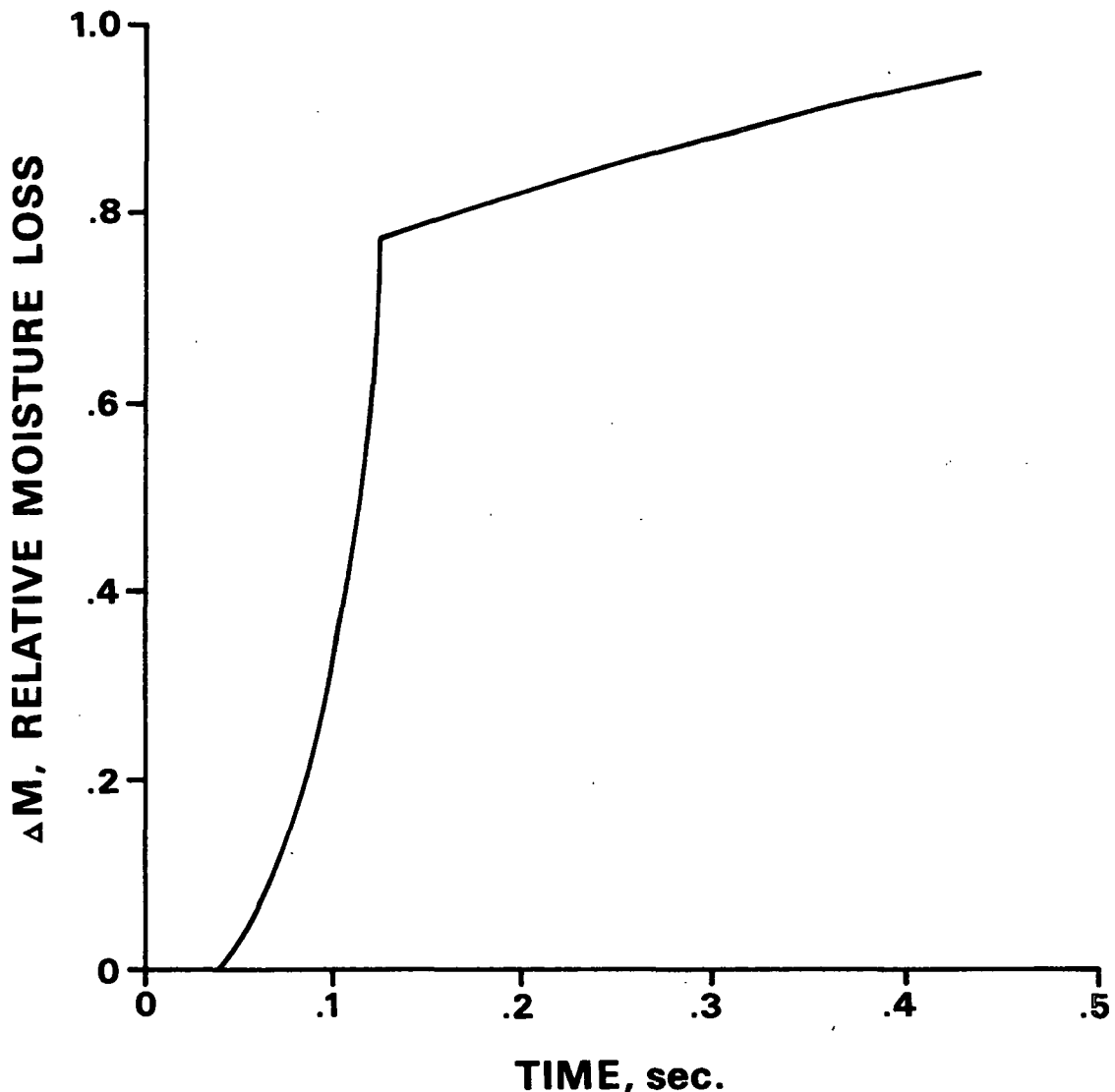


Figure 11. Moisture removal as a function of time for the RAMP base case.

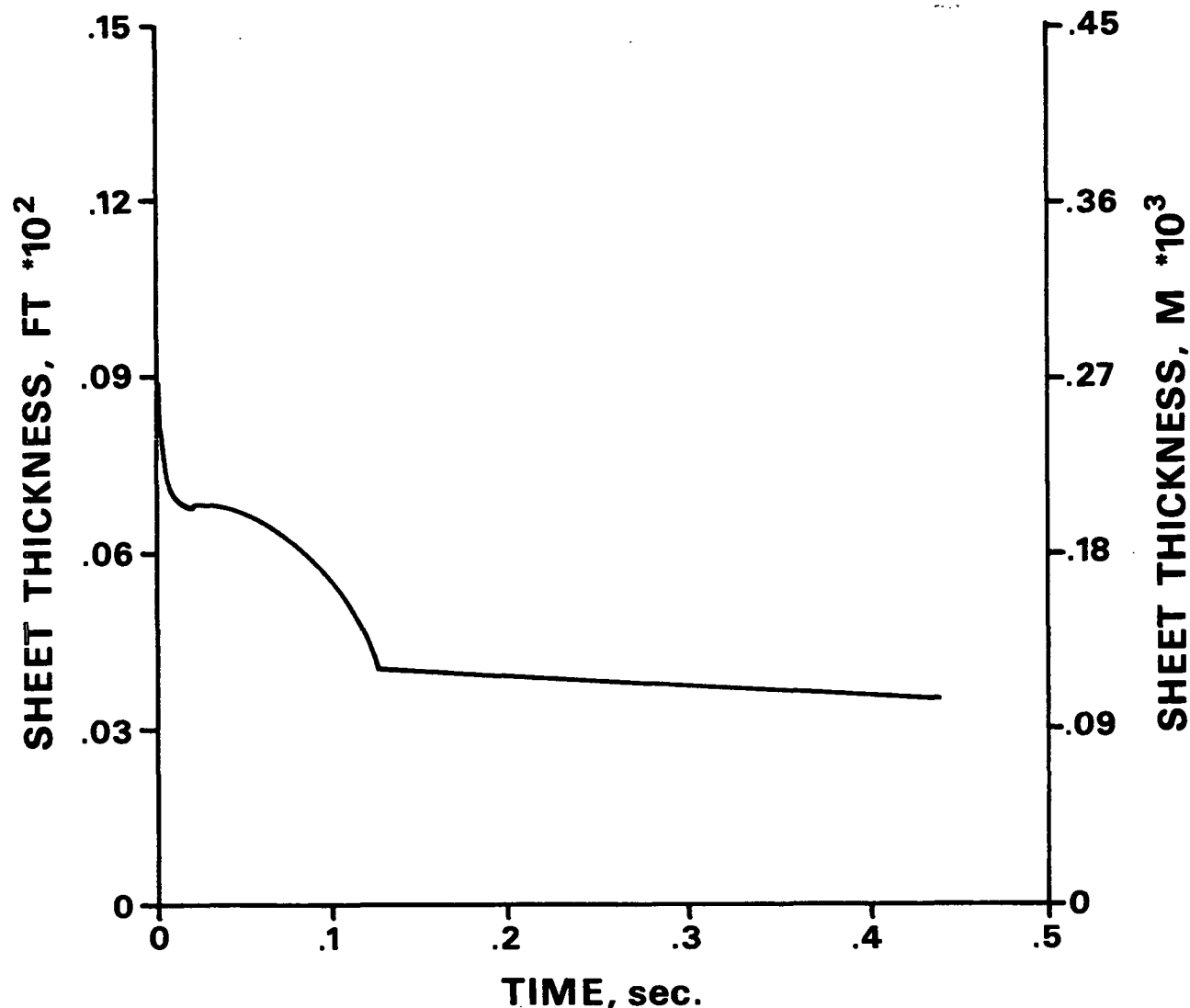


Figure 12. Sheet thickness as a function of time for the RAMP base case.

Figure 14 shows the temperature history of the interfaces.  $T_S$ ,  $T_1$ , and  $T_2$  move together until the transition regime starts.  $T_3$  begins to rise then because of the quantity of heat transferred by convecting liquid.  $T_1$  and  $T_2$  remain together until interface 2 moves faster than interface 1.  $T_2$  and  $T_3$  become identical when interface 2 reaches DELTAT and the linear regime starts.  $T_2$  rises as interface 2 moves back into the sheet so that a vapor pressure gradient (determined by sheet permeability) can be maintained.  $T_3$  is fixed at  $T_B$  since interface 3 is held at DELTAT.

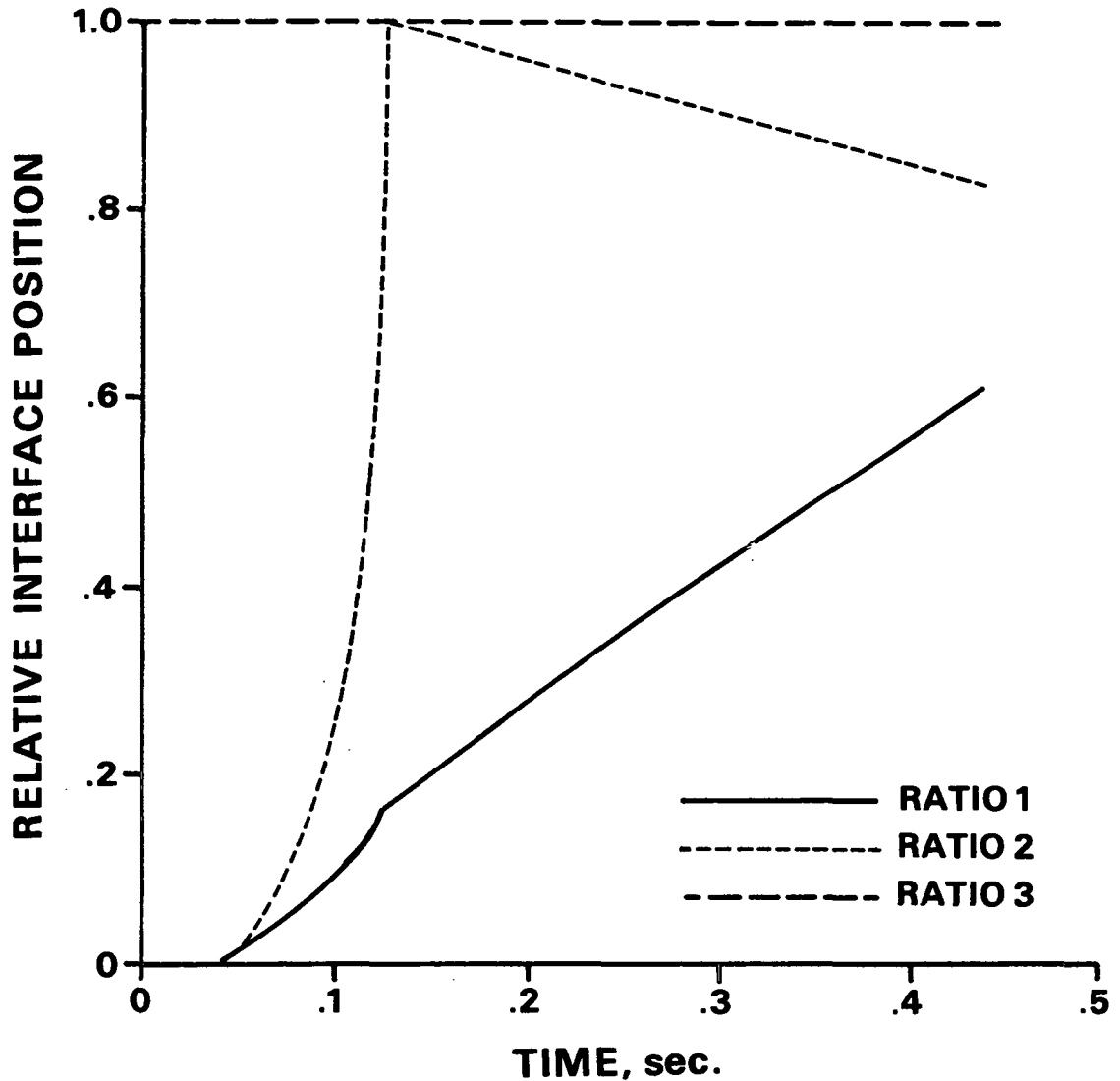


Figure 13. Interface positions relative to total sheet thickness as functions of time for the RAMP base case.

Figure 15 depicts the gage vapor pressure corresponding to the value of  $T_1$ . The two abrupt drops and recoveries of vapor pressure occur at points where a slug of liquid is pushed through the sheet and the heat rate has to "catch up" to sustain continued flow. The first point occurs as interfaces 1 and 2 move into the sheet. The second point occurs as interface 2 moves ahead of interface 1. In both cases a zone of high vapor permeability (relative to zone 3) is suddenly created. This causes  $T_1$  (and the vapor pressure corresponding to  $T_1$ ) to

drop since the flow resistance is reduced. As the interfaces progress,  $T_1$  must increase to sustain continued vapor and liquid flow at points in the interior of the sheet.

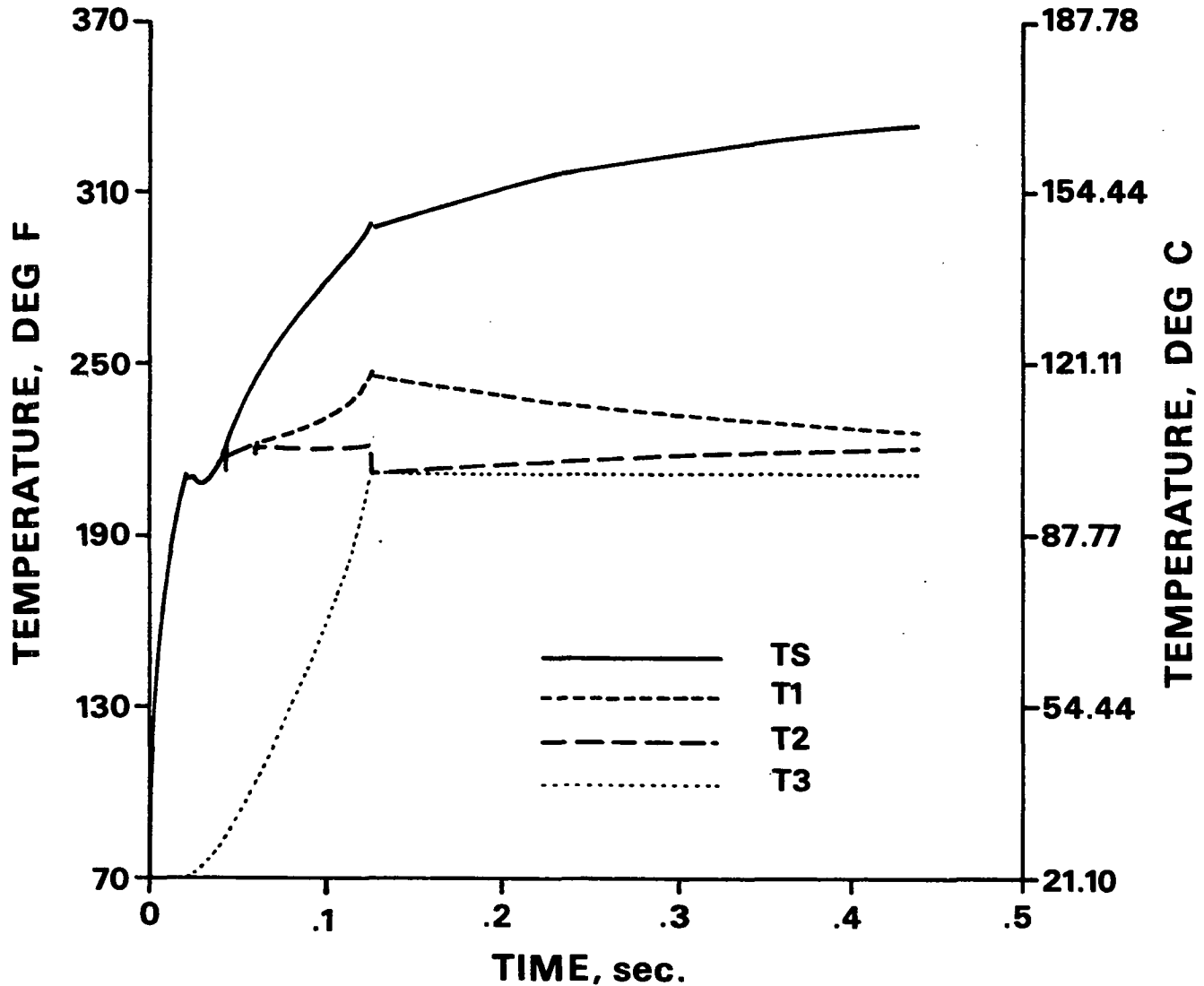


Figure 14. Sheet surface temperature and interface temperatures as functions of time for the RAMP base case.

Figure 16 traces the temperature at a point half way through the basis weight of the sheet. Since this does not always correspond to the instantaneous location of an interface,  $TMID$  has to be interpolated based on the positions of the interfaces relative to the total sheet basis weight. Conduction in the

compressing sheet during heatup causes the internal temperature to rise above its initial value earlier than the cool side does. The temperature rises steadily until the linear regime when the rate of compression and the drying rate slow significantly. TMID achieves a nearly constant level until interface 2 moves far enough back into the sheet to affect the thermal behavior of the sheet's interior.

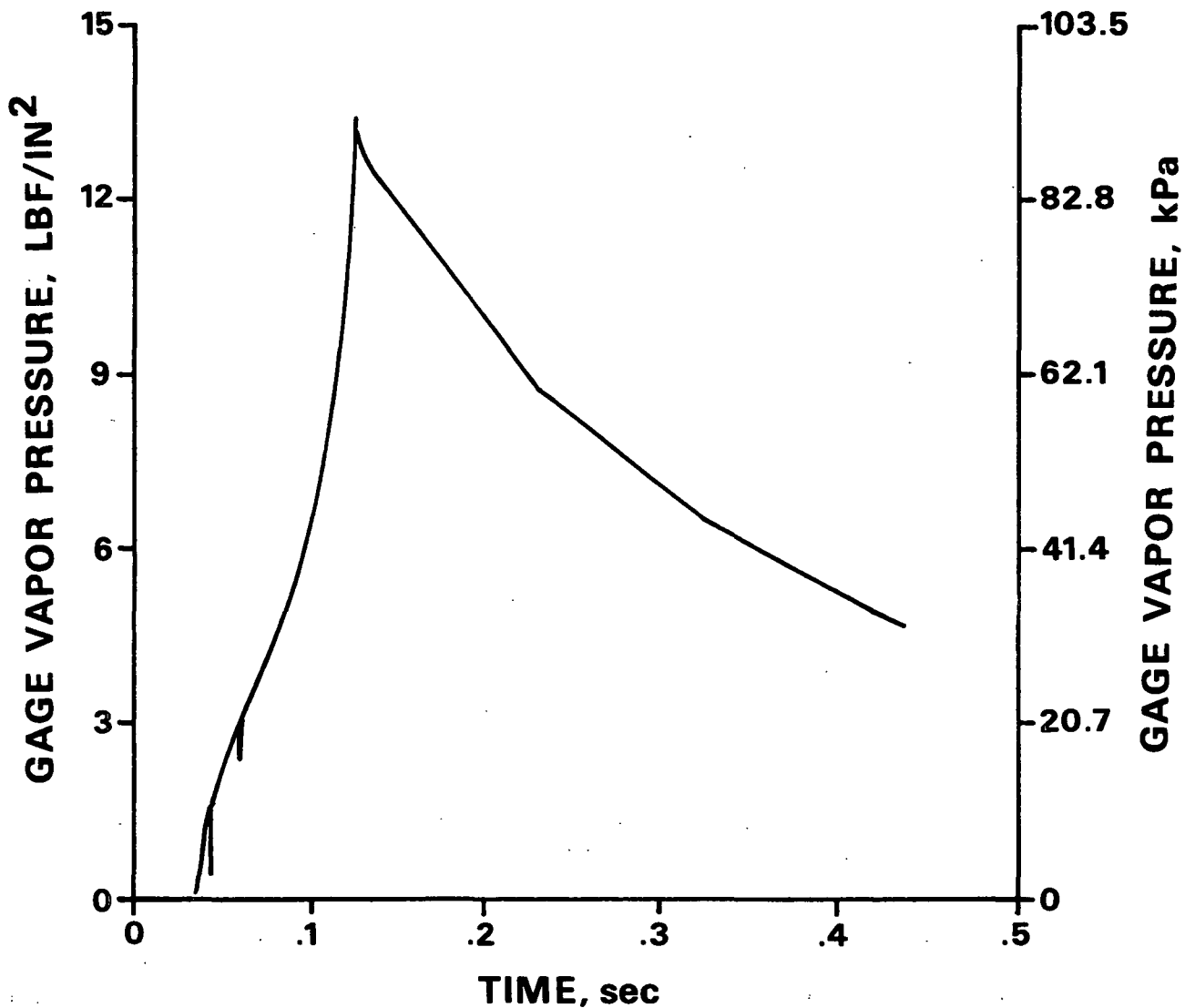


Figure 15. Gage vapor pressure corresponding to T1 as a function of time for the RAMP base case.

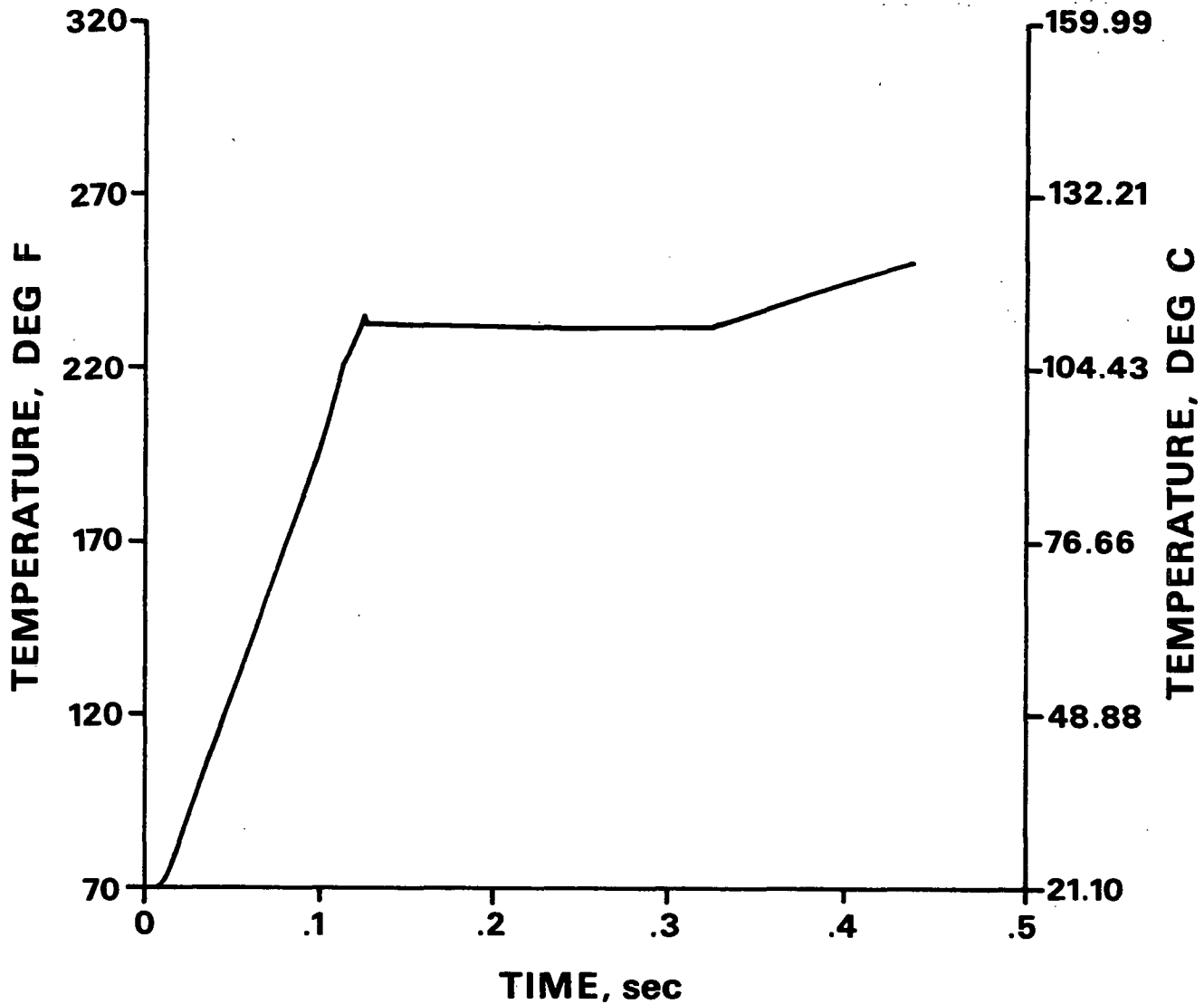


Figure 16. Temperature at one-half the sheet basis weight as a function of time for the RAMP base case.

Figure 17 graphs the heat flux from the hot surface to the sheet. Note that the hot surface temperature is assumed constant. The initial portion of the heat flux is controlled by the shape of the pressure pulse. The heat flux is initially zero and rises to its peak as the pressure peaks. When the pressure stabilizes, the heat penetrates the sheet, causing a temperature rise and a sharp drop in heat flux. Just as the transition regime begins, the drop in the heat flux moderates and when the linear regime begins the heat flux slowly

approaches an equilibrium value (zero) as the sheet approaches an equilibrium condition (dry).

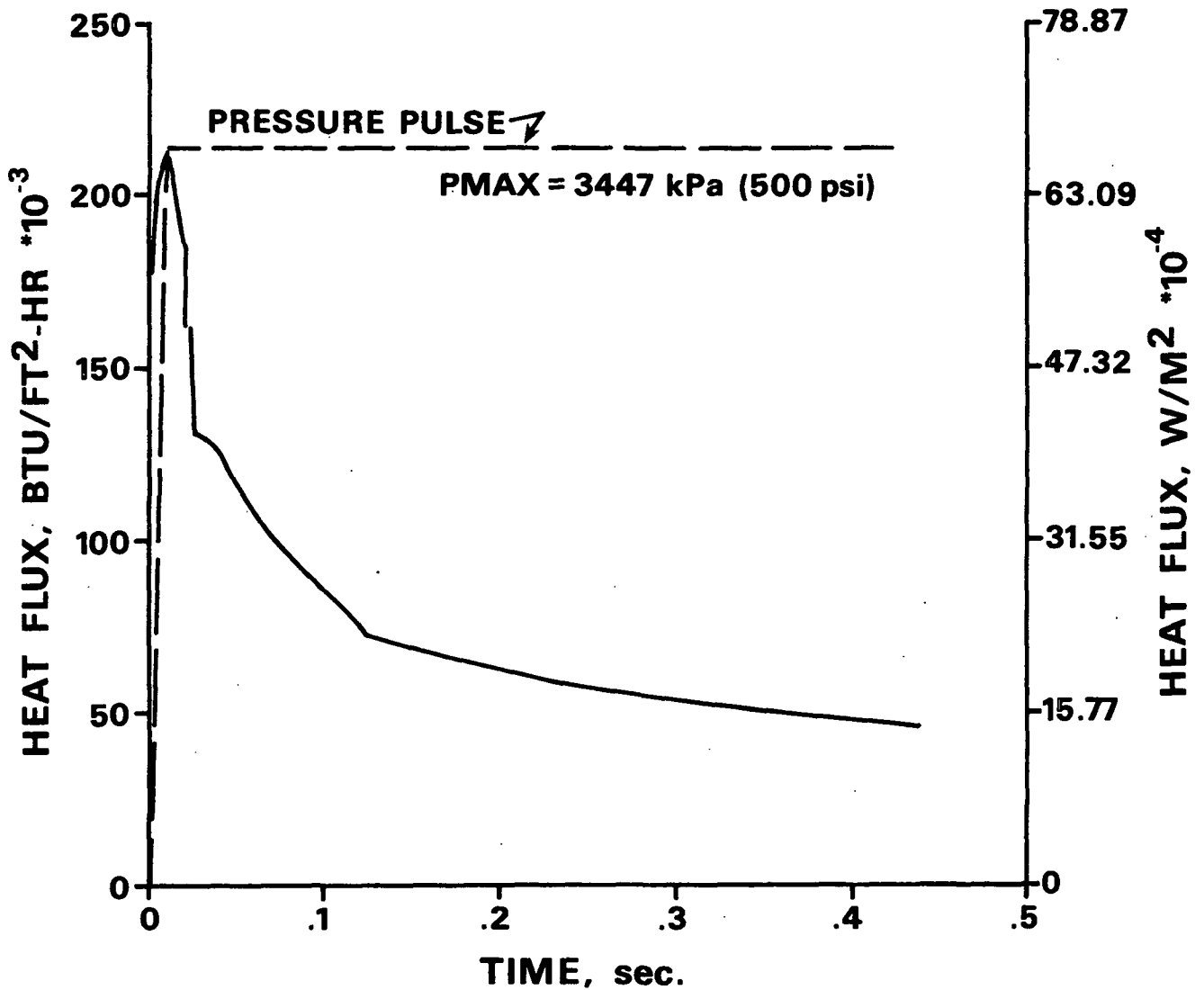


Figure 17. Heat flux as a function of time for the RAMP base case.

Figure 18 presents the history of the overall heat transfer coefficient. This quantity is calculated by dividing the heat flux by the difference between  $T_H$  and  $T_{MID}$ . OHTC parallels the heat flux curve until transition begins. As  $Q$  moderates and  $T_{MID}$  continues to rise, OHTC remains somewhat constant. As the

linear regime begins, OHTC again parallels  $Q$  since TMID stabilizes. As TMID starts to rise again, its increase is offset by the decrease in  $Q$  to yield a constant OHTC value.

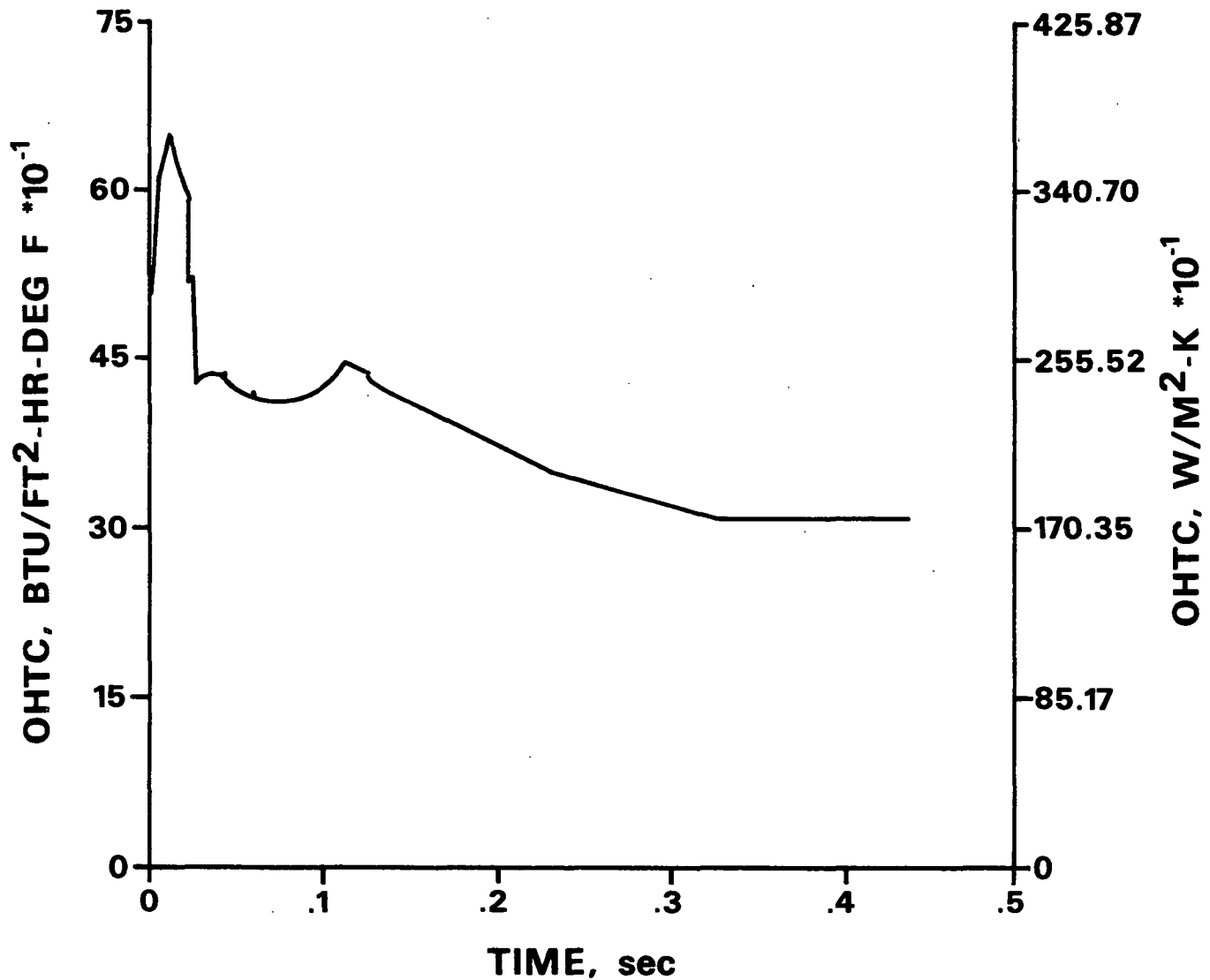


Figure 18. Overall heat transfer coefficient as a function of time for the RAMP base case.

The behavior of the base case for the niplike pressure pulse is not shown. The variables essentially match the RAMP pressure base case up until the peak



pressure is reached. After that, the values plateau and decline slightly as the pressure rapidly declines. The SINE case with 0.05 second RISTIM is the only niplike case that predicts any moisture removal. This is shown in a later figure in comparison with the moisture removal predicted for the various RAMP pressure rise times. (For the conditions selected the sheet is still in the heatup regime for all but this one SINE case.)

### Comparisons of Drying Behavior

Figures 19 through 24 show comparisons of the drying behavior for the values of the input parameters given in Table 1. Results from all cases are compared against the base case and are generated by varying the value of an individual parameter from its base value while maintaining all other parameters at their base values. The drying curve stops when the sheet reaches 6% moisture content or, in one case, when the niplike pressure pulse drops to its starting value. The heatup regime accounts for 5 to 10% of the total drying time; the transition regime accounts for 10 to 45% of the total time; and the linear regime accounts for 50 to 80% of the total time. The base case results for drying time to 6% moisture content fall in between the times predicted for the minimum and maximum parameter values.

Figure 19 displays the effect of hot surface temperature on the drying curve. As anticipated, higher hot surface temperature results in shorter drying time and there is nearly a one-to-one correspondence between drying time and the driving force ( $T_H - T_B$ ). The greatest benefits of higher hot surface temperature are reduction of the heatup time and higher driving force (drying rate) in the linear regime.

Figure 20 shows the effect of initial moisture ratio on the drying curve. There is little effect on total drying time because the moisture removal is

dominated by the (rapid) liquid dewatering mechanism. The time required to evaporate the remaining water during the linear regime is comparable for each initial moisture ratio case.

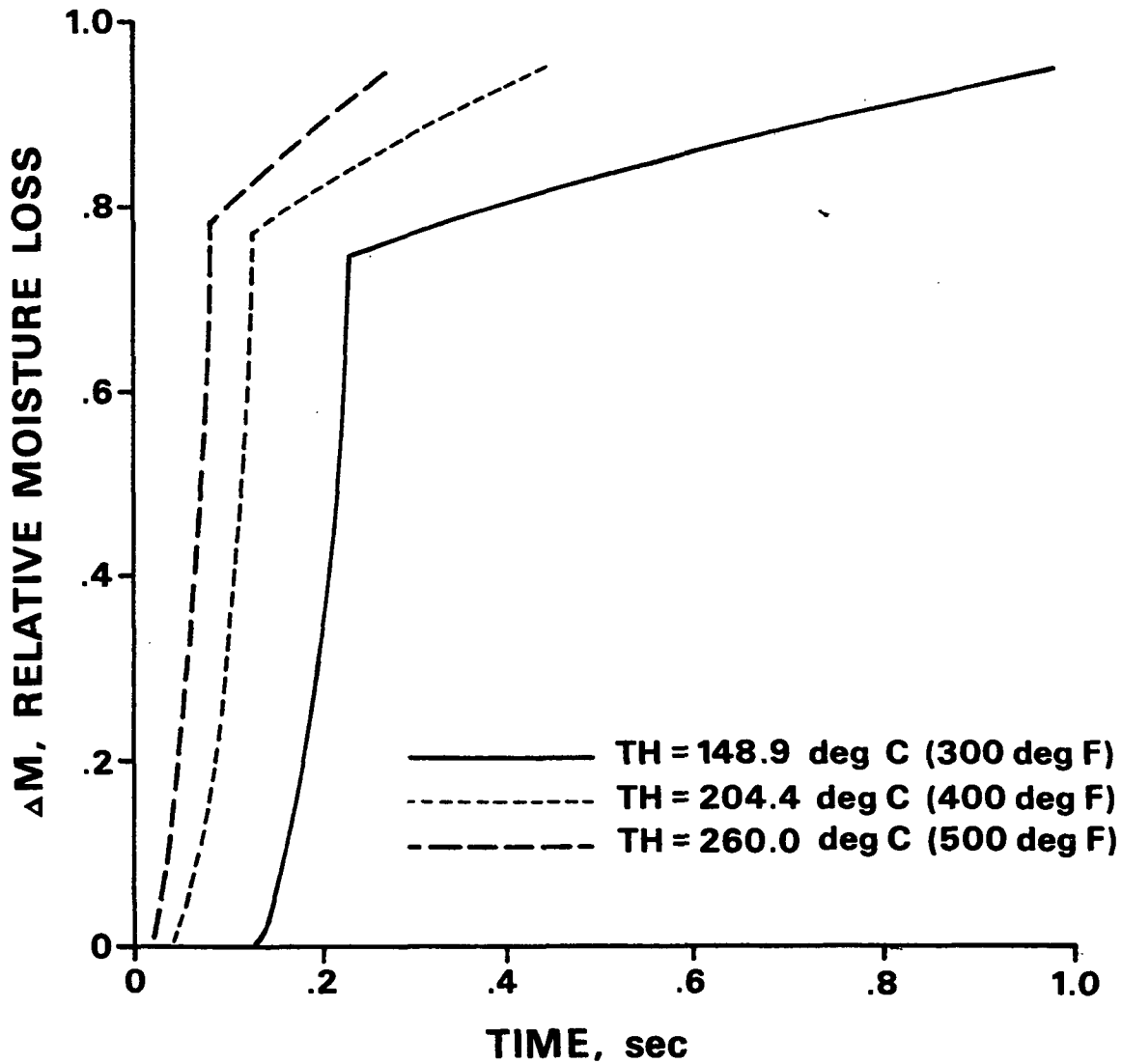


Figure 19. Effect of hot surface temperature on moisture removal for RAMP cases.

Figure 21 presents the effect of basis weight on drying. The heatup time for each basis weight is comparable, but the slopes of the liquid dewatering portion are distinctly different. In the lowest basis weight case, the heat can

penetrate far into the sheet in a short time and liquid motion can be sustained at its initial pace. In the heavier basis weights (thicker sheets), the heat only penetrates into a fraction of the total sheet thickness and after liquid motion starts, it takes some amount of time for a sufficient quantity of heat to penetrate further and sustain the flow. In the linear regime, the heat and mass have a shorter distance to travel in the lower basis weight cases and the drying rate is faster than in the heavier basis weight examples.

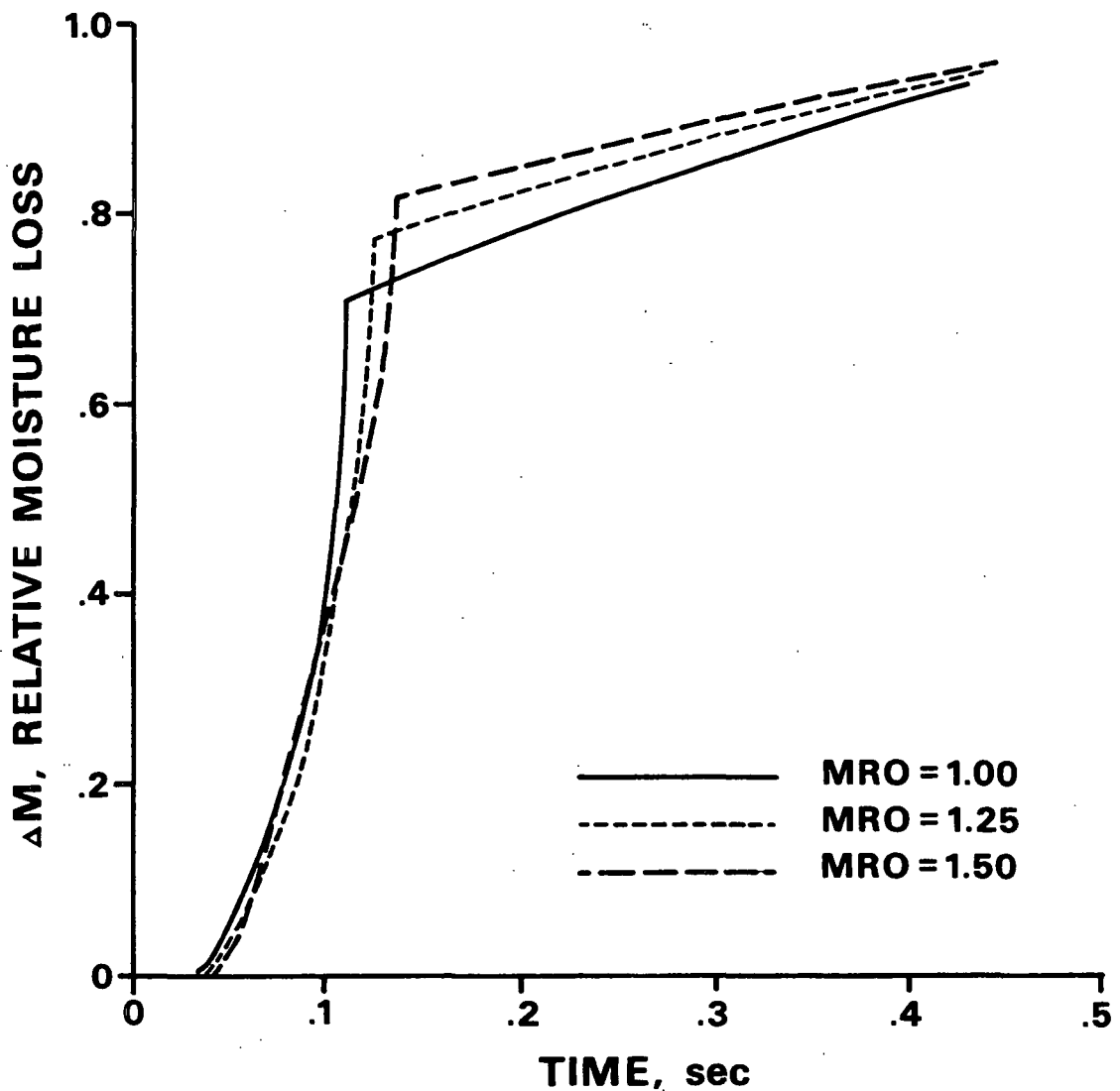


Figure 20. Effect of initial moisture ratio on moisture removal for RAMP cases.

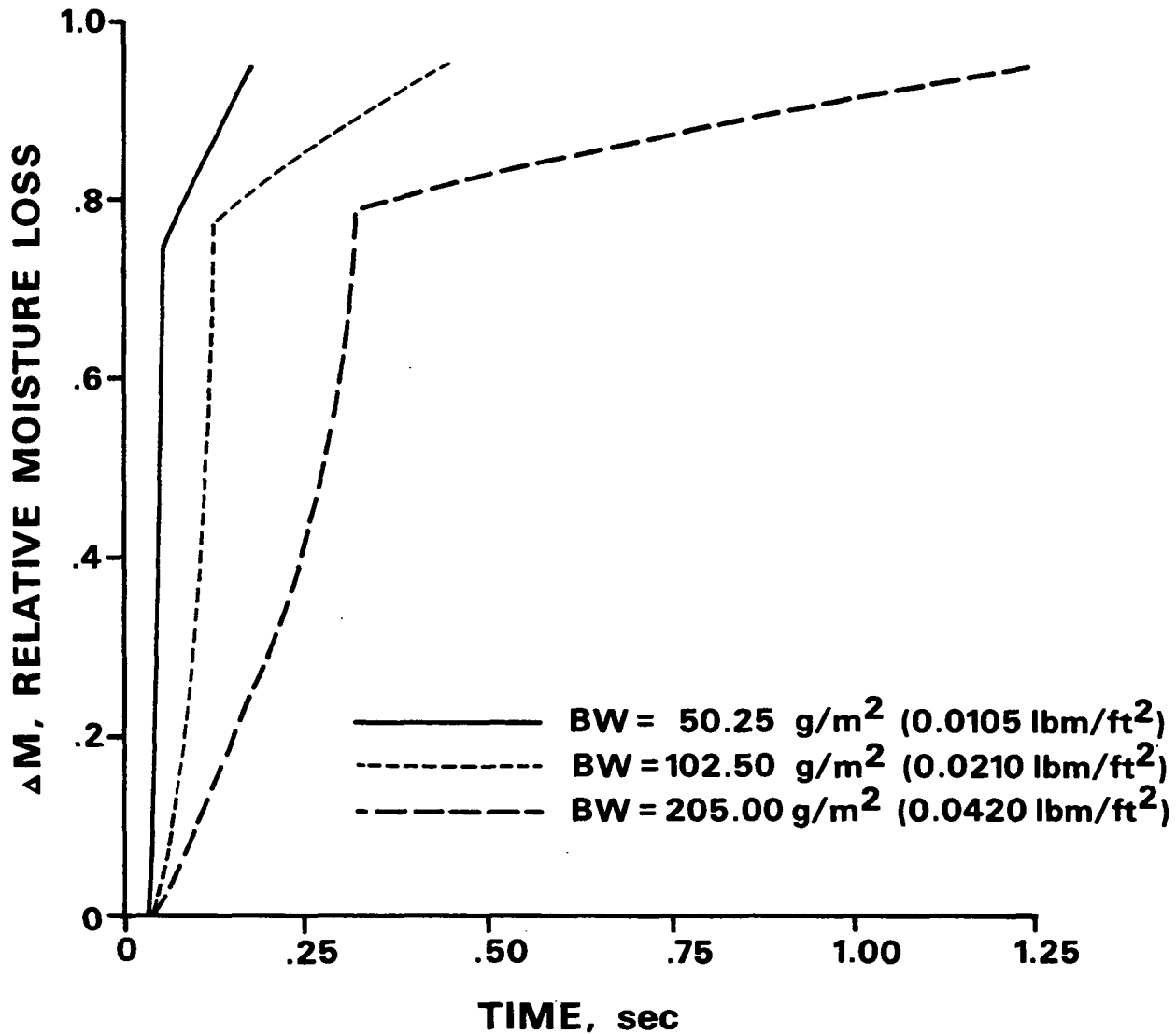


Figure 21. Effect of basis weight on moisture removal for RAMP cases.

Figure 22 shows how Canadian Standard Freeness affects drying. Lower CSF gives a more compressed sheet (at a given mechanical pressure), and in the case of 300 CSF liquid is removed from the sheet by mechanical dewatering in addition to the thermally induced liquid dewatering. The decrease in permeability accompanying lower CSF is not enough to offset the gains in drying resulting from a more compact sheet (which is better able to transfer heat) and the higher internal sheet temperatures going into the linear regime.

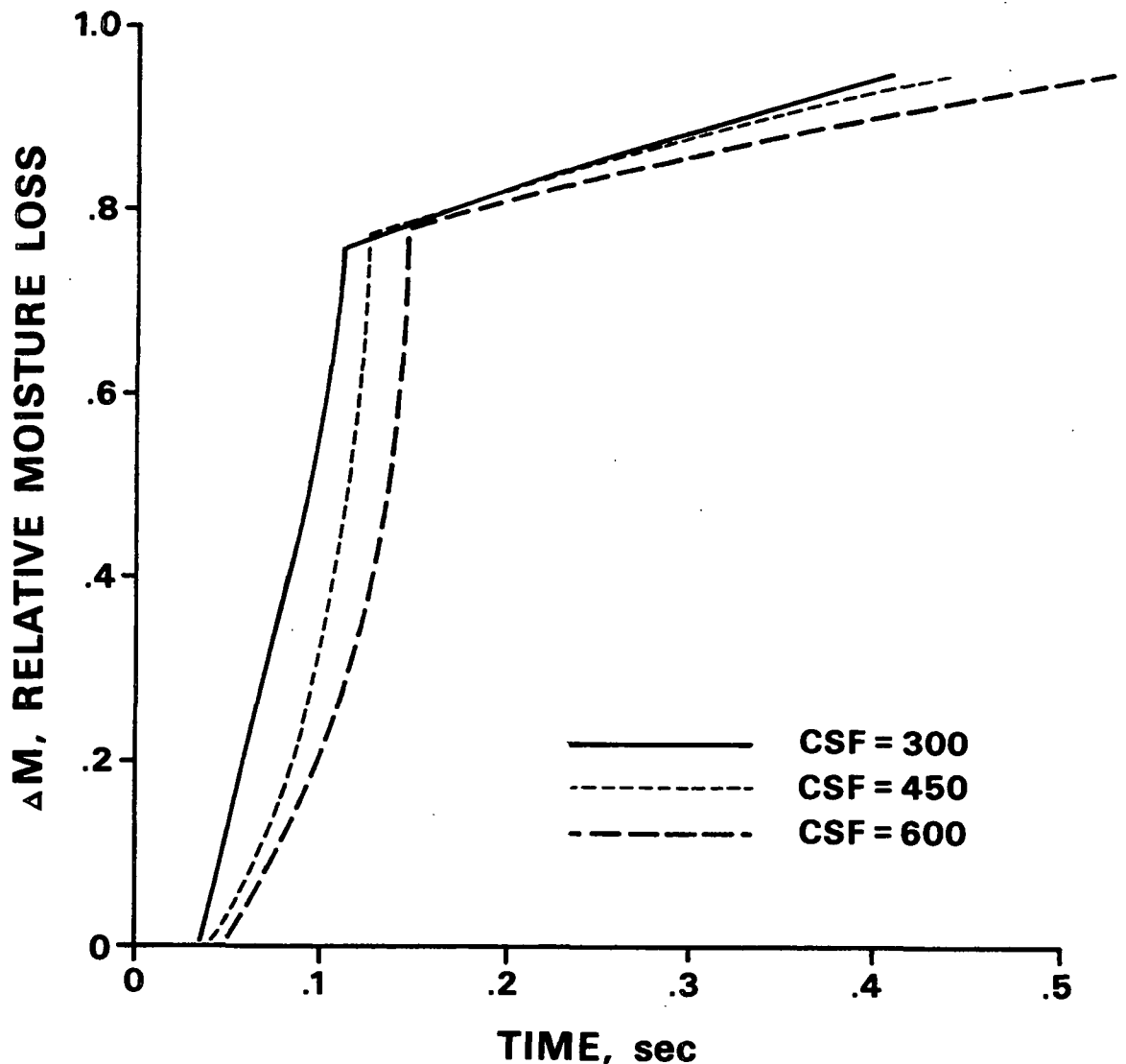


Figure 22. Effect of freeness on moisture removal for RAMP cases.

Figure 23 depicts the influence of peak pressure on drying. The curves are essentially parallel in slope but shifted in time. The results indicate that increasing pressure decreases drying time, but that the relative increase becomes smaller at higher pressures for the range of pressures examined here. This suggests that there may be some practical limit to the amount of pressure which is cost effective for a commercial implementation of high intensity drying technology.

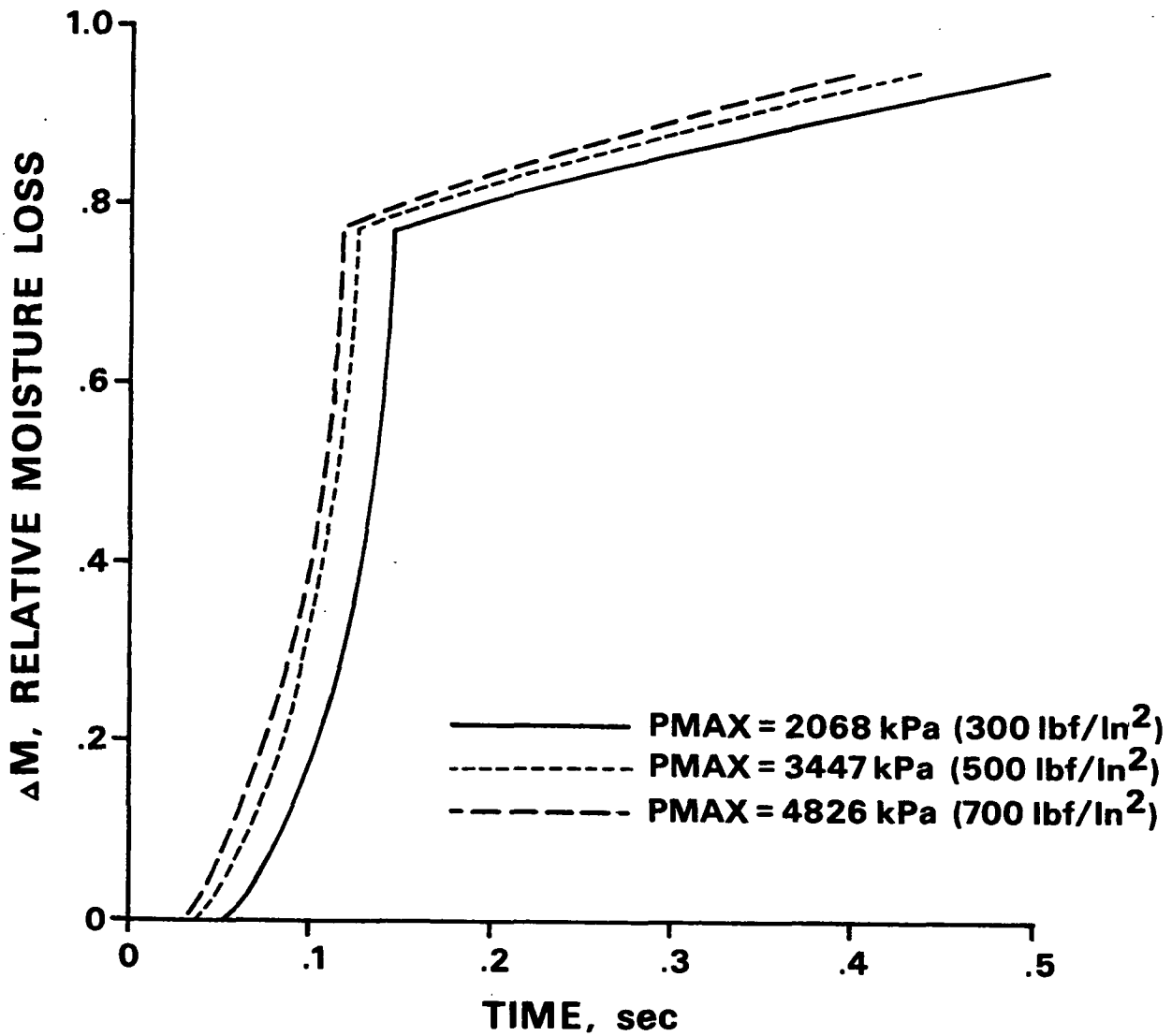


Figure 23. Effect of peak pressure on moisture removal for RAMP cases.

Figure 24 shows the effect of the pressure rise time, the time it takes to achieve the peak pressure. There is virtually no effect on drying time for the RAMP cases, since the rise time is such a small percentage of the total drying time needed. Comparing the SINE case to a RAMP case with the same rise time shows that they behave similarly until the SINE case pressure begins to drop rapidly. The SINE case continues to show a decreasing rate of dewatering as the

heat transfer to the sheet declines, and drying stops when the pressure reaches a point at which the heat transfer can no longer sustain liquid flow.

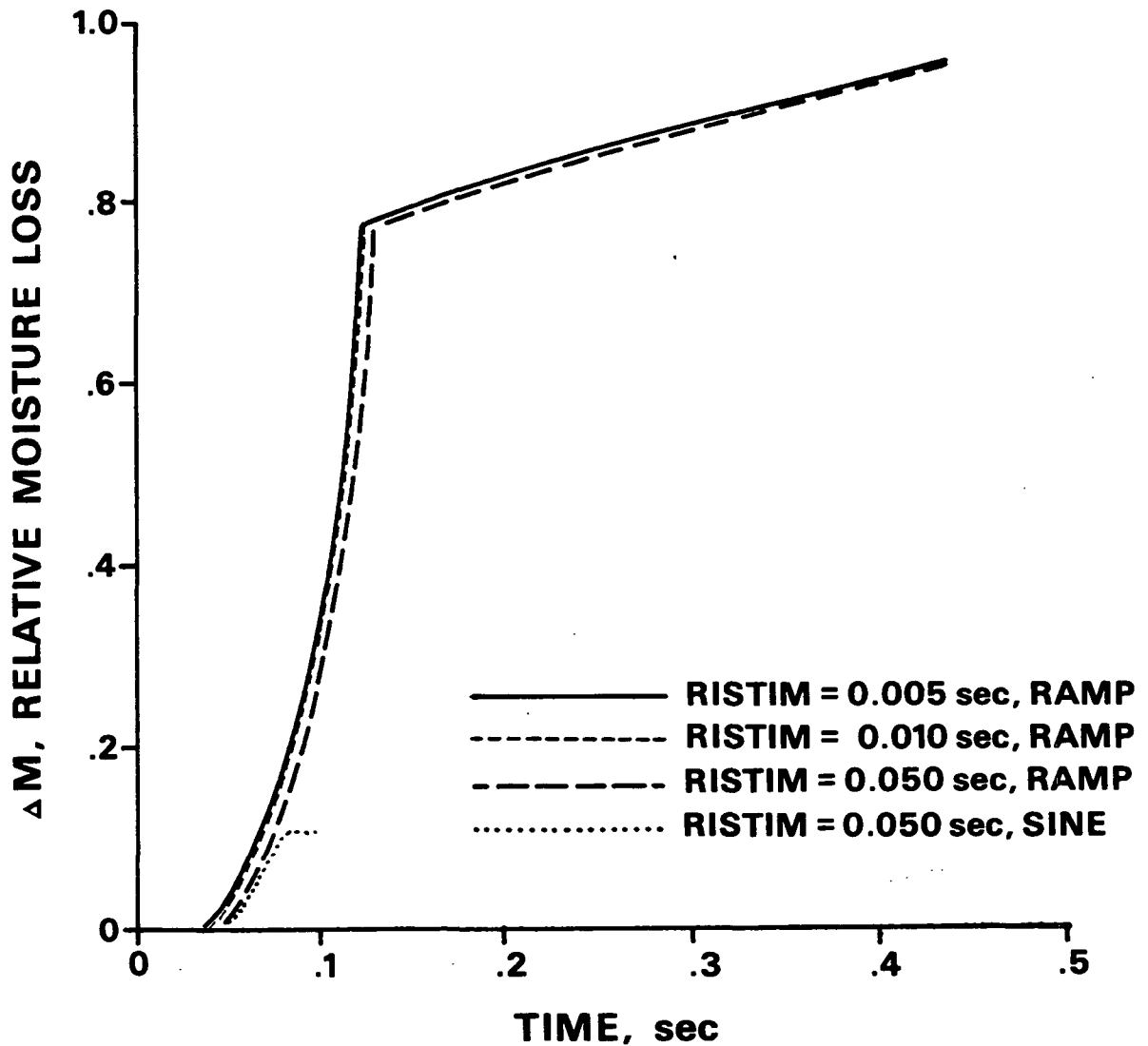


Figure 24. Effect of pressure rise time on moisture removal for RAMP cases and one SINE case.

The relative magnitudes of the changes are summarized in Table 2.

Table 2. Effect of changes in input parameters on drying time for RAMP cases.

<u>Parameter</u>	<u>Value Relative to Base Case Value</u>	<u>Change in Drying Time</u>
TH	- 25%	+123%
	+ 25%	- 39%
MRO	- 20%	- 2%
	+ 20%	+ 2%
BW	- 50%	- 60%
	+100%	+180%
CSF	- 33%	- 7%
	+ 33%	+ 18%
PMAX	- 40%	+ 16%
	+ 40%	- 9%
RISTIM	- 50%	<- 1%
	+400%	<+ 1%

#### SENSITIVITY ANALYSIS

The calculation method in HIDRYER1 requires that values be specified (in the program) for the number of grid points used in the finite difference equations (KMIN) and for the number of iterations used in determining the interface temperatures (IMAX). The default time increment (DTO) is an input parameter, and it too can influence the predicted drying output. There are no clear-cut methods of choosing appropriate values for these variables and so a sensitivity analysis is necessary to determine what numerical inputs give the best compromise between prediction accuracy and CPU ("computer") time.

Table 3 shows the results of variations in KMIN, IMAX, and DTO using the same inputs as for the RAMP base case (with the exception of DTO when sensitivity to DTO was tested, of course). The central line for each variable gives the value used in conducting the parametric study.



Table 3. Effect of grid spacing, iteration counter, and default time increment on drying time and CPU time.

<u>Variable and Value</u>		<u>Predicted Drying Time, s</u>	<u>CPU Time, hr:min:s</u>
KMIN	21	0.438	1:19:37
	101	0.432	0:28:20
	251	0.431	4:46:58
IMAX	5	0.432	0:22:26
	10	0.432	0:28:20
	15	0.432	0:35:34
DTO (hr)	10 <sup>-5</sup>	0.456	0:27:54
	10 <sup>-7</sup>	0.432	0:28:20
	10 <sup>-10</sup>	0.430	9:38:27

Changing the value of KMIN results in minor changes in predicted drying time and more drastic changes in CPU time. When KMIN is increased from 101 to 251, the increase in CPU time is a direct consequence of the increased amount of calculations required. When KMIN is decreased from 101 to 21, one might anticipate a reduction in calculation time. However, because HIDRYER1 uses a forward time difference procedure, interface 2 may be advanced to a location such that its temperature is less than TB. When this occurs, no drying takes place until heat transfer to the transition zone raises its temperature in the vicinity of interface 2 to the point at which T2 is calculated to be above TB. Thus, several time increments may elapse in which there is no drying. Using fewer grid points reduces the effective heat transfer by predicting a lower temperature at any given point inside the outer zone and therefore there are more time increments early in the process when the sheet is still heating up and not drying.

A change in the number of iterations for the interface temperature calculations is reflected directly in the amount of CPU time required. Since there is essentially no change in the predicted drying time or behavior, it appears that

5 iterations are sufficient and the system is "well behaved" with regard to interface temperature calculations.

Decreasing the default time increment has a tremendous effect on CPU time. Typically, the interface motion time increment restriction and the finite difference time increment stability criterion are more restrictive than the default time increment. These are dominant in the transition regime. In the linear regime the finite difference criterion is not operative and the interfaces are sufficiently separated that the default time increment becomes the more restrictive time step. It is in just this regime, however, that a larger time increment can be most useful, since the rate of drying slows relative to the liquid dewatering part of drying. Limiting the default time increment chiefly limits the number of calculations in the linear regime only. Clearly, maintaining DT0 on the order of  $10^{-7}$  hour produces a vast improvement in accuracy with little sacrifice in CPU time.

#### SUMMARY

The parametric study shows that hot surface temperature and basis weight have the greatest influence on drying time to 6% moisture content. Peak pressure and freeness have a more moderate effect, and initial moisture ratio and rise time have almost no effect.

Using about 101 finite difference grid points, 5 iterations for interface temperature calculations, and a default time increment on the order of  $10^{-7}$  hour appears to be an adequate compromise for balancing prediction accuracy and CPU time.

## EXPERIMENTAL COMPARISONS

### PURPOSE

Comparisons between experimental results and the model's predictions can suggest changes and improvements, can validate the mechanisms assumed in the model, and can identify areas requiring further experimental study.

### EXPERIMENTAL CONDITIONS

Two kinds of experiments were selected for comparisons to HIDRYER1 output based on the manner and magnitude of mechanical pressure application: ramp-and-hold high intensity drying and short duration (impulse) high intensity drying. Examination of the assumptions used in developing the model suggests that it should best predict cases of high hot surface temperature and moderate mechanical pressure (so that good thermal contact is promoted but capillary flow is discouraged by maintaining larger pores) and a ramp-and-hold pressure pulse (since a static compression equation is used).

HIDRYER1 appears to be impractical for modeling cases of mechanical pressure at or below 350 kPa (50 psi). HIDRYER, the earlier version of the program, gives reasonable results in much shorter times. At a mechanical pressure of 321 kPa (46.6 psi) and hot surface temperature of 274°C (525°F), HIDRYER requires about 2 minutes of CPU time but HIDRYER1 needs about 5 hours. HIDRYER gives a better estimate of the experimentally determined<sup>9</sup> drying time of 1.7 seconds: 1.4 seconds for HIDRYER and 0.68 second for HIDRYER1; and a better estimate of the peak vapor pressure of 120 kPa (17.4 psi): 125 kPa (18.1 psi) for HIDRYER and 24 kPa (3.5 psi) for HIDRYER1.

HIDRYER1 requires so much CPU time because it calculates all the properties and sheet behaviors, even when they change by only very small amounts. Conversely, HIDRYER has many built-in assumptions that eliminate the necessity for the

calculation of quantities that do not change much. For example, since HIDRYER takes values of thickness, absolute permeability, and the relative permeabilities as inputs and holds them fixed, it does not have to perform repetitive determinations of these quantities.

The chief drawback to using HIDRYER is that there are no simple guidelines for selecting valid "average" values representative of the quantities throughout the course of drying. Values for input parameters can be easily manipulated to produce good agreement with laboratory data, but the extent to which they reflect real sheet properties can always be questioned. HIDRYER1 attempts to provide an accurate picture at every instant of drying and was developed to address the chief drawback by removing the subjective aspect of running a simulation.

#### RAMP-AND-HOLD PRESSURE PULSE

Data are available<sup>93</sup> for a peak pressure of 4826 kPa (700 psi) at two hot surface temperatures: 149°C (300°F) and 274°C (525°F). Basis weight is 205 g/m<sup>2</sup> (0.042 lbm/ft<sup>2</sup>); moisture ratio is 1.3256; and freeness is 625 CSF. The hydraulic system for application of the pressure pulse causes a small overshoot of P<sub>MAX</sub> before it settles to the designated value. RISTIM is selected as the time at which the mechanical pressure first reaches the target (about 0.12 second). It takes about an equal amount of time for the system to then settle and hold the target pressure value.

Figures 25 and 26 show predicted moisture removal curves with representative experimental points for the two cases. The experimental points are determined gravimetrically. The agreement appears to be better in the higher temperature case. This is probably due to the decrease in capillary effects at the higher temperature from lowered surface tension and viscosity and from the higher vapor pressure generated near the hot surface.

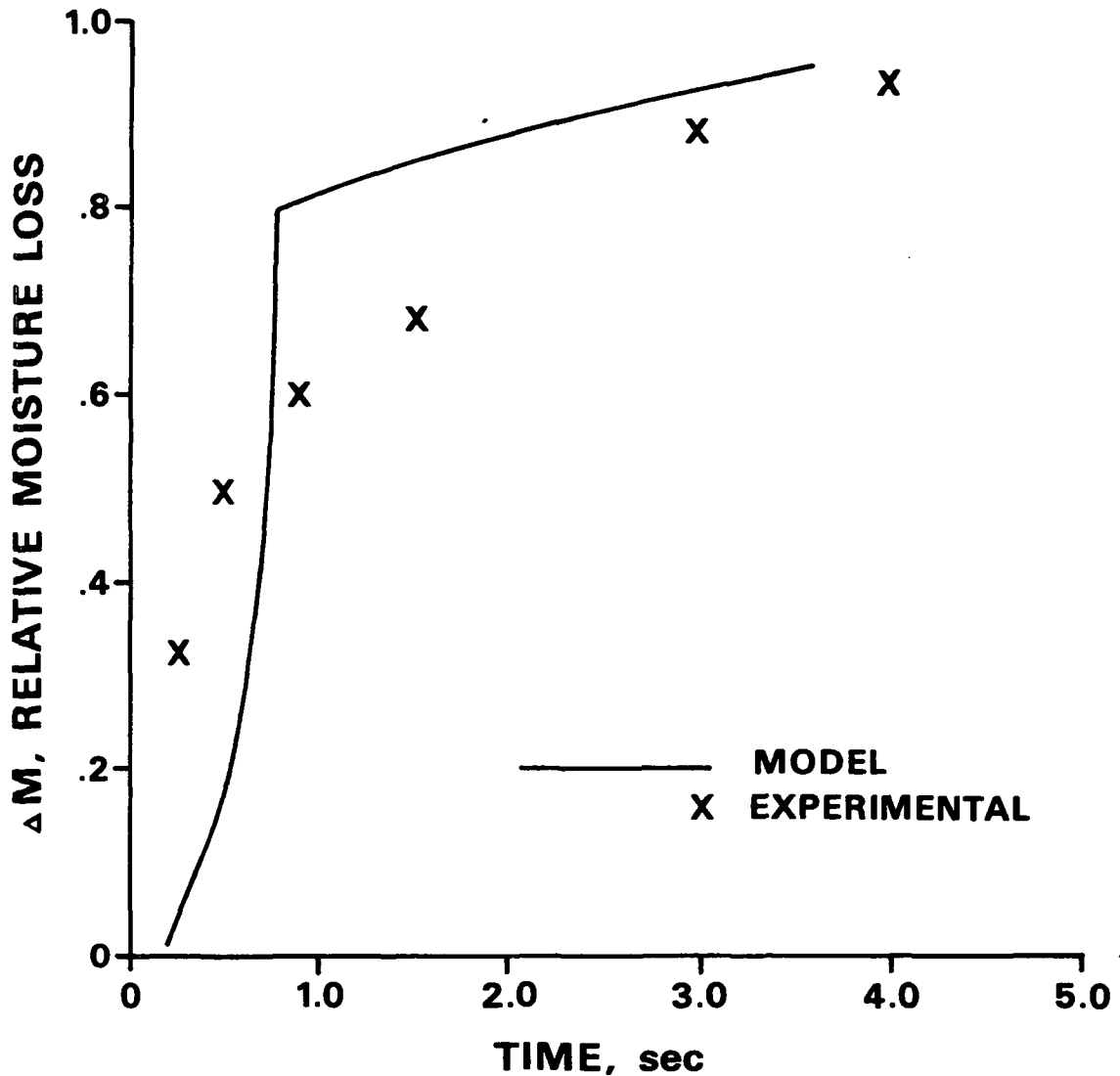


Figure 25. Predicted and measured moisture removal for 149°C (300°F) ramp-and-hold pressure pulse.

In both cases the model overpredicts the contribution of early liquid removal to overall moisture removal and underpredicts the rate of evaporative removal later in the process. Experimental results show liquid removal at about 30% of the total moisture removed,<sup>8</sup> but the model predicts values in the range of 80%. Also, the predicted drying times are about half the experimental ones. This behavior is probably a function of the uniform fiber wall density assumption, which fixes the amount of liquid available for flow; the assumption of no vapor

flow through the outer zone during transition, which limits the rate of rise of internal sheet temperature; and the calculated permeability for the outer zone, which controls the flow resistance.

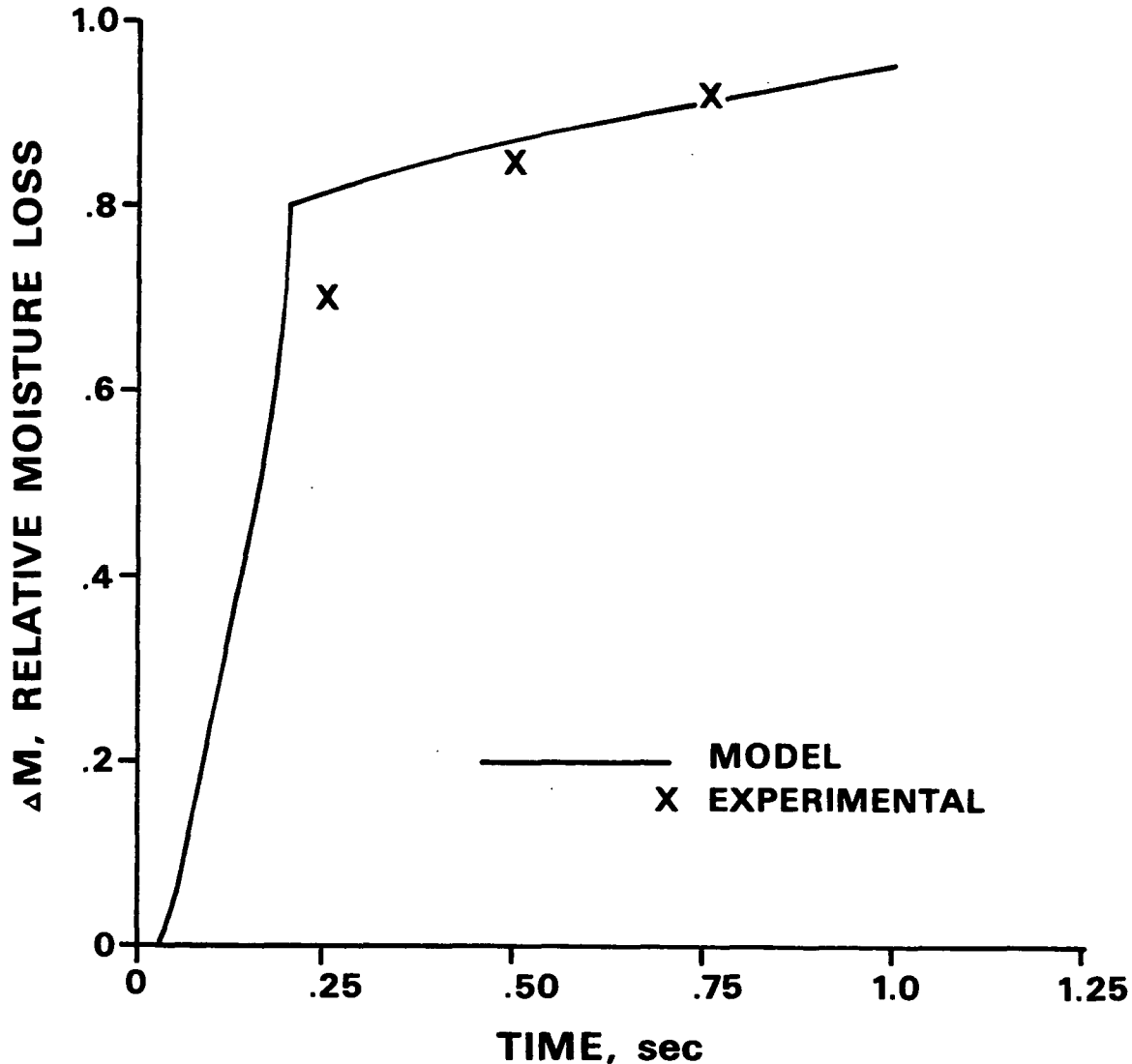


Figure 26. Predicted and measured moisture removal for 274°C (525°F) ramp-and-hold pressure pulse.

Figures 27 and 28 show heat flux comparisons for the two cases. The experimental heat flux is calculated from the measured hot surface temperature using Duhamel's Theorem. In both cases the model severely underpredicts the peak heat flux and less severely underpredicts the heat flux later in drying. The model curve also peaks before the experimental curve. This behavior is due to at

least two factors. First, the model assumes a constant hot surface temperature and determines heat flux by multiplying HC and the driving force ( $TH - TS$ ). Experimentally,  $TH$  drops by about 4% of its initial value, therefore the value that the model predicts for HC must be low relative to the true value. Second, the experimental pressure actually exceeds the nominal target and this makes a contribution to the true value for HC but not for the calculated value for HC. Thus, the thermal and mechanical pressure lags of the physical system are not completely described by the model.

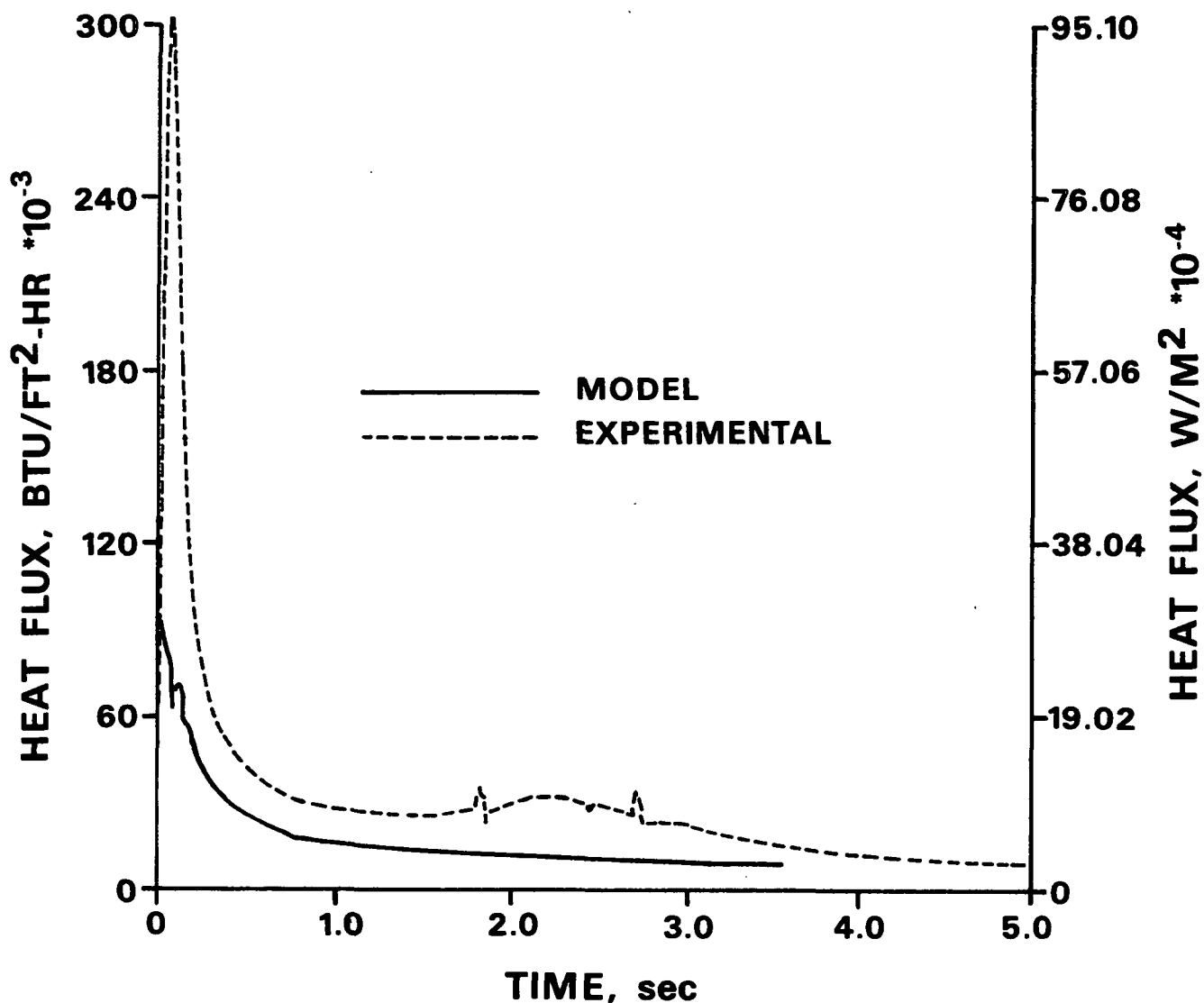


Figure 27. Predicted and measured heat flux for 149°C (300°F) ramp-and-hold pressure pulse.

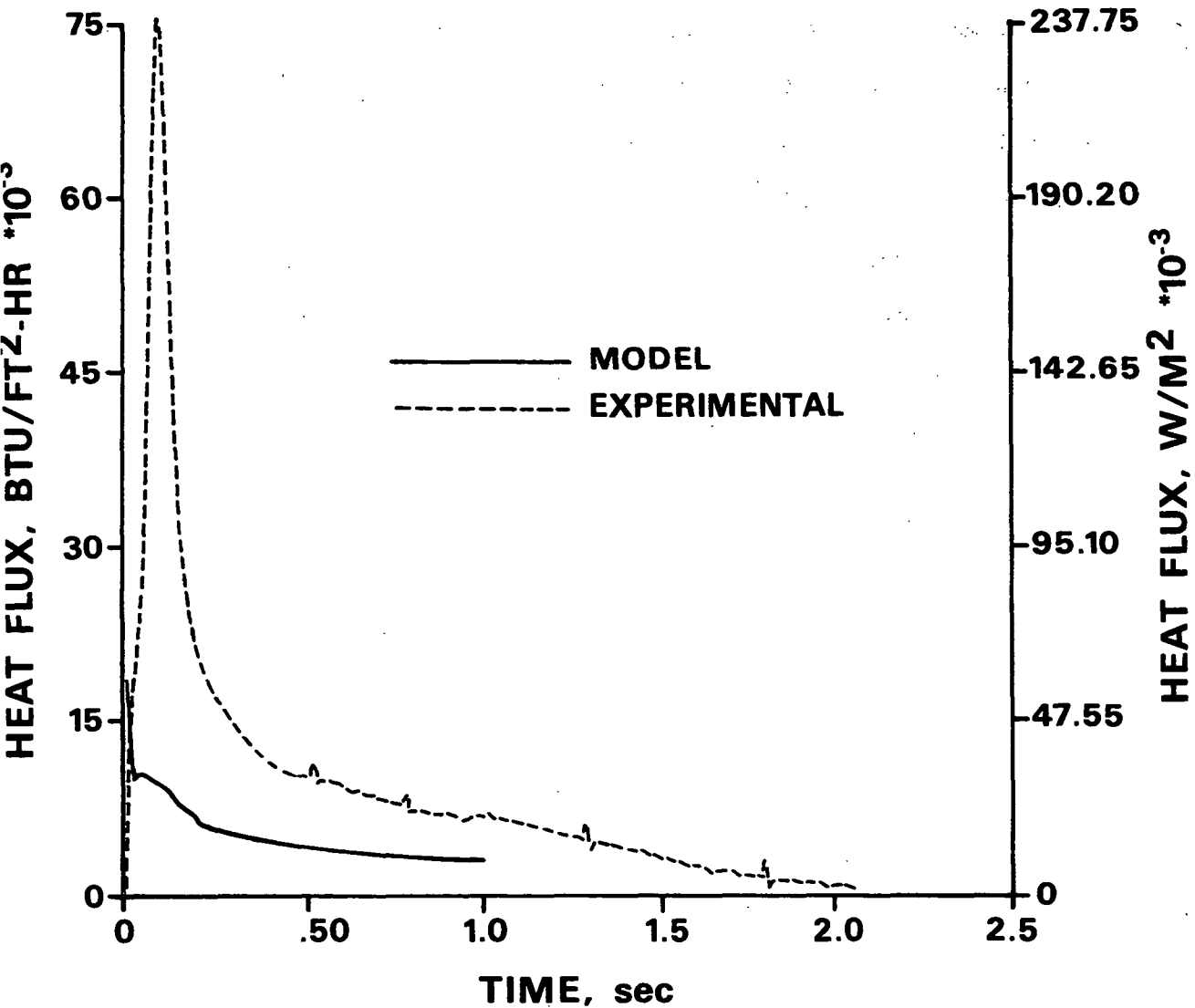


Figure 28. Predicted and measured heat flux for 274°C (525°F) ramp-and-hold pressure pulse.

Figures 29 and 30 show predicted and measured sheet thicknesses. The model curves qualitatively describe the compression pattern: a rapid compression ending in an abrupt change in compression rate followed by a moderate compression regime ending in an accelerating rate of compression followed by a quasi-equilibrium regime. The first regime results from the rapidly rising mechanical pressure. As the pressure attains the target value, heat transfer to the sheet begins to raise the hydraulic (vapor) pressure and the mechanical pressure plateaus, both of which slow the compression. Later, the heat flux drops, the interfaces move



into the sheet, moisture removal is dominated by liquid dewatering, and the vapor pressure decrease in the sheet increases the rate of compression. As the sheet enters the regime of drying by evaporation only the rate of moisture loss slows and the quasi-static compression regime starts. Quantitatively, the model underpredicts the initial sheet thickness and overpredicts the equilibrium thickness. This suggests a decrease in the M compression value and an increase in the N compression value would be appropriate so that the lower M value would dominate at lower pressures and the higher N value would dominate at higher pressures.

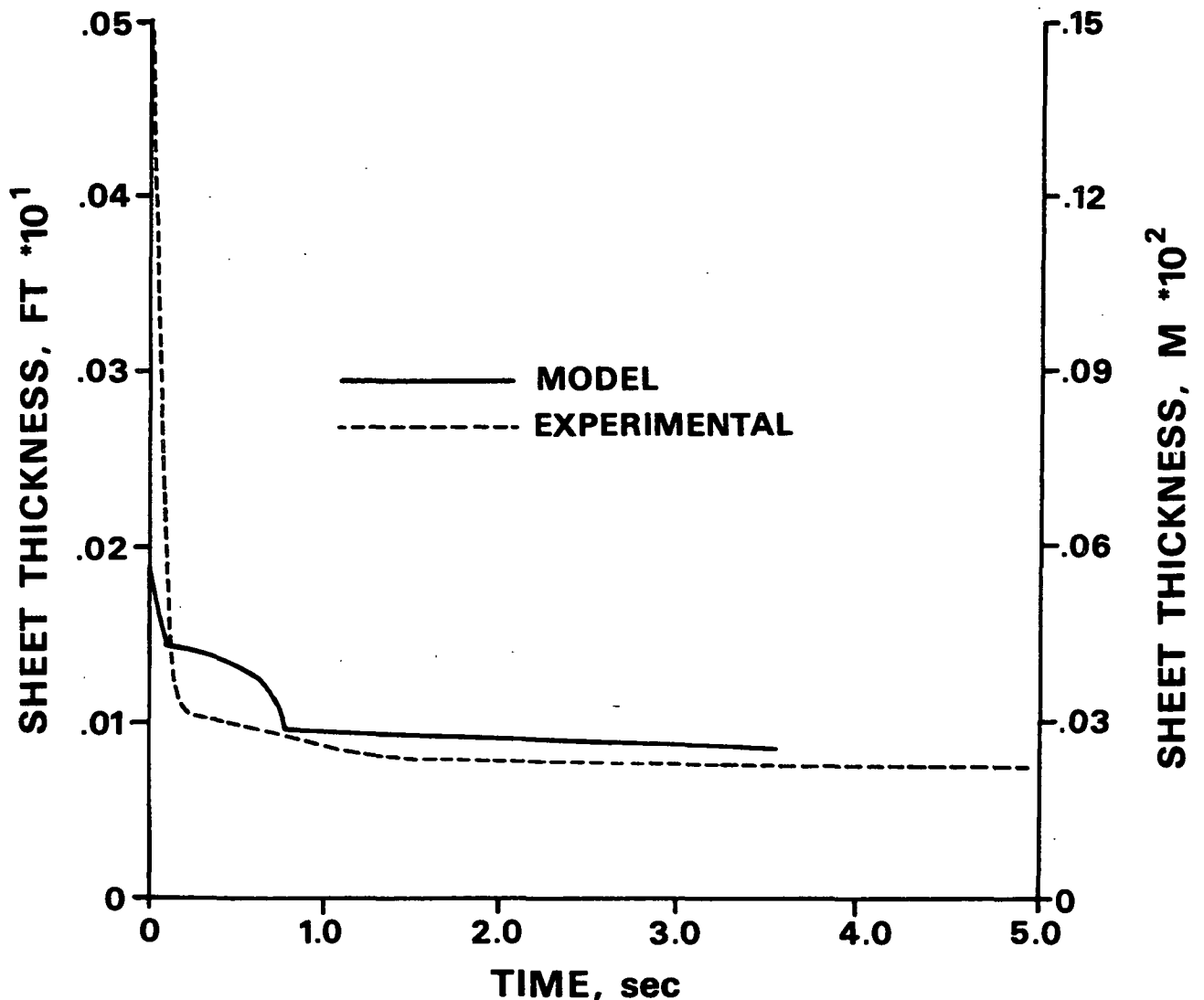


Figure 29. Predicted and measured sheet thickness for 149°C (300°F) ramp-and-hold pressure pulse.

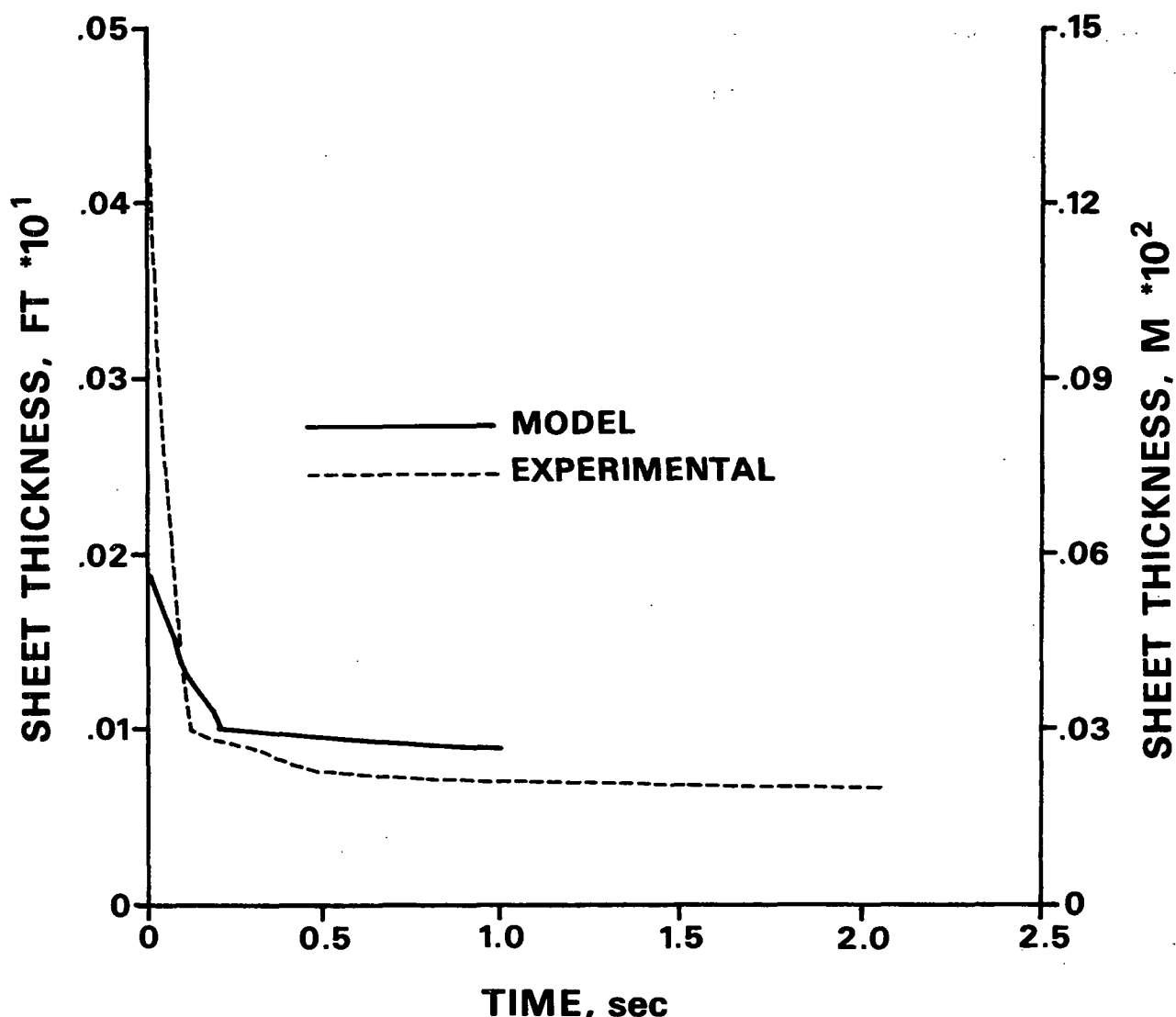


Figure 30. Predicted and measured sheet thickness for 274°C (525°F) ramp-and-hold pressure pulse.

Figures 31 and 32 again show that the model qualitatively describes these drying conditions. The temperature at a point midway through the basis weight of the sheet is plotted for both cases. The experimental curves indicate that the rate of heat transfer to the interior of the sheet is much higher than that predicted by the model. This is probably due to the model's assumption of no vapor flow through the outer zone during the transition regime. The large latent heat carried into the zone and released by vapor condensation raises the temperature there much faster than simple conduction would. Including this

effect would complicate the transition regime calculations by introducing a source term in the transient heat transfer equation and by requiring a more complicated mass balance (since the moisture ratio would be changing) but would be a reasonable next step in improving the model.

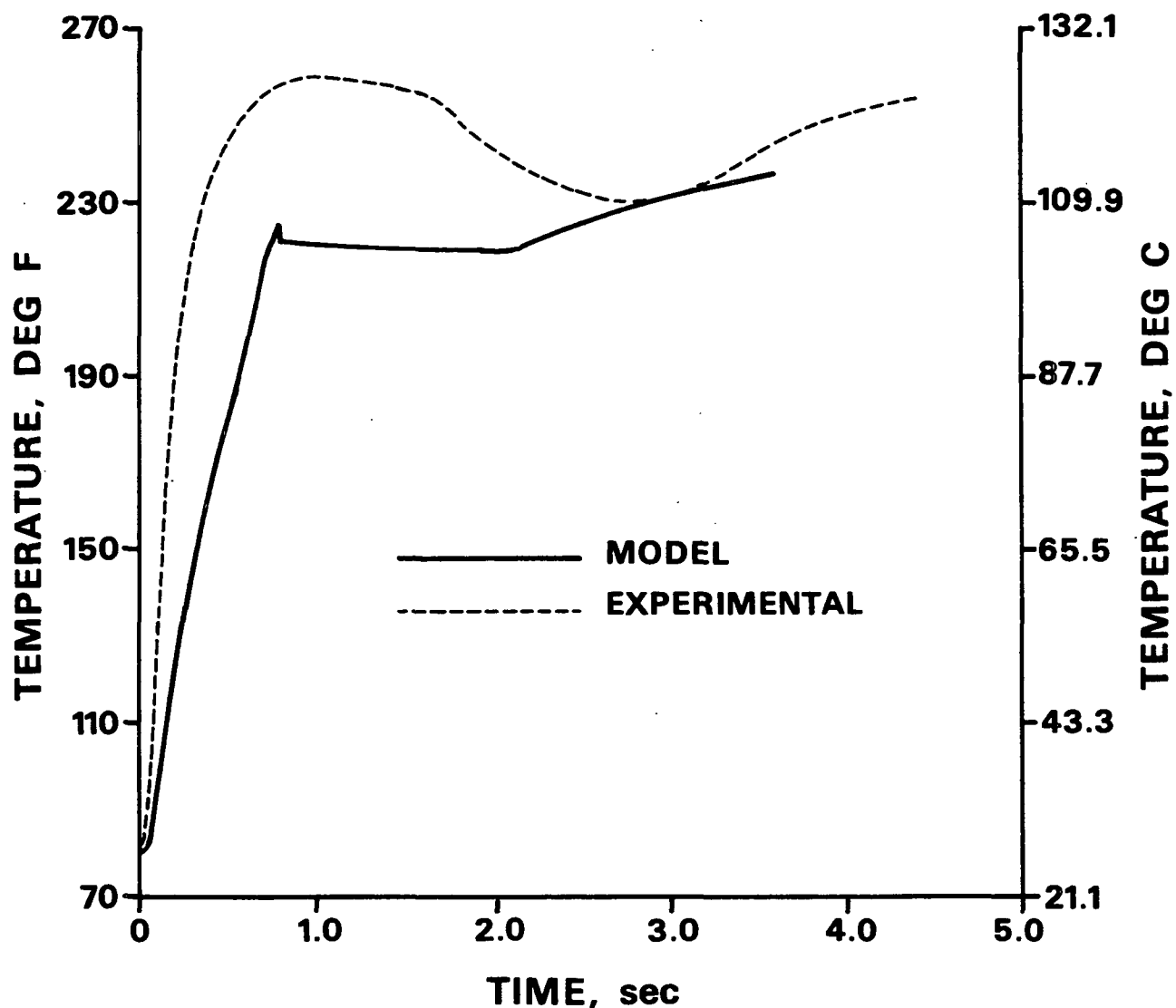


Figure 31. Predicted and measured midpoint temperature for 149°C (300°F) ramp-and-hold pressure pulse.

To demonstrate the effect of the proposed changes to the model, constants in the model were simultaneously modified by 10% of their original values. The reference values for contact coefficient and the N compression constant were increased. The apparent cell wall density, the absolute permeability, and the M

compression constant were decreased. To simulate the transport and condensation of vapor in the outer zone, the thermal conductivity was modified by the addition of a diffusion term for the heatup period<sup>94</sup> and a bulk vapor flow term for the transition period.<sup>95</sup> This combined "effective" conductivity can be orders of magnitude larger than the simple conductivity and should greatly increase heat transfer to the interior of the sheet. Note that no attempt was made to account for any changes in saturation from the condensing vapor. This approximation is reasonable because the large latent heat implies that only a small amount of condensation is necessary to produce a large change in temperature.

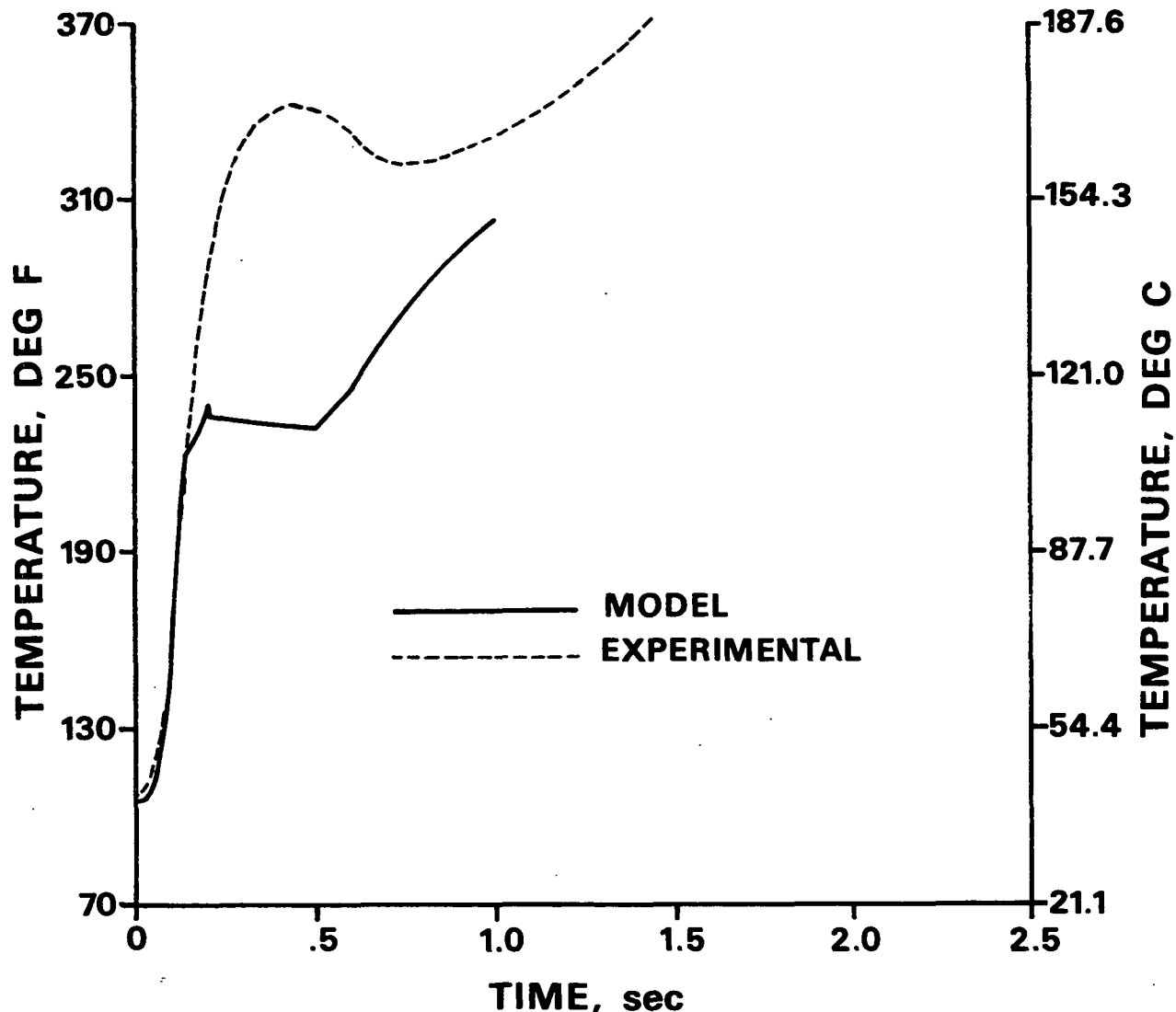


Figure 32. Predicted and measured midpoint temperature for 274°C (525°F) ramp-and-hold pressure pulse.

The results of this "optimization" are shown in Fig. 33 through 40 for the ramp-and-hold pressure cases. Figures 33 and 34 display the changes in drying behavior caused by the modifications. In both cases there is little effect on heatup time, since the diffusion term augmenting thermal conductivity is relatively small. The transition time is greatly reduced because the bulk flow term augmenting conductivity is very large. Trapping more water in the fibers causes a decrease in the amount of moisture removed in liquid form (from 80% down to 70%), and increases the drying time, since more moisture has to be removed by an evaporation mechanism.

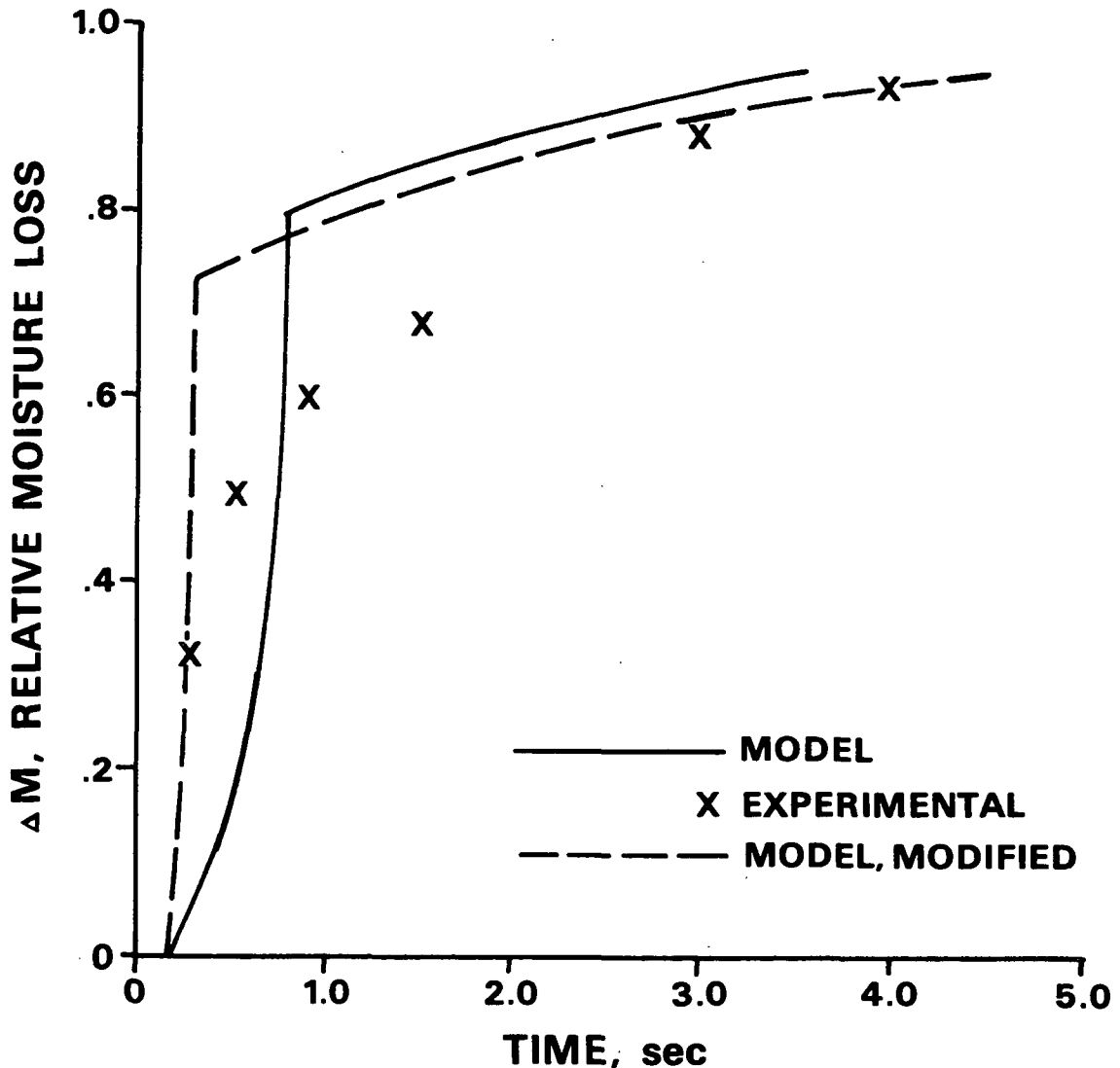


Figure 33. Predicted, measured, and modified model moisture removal for 149°C (300°F) ramp-and-hold pressure pulse.

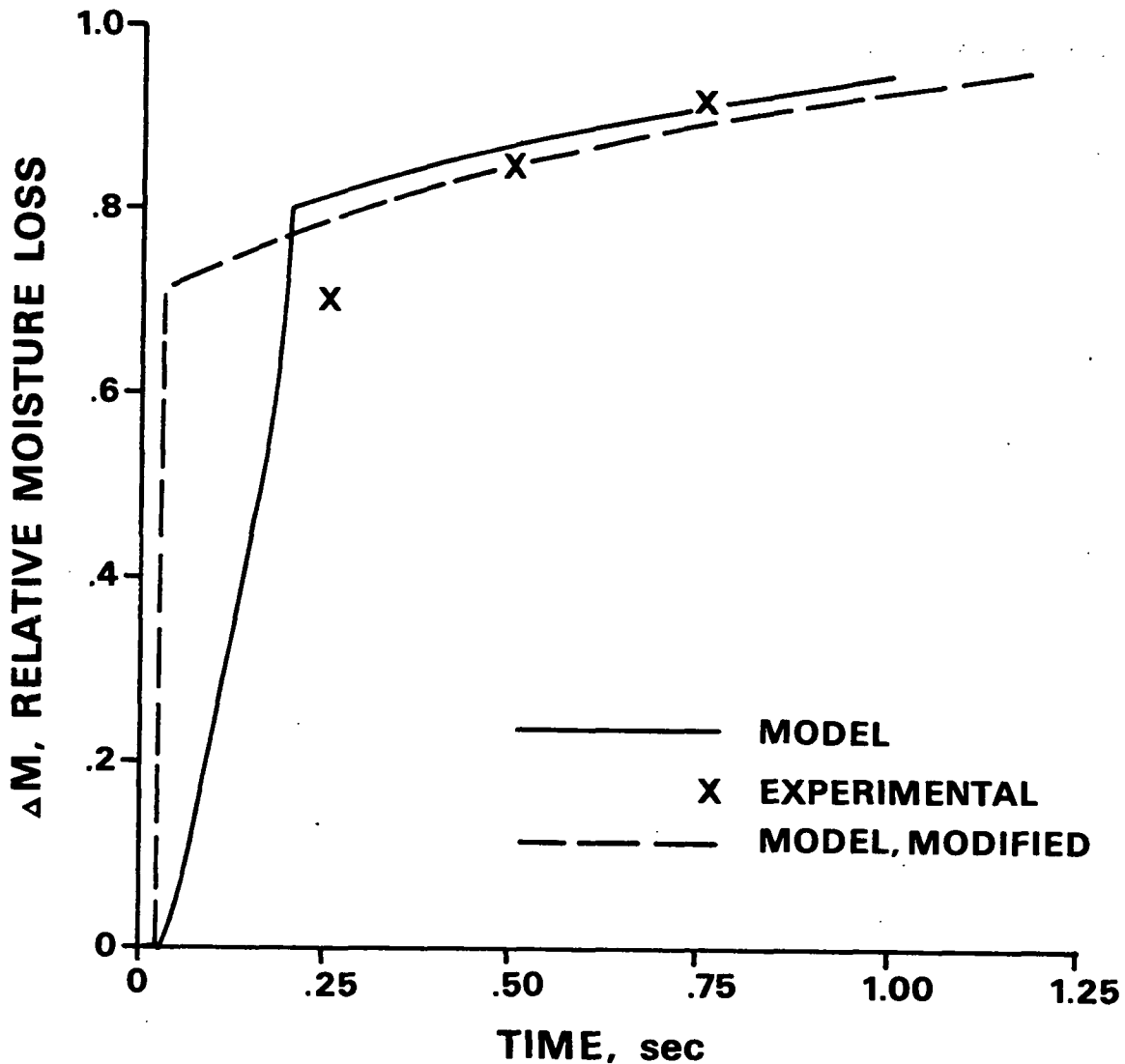


Figure 34. Predicted, measured, and modified model moisture removal for 274°C (525°F) ramp-and-hold pressure pulse.

Figures 35 and 36 show the influence on heat flux. In the 149°C (300°F) case the heat flux is decreased, which is the opposite of the anticipated trend. The change in compression constants causes a general increase in porosity and therefore an overall decrease in the contact coefficient even though the reference values for  $H_c$  were increased by 10%. In the 274°C (525°F) case, there is little effect because the higher driving force ( $T_H - T_S$ ) tends to mask the influence of changes in the  $H_c$  reference values and compression constants.

Figures 37 and 38 depict the changes in predictions of sheet thickness. Changing the constants causes a slight increase in the initial thickness

prediction and significant changes in the slope and duration of the intermediate compression regime. The increase in N is not enough to offset the decrease in M and the modified model predicts an even higher thickness in the third compression regime. The slope is also changed in the third regime and shows a more rapid compression in the later stages of drying.

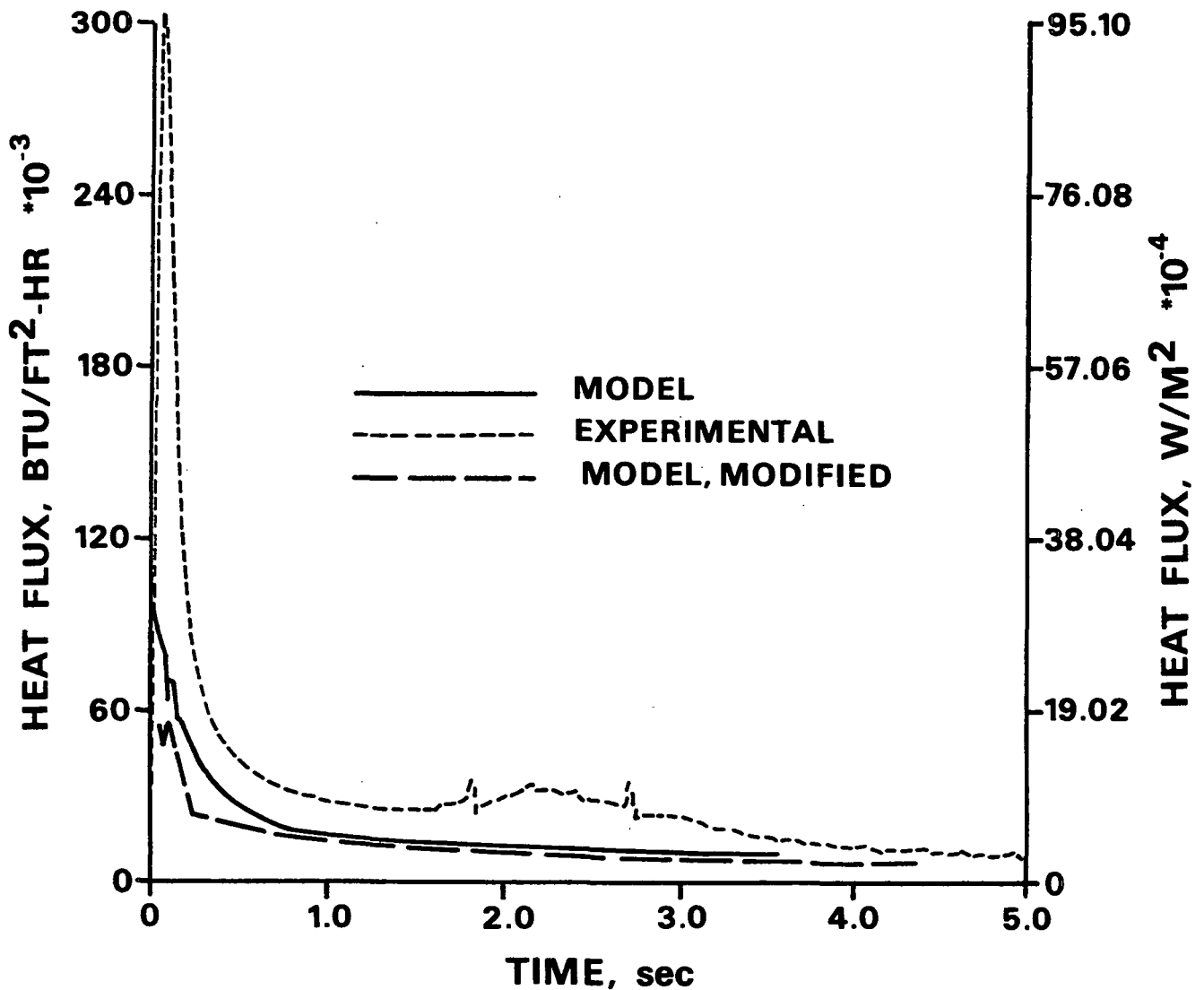


Figure 35. Predicted, measured, and modified model heat flux for 149°C (300°F) ramp-and-hold pressure pulse.

Figures 39 and 40 graph the effects of the modifications on the prediction of midpoint temperature. The first-peak midpoint temperature is significantly increased and the time required to achieve the peak is decreased. The duration of the predicted plateau period is increased. In a qualitative sense, the

changes benefit the lower temperature case more than the higher temperature case. This tends to indicate that the initial values for most constants were reasonable and that it is a change in mechanism going from lower temperature to higher temperature (such as the relative importance of capillary liquid flow) that causes the difference between measured and predicted behavior. Since the assumptions of HIDRYER1 are more appropriate to the higher temperature case, changing the constants should be expected to shift it away from its initially reasonable qualitative fit.

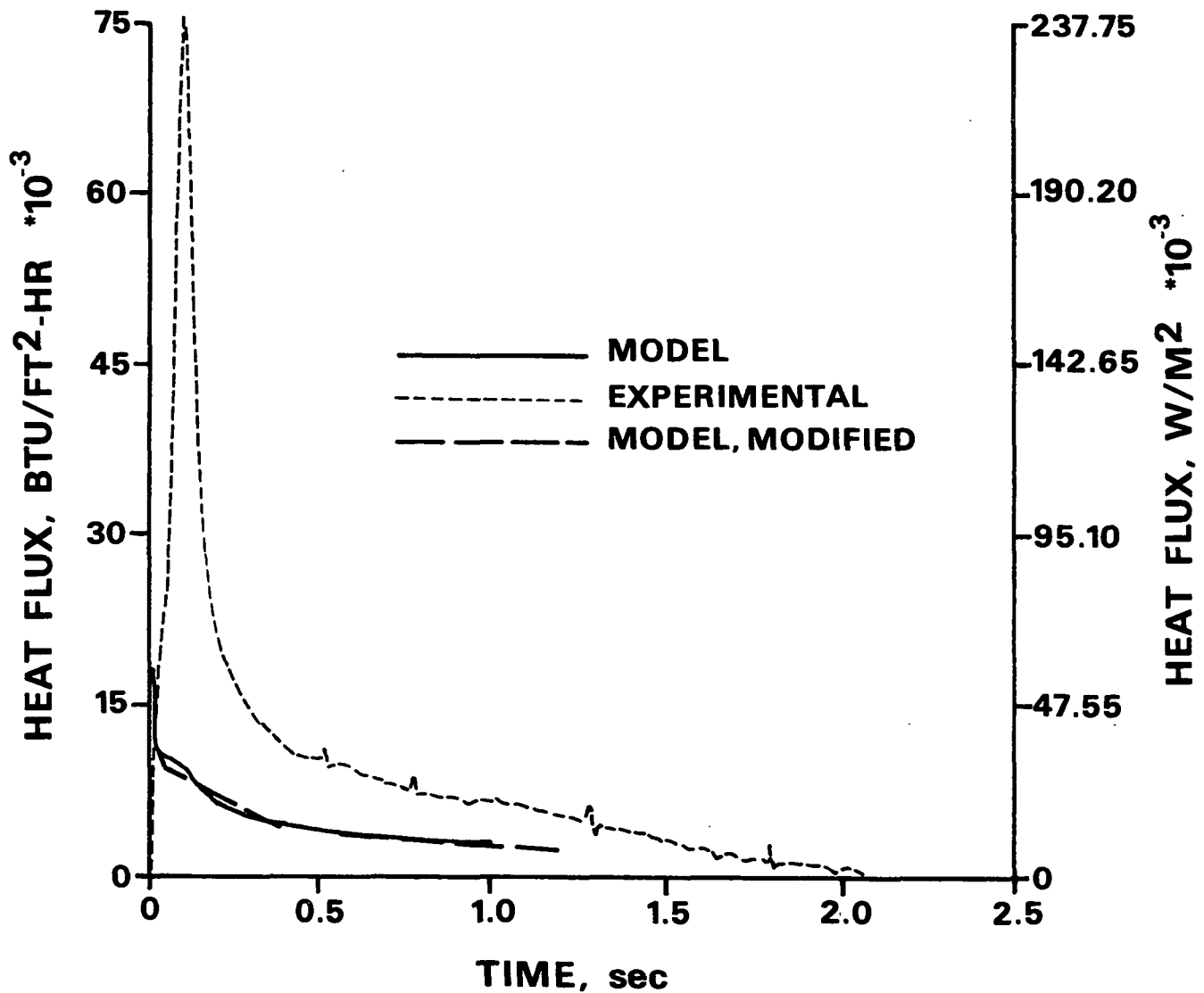


Figure 36. Predicted, measured, and modified model heat flux for 274°C (525°F) ramp-and-hold pressure pulse.



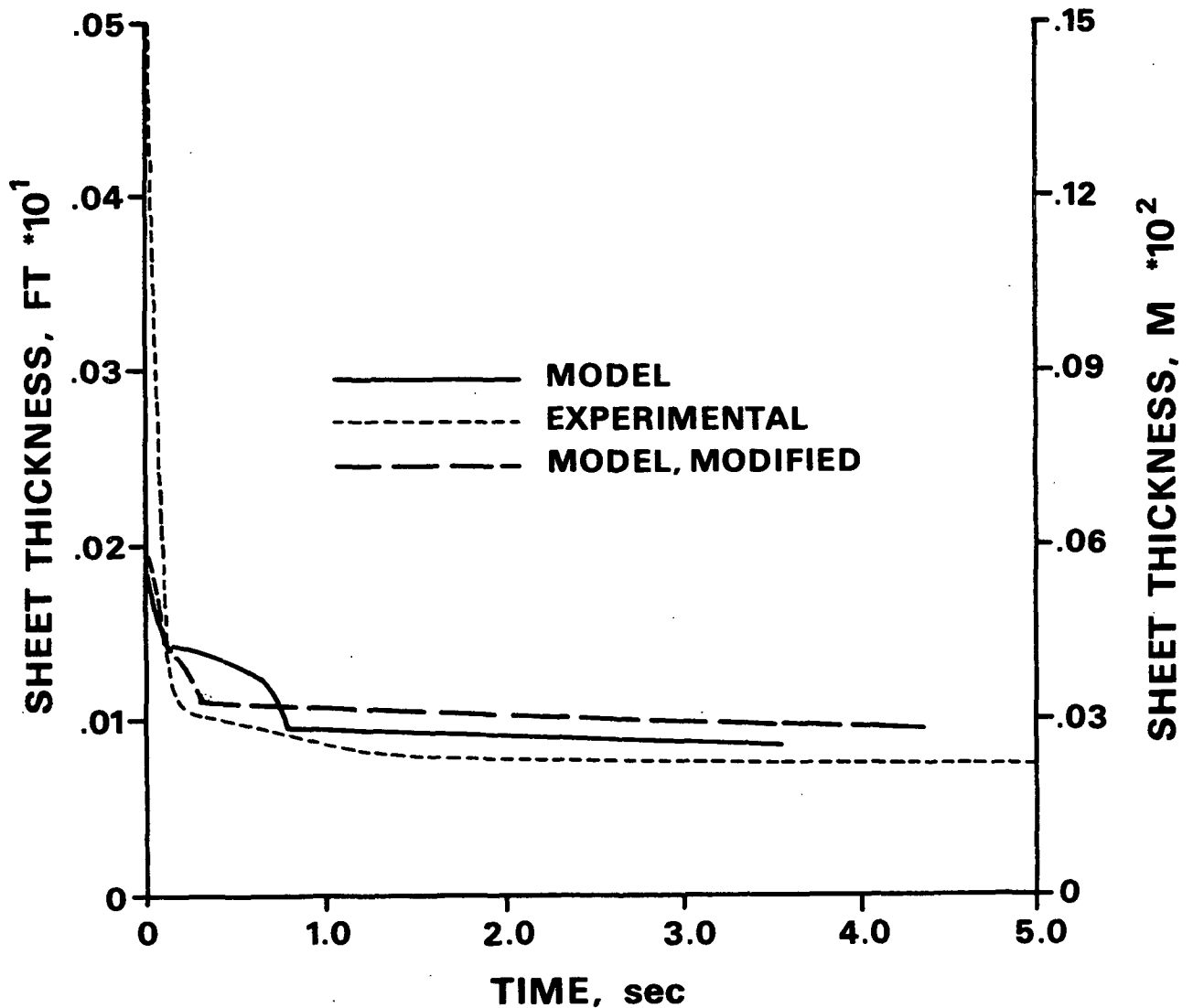


Figure 37. Predicted, measured, and modified model sheet thickness for 149°C (300°F) ramp-and-hold pressure pulse.

The previous figures clearly show that the model can be easily modified to alter its predictions by changing the constants in the model. An optimization of these constants in conjunction with further experimental information should be able to produce a highly accurate predictive tool.

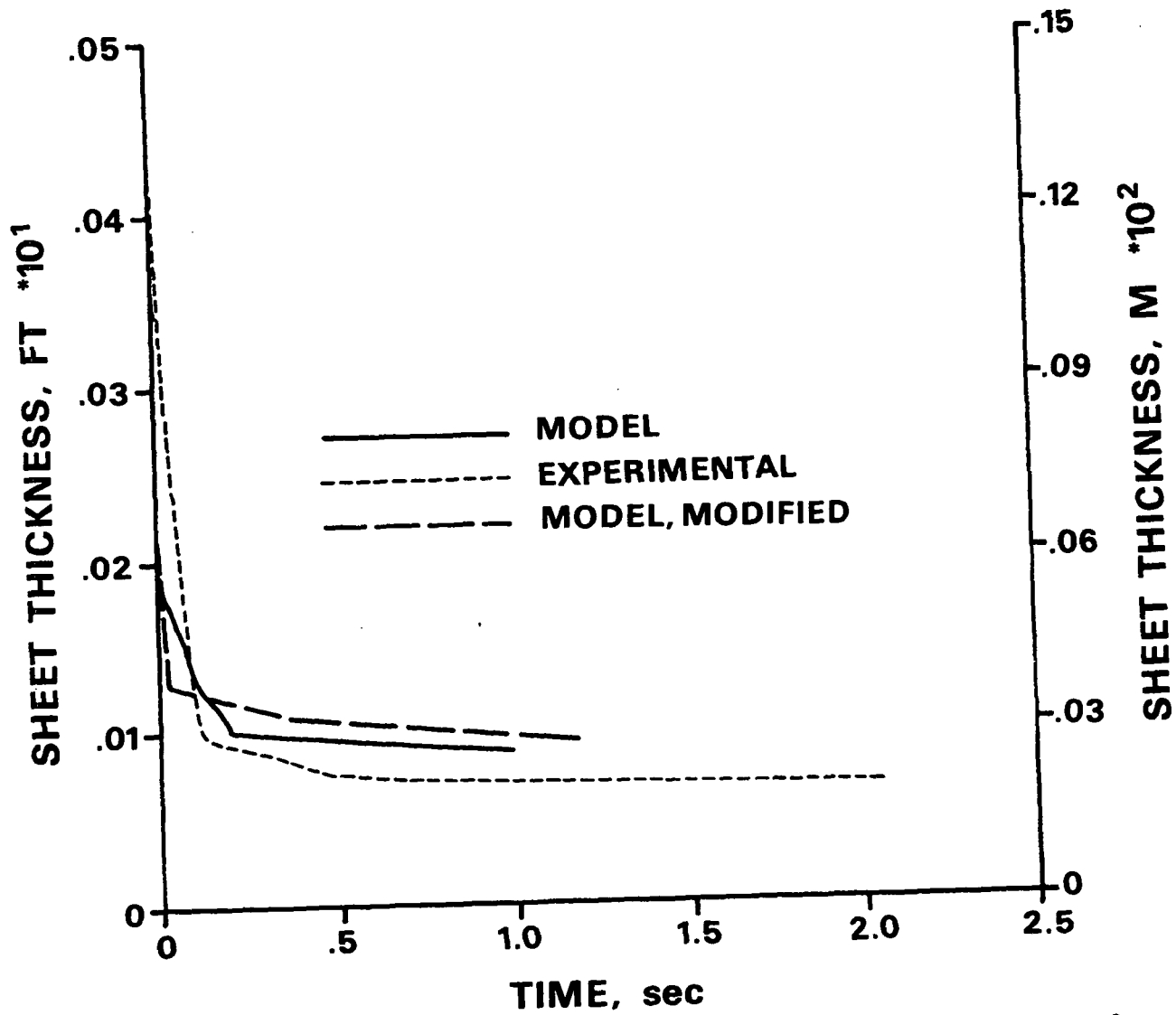


Figure 38. Predicted, measured, and modified model sheet thickness for 274°C (525°F) ramp-and-hold pressure pulse.

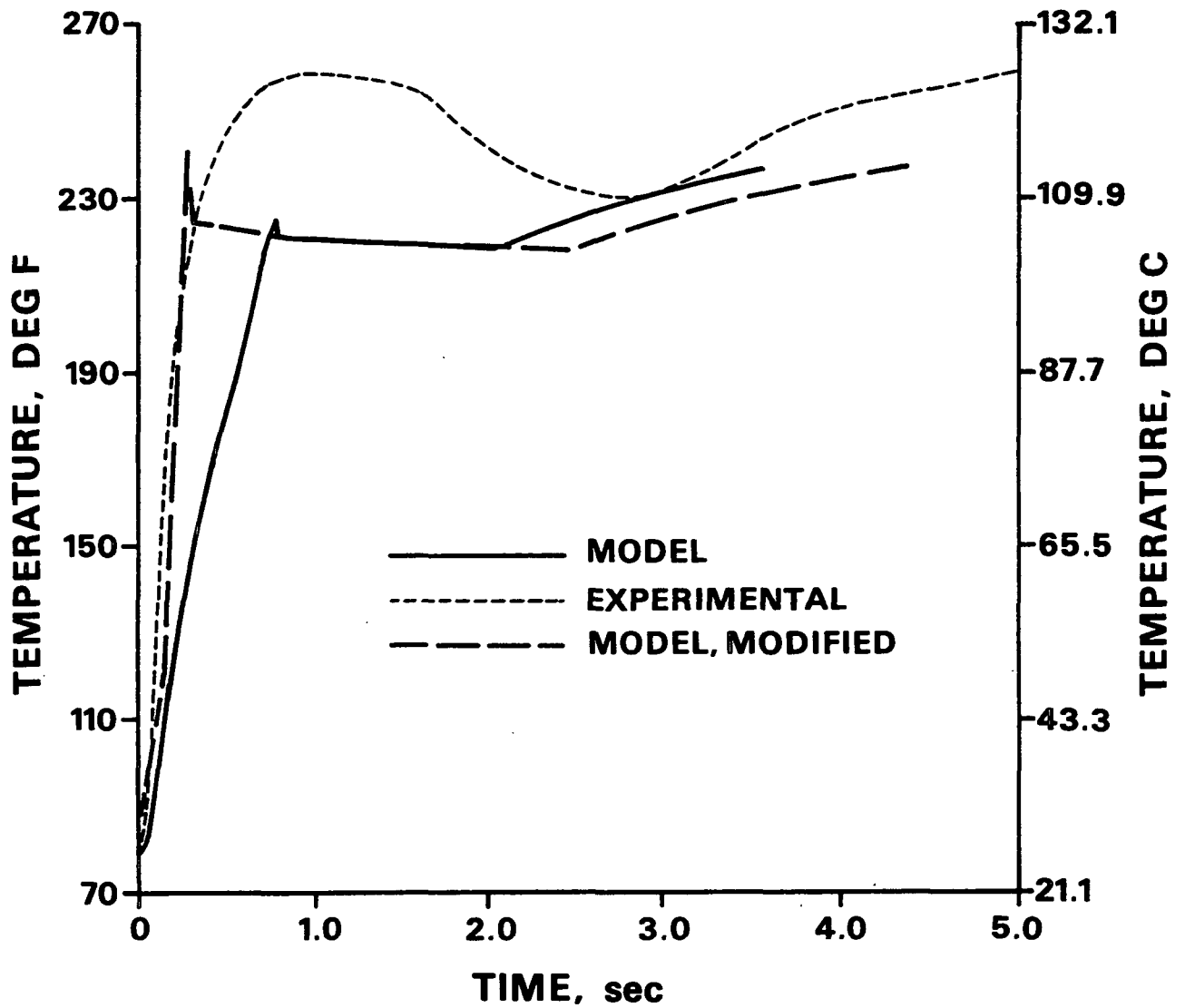


Figure 39. Predicted, measured, and modified model midpoint temperature for 149°C (300°F) ramp-and-hold pressure pulse.

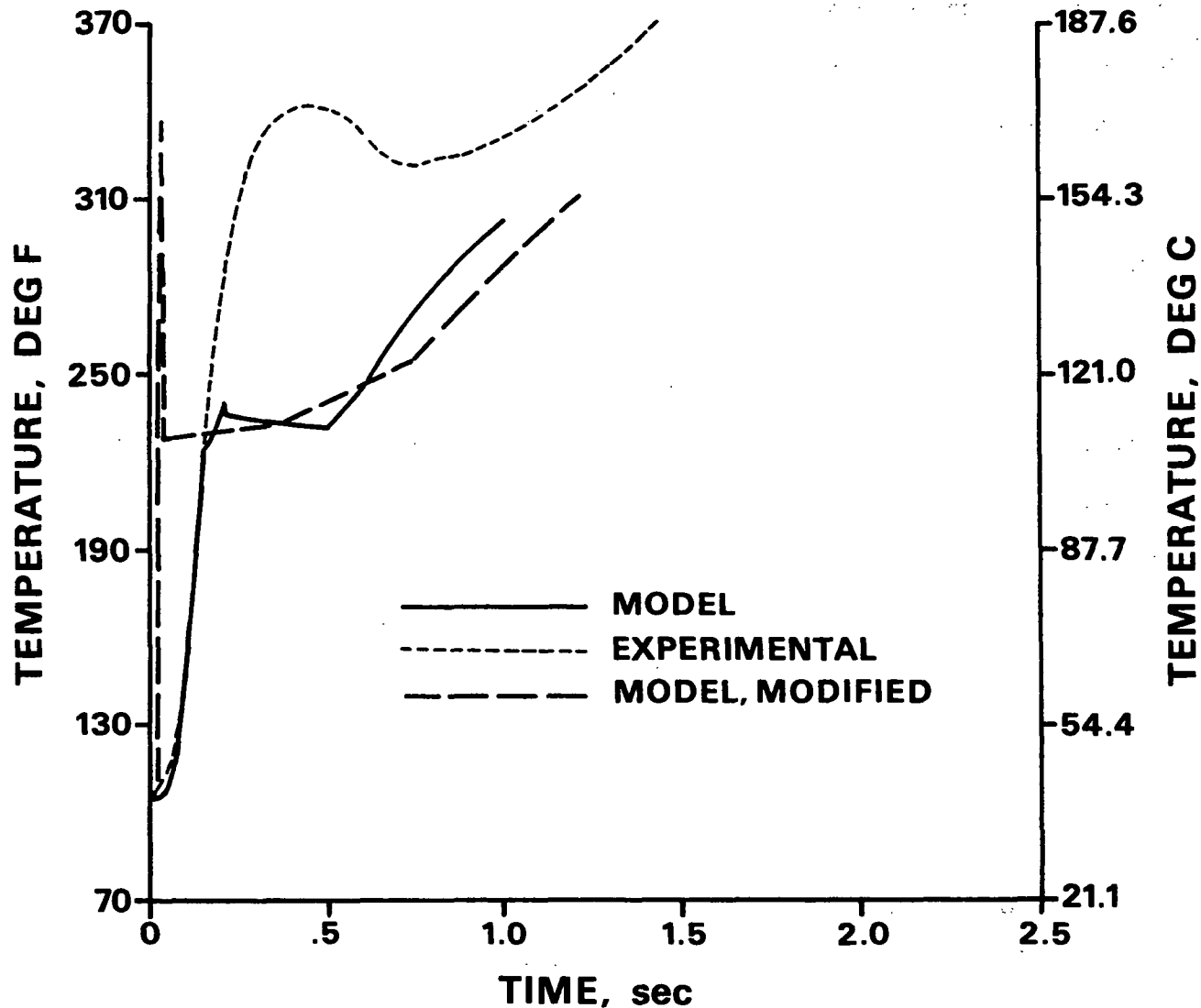


Figure 40. Predicted, measured, and modified model midpoint temperature for 274°C (525°F) ramp-and-hold pressure pulse.

#### SHORT DURATION (IMPULSE) PRESSURE PULSE

The time scale for the application of the mechanical pressure pulse in impulse drying is an order of magnitude shorter than the ramp-and-hold method. Rise times of a few milliseconds are possible. The heat and mass transfer phenomena that take place in both circumstances are fundamentally the same, but because of the dynamic nature of the impulse process the compression properties of the sheet assume great importance. The moisture loss by mechanical compression is

greater in the impulse case and the resulting sheet properties tend to be different. The impulse process is conceptually more identifiable with a (very high temperature) "heated wet pressing" operation than with a "drying" operation.

Figures 41 and 42 show comparisons of experimental and predicted sheet thicknesses for impulses delivered by a drop press simulator<sup>3</sup> at two hot surface temperatures.<sup>96</sup> Figure 42 corresponds to a wet pressing case since the temperature is only 18°C (65°F). The difference in magnitudes for the predicted and experimental results comes from the values used for M and N in the model and because the model calculates the thickness at every point in time (i.e., there is no initial thickness input to the model). If the model curve is simply shifted vertically so that the initial predicted thickness matches the initial measured thickness, a better comparison can be made. This is also shown in Fig. 41 and 42. Note that this method could be built into the model by supplying the initial thickness and correcting the model's predictions by a constant value equal to the difference between initial measured and predicted thicknesses. (An alternative would be to supply the initial measured thickness and modify M and N so that the initial predicted thickness would match.) Apart from the difference in magnitudes, the model exhibits an elastic type of behavior consistent with its compression equation. The experimental result shows how the paper fails to recover after the peak pressure has been achieved. This is due in part to the viscous nature of the fiber matrix and in part from irreversible alterations in the matrix structure. The depression in the center of the predicted curve results from the combination of rapid rate of change in pressure and N (which is a function of pressure) as the peak pressure is reached.

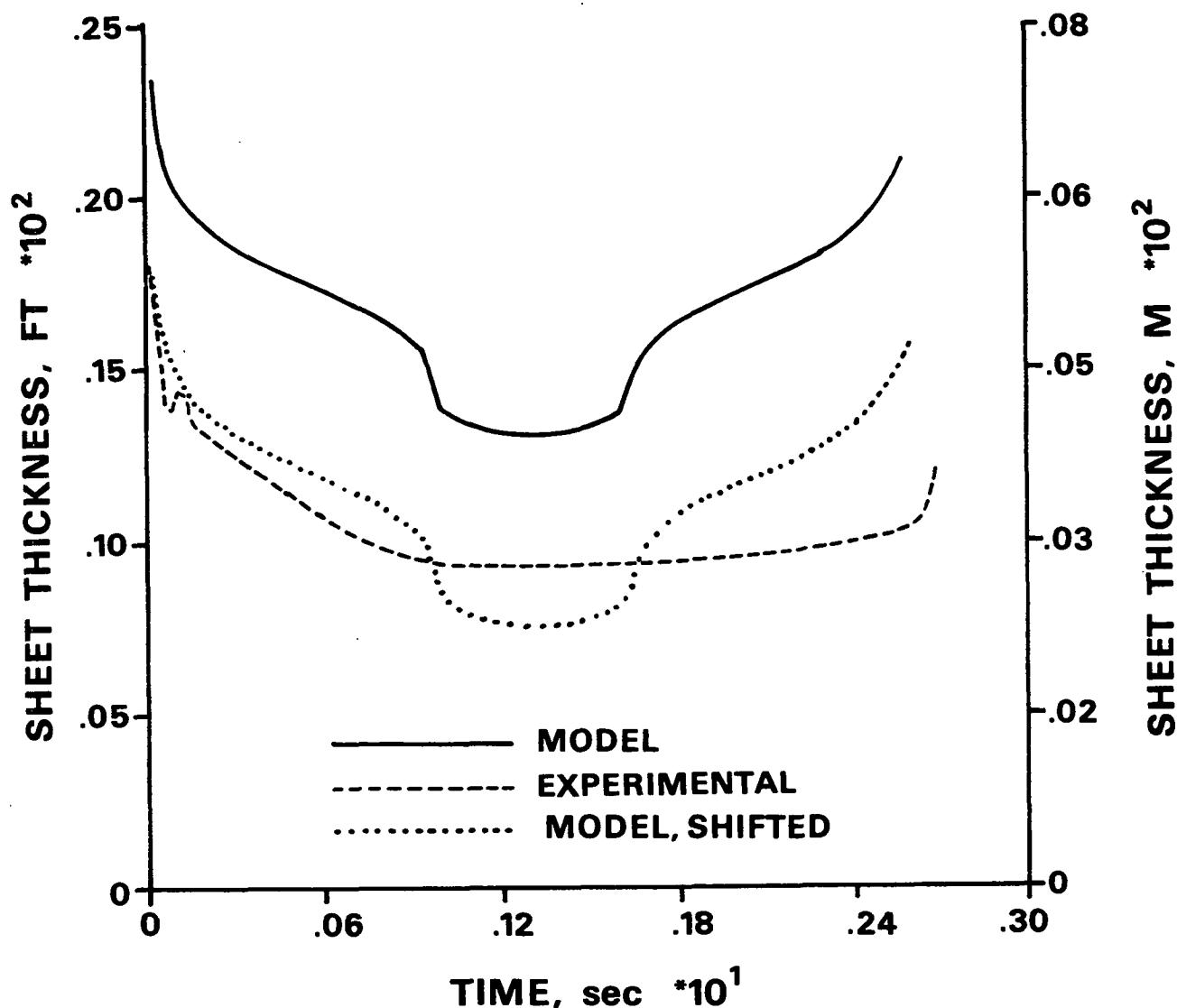


Figure 41. Predicted and measured sheet thickness for 18°C (65°F) impulse case.

In the 316°C (600°F) case, Fig. 42, the model more closely mimics the experimental result in a qualitative sense. Thermal softening at the elevated temperature moderates the rapid change in thickness as the peak pressure is attained. The model predicts a faster rate of compression in this case and a slower rate of thickness recovery relative to the lower temperature case. The experimental measurements show about the same rates in both cases. The model predicts a somewhat lower minimum thickness in the higher temperature case, which is the opposite of the experimental result. The model results are directly related to

the use of a compression equation in a drying model instead of using a heat transfer equation in a dynamic wet pressing model. A compression equation does not fully describe the internal sheet behavior to the extent necessary for direct application to impulse conditions.

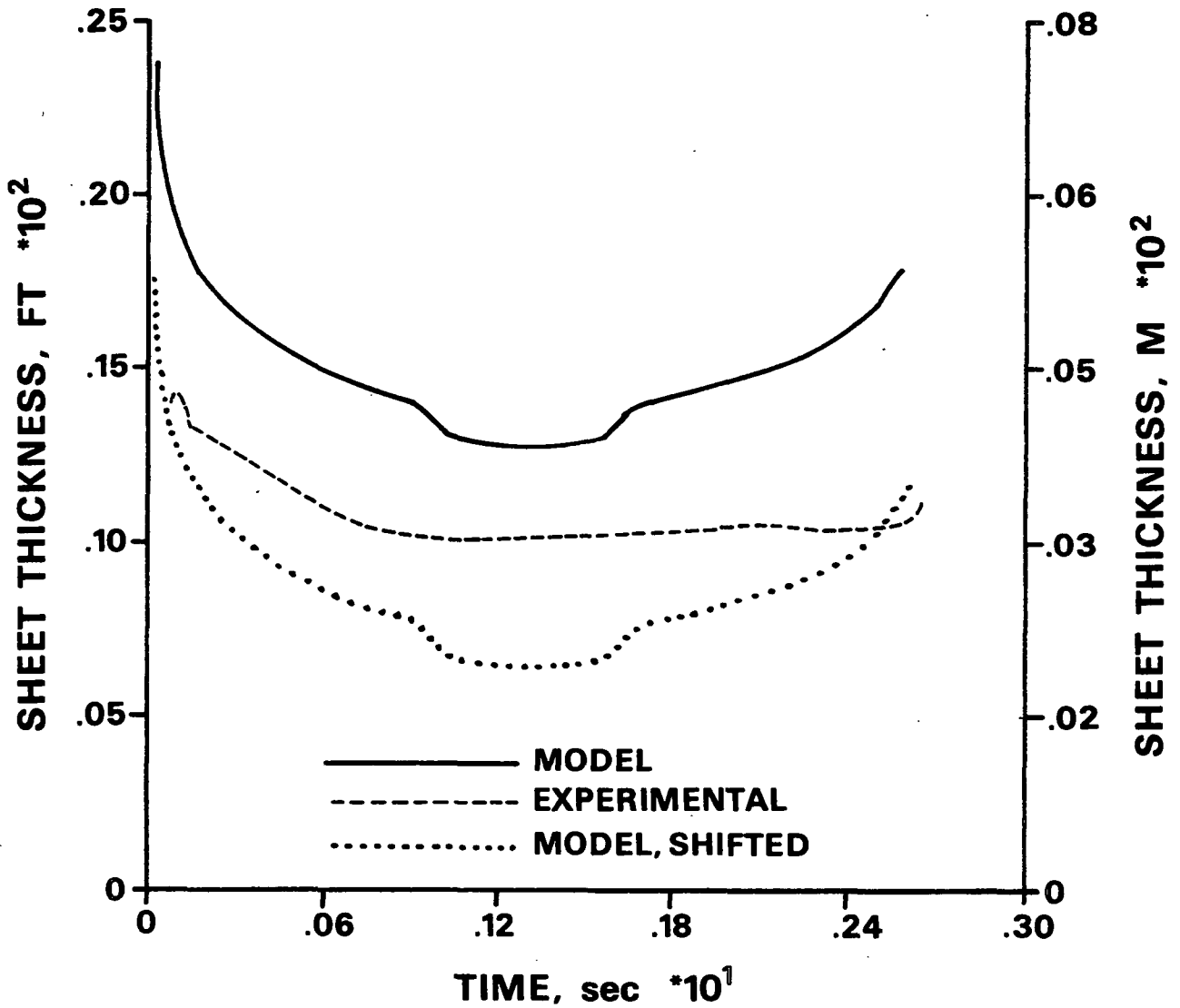


Figure 42. Predicted and measured sheet thickness for 316°C (600°F) impulse case.

Figure 43 shows the results from experiments in a heated, rotating roll press nip.<sup>97</sup> Equivalent dewatering can be achieved at many combinations of hot surface temperature and nip residence time.

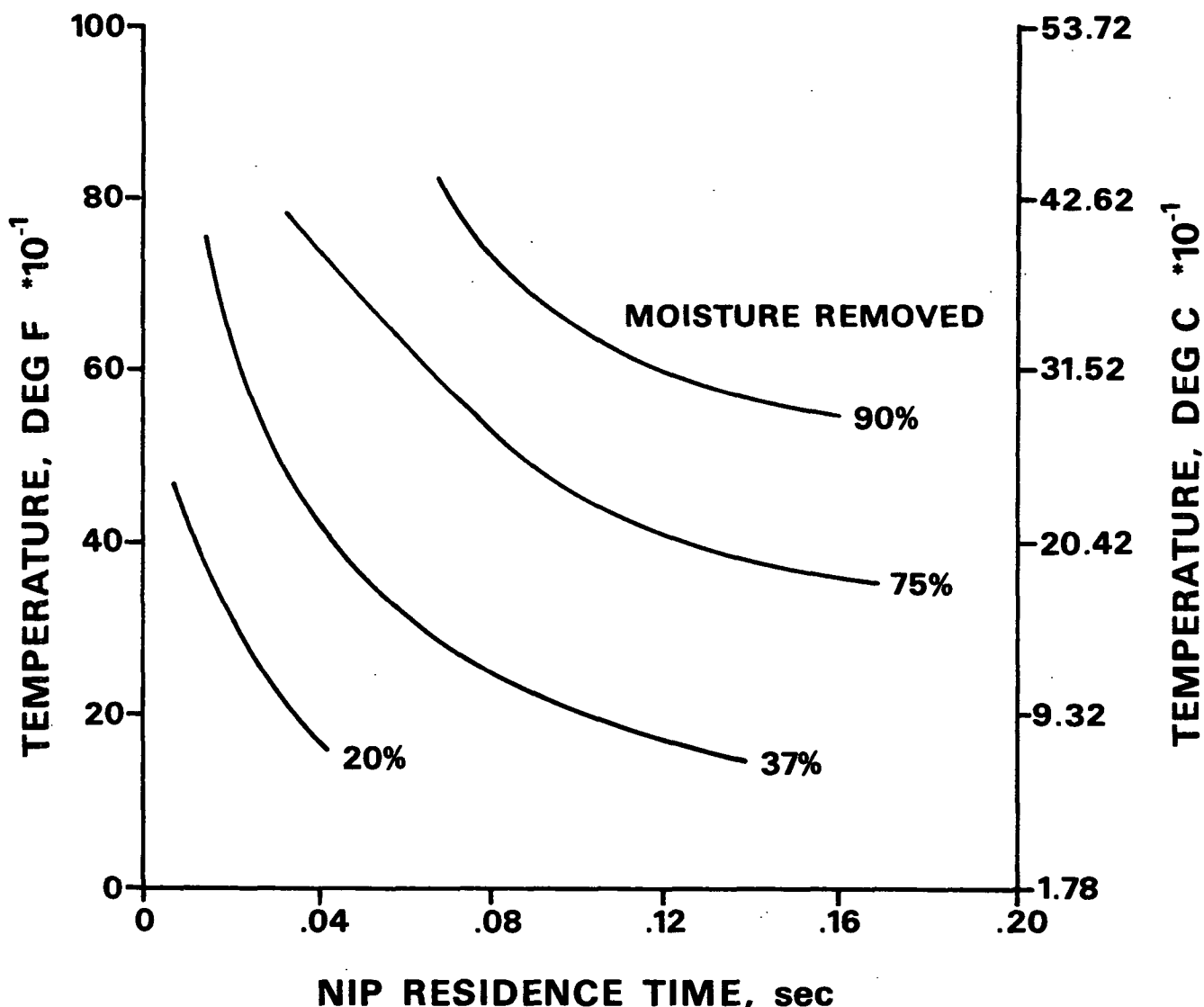


Figure 43. Impulse drying moisture removal for various combinations of hot surface temperature and nip residence time.

Table 4 summarizes the model's dewatering predictions for a variety of operating conditions selected from Fig. 43. The basis weight is 100 g/m<sup>2</sup> (0.0205 lbm/ft<sup>2</sup>); moisture ratio is 1.381; freeness is 570 CSF; and P<sub>MAX</sub> is 12144 kPa (1760 psi). There are certain combinations of time and temperature which cause the model to predict an apparent zone 3 density which is greater than the (assumed constant) effective fiber wall density of 1 g/cc. The higher temperature cases can complete the calculations at shorter nip residence times than the lower temperature cases. This is a consequence of the rate of dewatering (rates of heat transfer and vapor pressure generation) relative to the rate of compression.



Table 4. Comparison of predicted and measured moisture removal for impulse drying conditions.

<u>TH, °C (°F)</u>	<u>Nip Residence Time, s</u>	<u>Experimental Moisture Removal, %</u>	<u>Model Moisture Removal, %</u>
149 (300)	0.020	20	55 <sup>a</sup>
	0.060	37	33 <sup>a</sup>
204 (400)	0.011	20	30 <sup>a</sup>
	0.042	37	58 <sup>a</sup>
	0.130	75	75
260 (500)	0.030	37	64 <sup>a</sup>
	0.083	75	82
316 (600)	0.022	37	76
	0.063	75	83
	0.114	90	89
371 (700)	0.016	37	0 <sup>a</sup>
	0.044	75	83
	0.082	90	88

<sup>a</sup> Computation terminated when zone 3 porosity becomes lower than the minimum allowable porosity.

Higher temperatures produce faster drying and higher hydraulic (vapor) pressures before the critical density is achieved by compression so that these cases can run to completion. At a basis weight of 50 g/m<sup>2</sup> (0.01025 lbm/ft<sup>2</sup>) the model runs to completion but predicts no dewatering, even at 316°C (600°F) and 4137 kPa (600 psi), when the nip residence time is 5.4 milliseconds. Experimental moisture removals of up to 80% have been demonstrated for these conditions.<sup>98</sup>

In Table 4 all model cases overpredict the amount of moisture removed but the trend of increasing removal with increasing time is intact. The overprediction is a function of the assumed fiber wall density which determines the amount of (trapped) moisture unavailable for liquid flow. Decreasing the density would lower the amount available for flow but would raise the minimum porosity (lower

the effective critical density). The model therefore needs to be modified to treat both a compressible matrix, so that sheet thickness is a function of mechanical pressure; and compressible fibers, so that the liquid available for flow becomes a function of mechanical pressure and the limiting density is the density of cellulose (at a porosity of zero).

#### SUMMARY

HIDRYER1 gives good qualitative agreement with experimental results. The quantitative agreement could be improved by varying some of the constants used in the model and modifying the model to account for the phenomena of vapor flow and condensation during the transition regime and liquid expression from the fiber walls.

## SUMMARY

This mathematical model is a significant first effort in the development of a convenient predictive tool for investigating high intensity drying options. The zone concept and simple solution method provide a methodology and framework for easy modification, expansion, and improvement.

The model requires few input parameters (hot surface temperature, boiling point temperature, basis weight, Canadian Standard Freeness, initial moisture ratio, mechanical pressure pulse) and qualitatively accounts for the observed macroscopic phenomena: internal sheet temperature, heat flux, sheet thickness, and moisture removal in liquid and vapor form. The degree of quantitative agreement varies with drying conditions. The agreement with all experimentally measured quantities could be improved by the specific suggestions in the thesis using a mathematical optimization procedure (with the empirical results as constraints on the output).

Capillary liquid flow appears to be significant at lower hot surface temperatures. Vapor flow with condensation appears to be significant during the transition regime under all conditions. A better model of dynamic sheet compression at high temperatures needs to be developed and tested.

## RECOMMENDATIONS

The first extension of this work should be the modification of HIDRYER1 to run faster. This could be accomplished in several ways. The number of finite difference grid points could be reduced; the number of iterations for the calculation of the interface temperatures could be reduced; an alternative to the finite difference method could be used; or a reorganization of the computational algorithm could be performed. Any reduction in the CPU time would encourage more use of the model and allow a more comprehensive parametric investigation.

Second, a mathematical optimization of the model's constants would yield improvements in its quantitative predictions. There is already enough empirical evidence to make a reasonable effort in this area.

The third area for future research involves permeability. Transport models for paper have been limited in that a thorough investigation of the factors (freeness, moisture ratio, etc.) affecting permeability has not been performed. Isolated efforts are apparent, but are limited in scope and depth.

The fourth area is related to the compression properties of paper. The quantitative effects of moisture ratio, temperature, mechanical pressure, and freeness for a wide range of conditions are unknown. Each should be investigated individually and in combination to cover the complete range of process possibilities from wet pressing to high intensity drying.

#### ACKNOWLEDGMENTS

I would like to thank The Institute of Paper Chemistry for providing the facilities and financial support for this thesis.

The members of my advisory committee, Nai Chang, Peter Parker, and Douglas Wahren, offered many helpful insights and suggestions. My friend and principal adviser, Fred Ahrens, always found a way to keep me on the right track, whether by example, encouragement, or experience.

Finally, I would like to express my love and gratitude to my wife Deborah and my son Daniel for their endless supply of patience, support, love, and understanding.

# NOMENCLATURE

The abbreviations for SI units in this section are: m (meter), s (second), kg (kilogram), K (kelvin), J (joule), N (newton), W (watt) , and Pa (pascal).

a	fraction of liquid water external to fibers
Al-4	equation constants
b	equation constant
Bl-5	equation constants
BI	heat transfer Biot number
BW	mass of dry fibers per unit sheet area, $\text{kg/m}^2$
BW1-4	BW of individual zones, $\text{kg/m}^2$
C	mass of dry fibers per unit sheet volume, $\text{kg/m}^3$
C1,C2	equation constants
COEFF	arbitrary equation coefficient
CONST	arbitrary equation constant
Cpf	specific heat of cellulose, $\text{J}/(\text{kg K})$
Cpv	specific heat of gas or vapor, $\text{J}/(\text{kg K})$
Cpw	specific heat of liquid water, $\text{J}/(\text{kg K})$
CSF	Canadian Standard Freeness
D	equation constant
Dl-7	equation constants and rates of change
DBWxDT	rate of change of zone x basis weight, $\text{kg/m}^2 \text{ s}$
Dc	equation constant
DIFF'	relative position increment
DIFF''	relative position increment
DT0	default time increment, s

E1,E2	equation constants
F1,F2	equation constants
G1-6	equation constants
H1-4	equation constants
Hc	hot surface to paper contact coefficient, $W/(m^2 K)$
$\Delta h$	latent heat of vaporization, J/kg
$\Delta h'$	incremental latent heat of desorption, J/kg
$\Delta h^*$	average latent heat of desorption, J/kg
I1	equation constant
i'	grid point designation
i''	grid point designation
IMAX	iteration counter
J1-5	equation constants
K	thermal conductivity, $W/(m K)$
K1-3	equation constants or zone thermal conductivities
KAKV	product of $Ka3$ and $Kv$ , $m^2$
KAKW	product of $Ka3$ and $Kw$ , $m^2$
Ka	absolute permeability, $m^2$
Ka2-4	zone absolute permeabilities, $m^2$
Kd	dry zone thermal conductivity, $W/(m K)$
KMIN	minimum number of grid points
Kv	relative gas or vapor permeability
Kw	relative liquid permeability
$\bar{L}$	distance in zone, m
L	zone thickness, m
L1-3	equation constants or zone thicknesses
M	compression equation constant, $(kg/m^3)/Pa^N$

M'	modified M value, $(\text{kg}/\text{m}^3)/\text{Pa}^N$
M1	equation constant
Mo	initial mass of water per unit area, $\text{kg}/\text{m}^2$
MR	mass of water per unit mass of dry fiber
MRi	starting MR
MRf	ending MR
MREL	mass of water removed divided by initial mass
MRO	initial MR
N	compression equation constant
N1,N2	equation constants
OHTC	overall heat transfer coefficient, $\text{W}/(\text{m}^2 \text{ K})$
P	pressure, Pa
Patm	ambient pressure, Pa
Pcap	capillary pressure, Pa
PMAX	maximum gage mechanical pressure, Pa
Pmech	absolute mechanical pressure, Pa
Pmechg	gage mechanical pressure, Pa
PROP	arbitrary vapor or liquid property
Pv	vapor pressure, Pa
Pw	liquid pressure, Pa
$\overline{Pw}$	average hydraulic pressure, Pa
Q	conduction heat flux, $\text{W}/\text{m}^2$
r	pore radius, m
R	specific filtration resistance, $\text{m}/\text{kg}$
RATE1-3	rates of advance, $\text{m}/\text{s}$
RATIO1-3	interface position divided by DELTAT
RISTIM	time required to attain PMAX, s



S	saturation
S'	interfiber saturation
S2,S3	zone saturations
SEC	time, s
t	time, s
$\Delta t$	time increment, s
t'	time, s
T	temperature, K
T'	grid point temperature, K
T''	grid point temperature, K
T1-3	interface temperatures, K
TB	boiling point temperature, K
TBAR	average zone temperature, K
TH	hot surface temperature, K
TI	initial sheet temperature, K
TIME	time, s
TS	sheet surface temperature, K
U	same as OHTC, $W/(m^2 K)$
Vf	velocity of fibers, m/s
Vf'	interface velocity, m/s
Vgas	gas velocity, m/s
Vv	superficial vapor velocity relative to Vf, m/s
Vw	superficial liquid water velocity relative to Vf, m/s
Vwater	velocity of liquid water, m/s
x	relative position
$\Delta x$	relative position increment
z	position coordinate, m

$\gamma$	surface tension, N/m
$\delta$	thickness, m
$\delta'$	grid point coordinate, m
$\delta''$	grid point coordinate, m
$\delta_{1-3}$	interface positions, m
$\delta_T$	total thickness, m
$\epsilon$	porosity
$\epsilon'$	interfiber porosity
$\epsilon_{2,3}$	zone porosities
$\theta$	contact angle, radians
$\mu_v$	vapor viscosity, N s/m <sup>2</sup>
$\mu_w$	liquid viscosity, N s/m <sup>2</sup>
$\rho_F$	fiber density, kg/m <sup>3</sup>
$\rho_v$	vapor density, kg/m <sup>3</sup>
$\rho_w$	liquid density, kg/m <sup>3</sup>
$\tau$	time parameter
$\phi$	equation coefficient
$\overline{\phi}$	averaged equation coefficient
$\psi$	equation coefficient

LITERATURE CITED

1. Byrd, V. Drying and heat transfer characteristics during bench-scale press drying of linerboard. *Drying 82*. A. Mujumdar, ed., Washington, Hemisphere Publishing, 1982:83-90.
2. Lehtinen, J. A new vacuum-drying method for paper, board, and other permeable mats. *Drying 80: Vol. 2 Proceedings of the 2nd International Drying Symposium*. A. Mujumdar, ed., Washington, Hemisphere Publishing, 1980:347-54.
3. Arenander, S.; Wahren, D. Impulse drying adds new dimension to water removal. *Tappi* 66(9):123-6(Sept., 1983).
4. Ahrens, F.; Kartsounes, G.; Ruff, D. A laboratory study of hot surface drying at high temperature and mechanical loading. Preprints of the 68th annual CPPA Technical Section meeting, Montreal, Jan. 26-29, 1982, Vol. B, B93-B97 and *Pulp Paper Canada* 85(3):T63-7(March, 1984).
5. Ahrens, F. Heat transfer aspects of hot surface drying at high temperature and mechanical loading. *J. Pulp Paper Sci.* 9(3):TR79-82(July, 1983).
6. Fang, Y., The Institute of Paper Chemistry, Personal communication, April 4, 1983.
7. Burton, S. A dynamic simulation of impulse drying. A291 final report. Appleton, WI, The Institute of Paper Chemistry, 1983. 95 p.
8. Devlin, C., The Institute of Paper Chemistry, Personal communication, March 25, 1985.
9. Ahrens, F.; Astrom, A. High intensity drying of paper. Submitted to *Drying Technology: An International Journal*, December 31, 1984.
10. Udell, K. Heat transfer in porous media heated from above with evaporation, condensation, and capillary effects. *J. Heat Transfer* 105(3):485-92 (Aug., 1983).
11. Chi, S. Heat pipe theory and practice. Washington, Hemisphere Publishing, 1976.
12. Holden, G., U.S. pat. 3,284,285(Nov. 8, 1966).
13. Kawka, W.; Rogut, R., *Przegląd Papier.* 26(2):52-6(Feb., 1970).
14. Kawka, W.; Ingielewicz, H., *Przegląd Papier.* 28(11):381-7(Nov., 1972).
15. Kawka, W., *Przegląd Papier.* 30(1):10-18(Jan., 1974).
16. Kawka, W.; Ingielewicz, H., *Przegląd Papier.* 34(2):53-8(Feb., 1978).

17. Kawka, W.; Ingielewicz, H.; Marek, I., *Przegląd Papier*. 34(3):82-7(March, 1978).
18. Kawka, W.; Stepien, K., *Przegląd Papier*. 35(11):402-4(Nov., 1979).
19. Kawka, W.; Szwarczajtajn, E. EUCEPA-79 International Conference, London, May 21-24, 1979, Paper No. 31.
20. Kawka, W., *Przegląd Papier*. 39(11/12):403-7(Nov.-Dec., 1983).
21. Carr, W.; Holcombe, W.; Pearson, K.; Robertson, S.; Carter, W. Assessing the Machnozzle as a predrying device. *Textile Chemist Colorist* 15(8):21-6 (Aug., 1983).
22. Luikov, A.; Vasiliev, L. Heat and mass transfer in capillary porous bodies blown by a rarefied gas flow. *Low Temperature Heat Mass Transfer* 5(1970) as quoted in: Tolubinsky, V.; Antonenko, V.; Ostrovsky, Y.; Shevchuk, E. Drop carry-over phenomenon in liquid evaporation from capillary structures. *Letters Heat Mass Transfer* 5(6):339-47(Nov.-Dec., 1978).
23. Andersson, L.; Back, E. The effect of temperature up to 90°C on dewatering of wet webs, evaluated in a press simulator. *TAPPI 1981 Engineering Conference Proceedings*. Book 1:311-23(1981).
24. Andersson, L.; Back, E. Improvements in dewatering at increased pressing temperatures, a press simulator evaluation. *Tappi* 65(7):75-80(July, 1982).
25. Cutshall, K. Cross machine moisture control via hot pressing. *TAPPI 1984 Engineering Conference Proceedings*. Book 3:637-41(1984).
26. van Brakel, J.; Heertjes, P. *Proceedings of the 1st International Drying Symposium*. 70(1978) as quoted in: Brown, L.; Kashiwa, B.; Vanderborgh, N.; Corlett, R. The kinetic behavior of subbituminous coal drying; effects of confining pressure. *Drying 80: Vol. 2 Proceedings of the 2nd International Drying Symposium*. A. Mujumdar, ed., Washington, Hemisphere Publishing, 1980:425-433.
27. Ingersoll, L.; Zobel, O.; Ingersoll, A. *Heat conduction with engineering, geological, and other applications*. Madison, WI, University of Wisconsin Press, 1954:190-199.
28. Muehlbauer, J.; Sunderland, J. Heat conduction with melting or freezing. *Applied Mechanics Reviews* 18(12):951-9(Dec., 1965).
29. Tien, R.; Geiger, G. A heat transfer analysis of the solidification of a binary eutectic system. *J. Heat Transfer* 89(3):230-4(Aug., 1967).
30. Cho, S.; Sunderland, J. Heat conduction problems with melting or freezing. *J. Heat Transfer* 91(3):421-6(Aug., 1969).
31. Eckert, E.; Drake, R. *Analysis of heat and mass transfer*. New York, McGraw-Hill, 1972:224-8.

32. Cho, S.; Sunderland, J. Phase change problems with temperature dependent thermal conductivity. *J. Heat Transfer* 96(2):214-17(May, 1974).
33. White, R. A modified finite difference scheme for the Stefan problem. *Mathematics of Computation* 41(164):337-47(Oct., 1983).
34. Chawla, T.; Pedersen, D.; Leaf, G.; Minkowycz, W.; Shouman, A. Adaptive collocation method for simultaneous heat and mass diffusion with phase change. *J. Heat Transfer* 106(3):491-7(Aug., 1984).
35. Selim, M.; Seagrave, R. Solution of moving boundary transport problems in finite media by integral transforms, Parts I, II, III. *I&EC Fundam.* 12(1): 1-8, 9-13, 14-17(Feb., 1973).
36. Solomon, A. Some remarks on the Stefan problem. *Mathematics of Computation* 20:347-60(1966).
37. Bonacina, C.; Comini, G.; Fasano, A.; Primicerio, M. Numerical solution of phase change problems. *Int. J. Heat Mass Transfer* 16(10):1825-32(Oct., 1973).
38. Voller, V.; Cross, M. Accurate solutions of moving boundary problems using the enthalpy method. *Int. J. Heat Mass Transfer* 24(3):545-56(March, 1981).
39. Voller, V.; Shadabi, L. Enthalpy methods for tracking a phase change boundary in two dimensions. *Int. Comm. Heat Mass Transfer* 11(3):239-49(May-June, 1984).
40. Talmon, Y.; Davis, H.; Scriven, L. Progressive freezing of composites analyzed by isotherm migration methods. *AIChE J.* 27(6):928-37(Nov., 1981).
41. Talmon, Y.; Davis, H.; Scriven, L. Moving boundary problems in simple shapes solved by isotherm migration. *AIChE J.* 29(5):795-800(Sept., 1983).
42. Cho, S. An exact solution of the coupled phase change problem in a porous medium. *Int. J. Heat Mass Transfer* 18(10):1139-42(Oct., 1975).
43. Hilding, W.; Cheh, U. Transient temperature response during heating of an initially saturated plane porous wall. *Heat Transfer* 82: Vol. 6 Proceedings of the 7th International Heat Transfer Conference. U. Grigull; E. Hahne; K. Stephan; J. Straub, eds., Washington, Hemisphere Publishing, 1982:67-72.
44. Szentgyorgyi, S.; Molnar, K. Calculation of drying parameters for the penetrating evaporation front. *Drying* 84. A. Mujumdar, ed., Washington, Hemisphere Publishing, 1984:76-82.
45. Szentgyorgyi, S.; Molnar, K.; Orvos, M. Computer calculation method of the falling rate period of drying. *Drying* 84. A. Mujumdar, ed., Washington, Hemisphere Publishing, 1984:83-7.
46. Lin, S.; Chou, T. A parametric study of the freeze-dry process for preservation of activities of biological substances. *Drying* 84. A. Mujumdar, ed., Washington, Hemisphere Publishing, 1984:99-104.

47. Kisakurek, B.; Celiker, H. Modeling of simultaneous heat and mass transfer in freeze drying. Drying 84. A. Mujumdar, ed., Washington, Hemisphere Publishing, 1984:324-29.
48. Adesanya, B. Heat and mass transfer in a capillary porous body with particular reference to lumber. Doctoral Dissertation. Clemson, SC, Clemson University, 1982. 189 p.
49. Beard, J.; Rosen, H.; Adesanya, B. Temperature distributions and heat transfer during the drying of lumber. Drying Technology: An International Journal 1(1):117-40(Feb., 1983).
50. Dorri, B.; Emery, A.; Malte, P. Drying rate of wood particles with longitudinal mass transfer. J. Heat Transfer 107(1):12-18(Feb., 1985).
51. Hallstrom, A. Drying of porous hygroscopic materials: an extended shrinking core model. Drying 82. A. Mujumdar, ed., Washington, Hemisphere Publishing, 1982:19-24.
52. Sato, K.; Ishida, M.; Shirai, T. Prediction of pressure increase and evaporation temperature during the course of drying of porous solid soaked with water. J. Chem. Eng. Japan 9(1):35-9(1976).
53. Cross, M.; Gibson, R.; Young, R. Pressure generation during the drying of a porous half-space. Int. J. Heat Mass Transfer 22(1):47-50(Jan., 1979).
54. Gibson, R.; Cross, M.; Young, R. Pressure gradients generated during the drying of porous shapes. Int. J. Heat Mass Transfer 22(6):827-30(June, 1979).
55. Streck, F.; Nastaj, J. Mathematical modeling and simulation of vacuum contact drying of porous media in the falling rate period (boundary condition of the first kind). Drying 80: Vol. 2 Proceedings of the 2nd International Drying Symposium. A. Mujumdar, ed., Washington, Hemisphere Publishing, 1980:135-43.
56. Baines, W. Analysis of transient effects in drying of paper. Pulp Paper Can. 74(2):58-64(Feb., 1973).
57. Ahrens, F. Fundamentals of drying, project 3470. Status report to the Engineering and Colloid Science Research Advisory subcommittee. Appleton, WI, The Institute of Paper Chemistry, March 23-24, 1983:117-36.
58. Kreith, F. Principles of Heat Transfer. Scranton, Pa., International Textbook Company, 1958:430-6.
59. Yiannos, P. The apparent cell wall density of wood and pulp fibers. Tappi 47(8):468-71(Aug., 1964).
60. Devlin, C. An investigation of the drying mechanism of paper at high temperatures and mechanical pressures, A400 Revised Thesis Proposal. Appleton, WI, The Institute of Paper Chemistry, 1982:19.

61. Ahrens, F.; Journeaux, I. An experimental and analytical investigation of a thermally induced vacuum drying process for permeable mats. Drying 84. A. Mujumdar, ed., Washington, Hemisphere Publishing, 1984:281-91.
62. Han, S. Heat and mass transfer in hot-surface drying of fiber mats. Pulp Paper Can. 65(12):T537-49(Dec., 1964).
63. Carlsson, G.; Lindstrom, T.; Floren, T. Permeability to water of compressed pulp fiber mats. Svensk Papperstid. 86(12):R128-34(Sept., 1983).
64. Emmons, H. The continuum properties of fiber suspensions. Tappi 48(12): 679-87(Dec., 1965).
65. Leonard, B. A survey of finite differences of opinion in numerical muddling of the incompressible defective convection equation. Finite Element Methods for Convection Dominated Flows, AMD Vol. 34. T. Hughes, ed., New York, ASME, 1979:1-17.
66. Patankar, S. Numerical heat transfer and fluid flow. Washington, Hemisphere Publishing, 1980:50-2.
67. Pounder, J. A400 Progress Report 5. Appleton, WI, The Institute of Paper Chemistry, Jan. 27, 1984. 26 p.
68. Prahl, J. Thermodynamics of paper fiber and water mixtures. Doctoral Dissertation. Cambridge, Harvard University, 1968. 159 p.
69. Pounder, J. A400 Progress Report 8. Appleton, WI, The Institute of Paper Chemistry, Oct. 19, 1984. 23 p.
70. Han, S. Drying of paper. Tappi 53(6):1034-46(June, 1970).
71. Fang, Y., The Institute of Paper Chemistry, Personal communication, March 20, 1983.
72. Pounder, J. A400 Progress Report 6. Appleton, WI, The Institute of Paper Chemistry, April 27, 1984. 24 p.
73. Campbell, W. The physics of water removal. Pulp Paper Can. 48:103-9, 122 ("Convention Issue", 1947).
74. Chang, N. Dynamic compression of handsheets. TAPPI 1978 Engineering Conference Proceedings. Book 1:93-106(1978).
75. Consolvo, W. Dynamic compression of a fiber mat. A291 final report. Appleton, WI, The Institute of Paper Chemistry, 1981. 33 p.
76. Caulfield, D.; Young, T.; Wegner, T. The role of web properties in water removal by wet pressing. Tappi 65(2):65-9(Feb., 1982).
77. Ceckler W.; Thompson, E. Final Report of the University of Maine at Orono Wet Pressing Project. Washington, U.S. Department of Energy, 1982. 335 p.

78. Gren, U.; Ljungkvist, K. Compressibility and permeability of chemical pulps. *Cellulose Chem. Tech.* 17(5):515-23(Sept.-Oct., 1983).
79. Hung, J.; Holm, R. A study of the drying of linerboard, Progress Report 2, Project 2693. Appleton, WI, The Institute of Paper Chemistry, 1969. 69 p.
80. Pounder, J. IPC Research Notebook 3711, March 2, 1985:60-3.
81. Pounder, J. IPC Research Notebook 3711, March 2, 1985:63-5.
82. Davies, C. The separation of airborne dust and particles. *Institution of Mechanical Engineers* 1B:185-98(1952).
83. Labrecque, R. The effects of fiber cross-sectional shape on the resistance to the flow of fluids through fiber mats. *Tappi* 51(1):8-15(Jan., 1968).
84. Ellis, E. Compressibility and permeability of never dried bleached softwood kraft pulp and its application to the prediction of wet press behavior. Doctoral Dissertation. Orono, ME, University of Maine at Orono, 1981. 287 p.
85. Guzy, C. Flow and retention in fibrous porous media. Doctoral Dissertation. Albuquerque, NM, University of New Mexico, 1983. 259 p.
86. El-Hosseiny, F.; Yan, J. Analysis of Canadian Standard Freeness Part 1: theoretical considerations. *Pulp Paper Can.* 81(6):T113-16(June, 1980).
87. Boyd, K. Canadian Standard Freeness. A347 term report. Appleton, WI, The Institute of Paper Chemistry, 1983. 26 p.
88. Ingmanson, W.; Whitney, R. The filtration resistance of pulp slurries. *Tappi* 37(11):523-41(Nov., 1954).
89. Wilder, J. Paper capillarity and rewetting during pressing. *Tappi* 51(2):104-9(Feb., 1968).
90. Robertson, A. The physical properties of wet webs, part 2, fiber properties and wet web behavior. *Svensk Papperstid.* 66(12):477-97(June 30, 1963).
91. Pounder, J. A400 Progress Report 4. Appleton, WI, The Institute of Paper Chemistry, Oct. 18, 1983. 29 p.
92. Pounder, J. A400 Progress Report 7. Appleton, WI, The Institute of Paper Chemistry, July 20, 1984. 28 p.
93. Devlin, C., Institute of Paper Chemistry, Personal communication, May 9, 1985.
94. Herminge, L. Heat transfer in porous bodies at various temperatures and moisture contents. *Tappi* 44(8):570-5(Aug., 1961).



95. Ahrens, F. An analysis of a thermally induced vacuum drying process for permeable mats. Heat Transfer 82: Vol. 6 Proceedings of the 7th International Heat Transfer Conference. U. Grigull; E. Hahne; K. Stephan; J. Straub, eds., Washington, Hemisphere Publishing, 1982:509-14.
96. Burton, S. Dynamics of densification in impulse drying. Engineering Project Advisory Committee Report. Appleton, WI, The Institute of Paper Chemistry, April 3-4, 1985:24-45.
97. Ahrens, F. Fundamentals of drying, Project 3470. Engineering Project Advisory Committee Report. Appleton, WI, The Institute of Paper Chemistry, March 21-22, 1984:53-64.
98. Belisle, S. A study of the characteristics of impulse drying. A291 final report. Appleton, WI, The Institute of Paper Chemistry, 1984. 46 p.

## APPENDIX I

### HIDRYER1 PROGRAM AND DOCUMENTATION

#### HIDRYER1/USE

To run HIDRYER1 the user needs to have or must be able to access three files on the Burroughs B6900 main frame:

HIDRYER1/JOB, the WFL job deck to run the object code;  
OBJECT/HIDRYER1, the compiled and saved FORTRAN object code; and  
HIDRYER1/PARAMS, the data file containing input parameters.

HIDRYER1/JOB is the following WFL job deck:

```
BEGIN JOB HIDRYER1(INTEGER Q,STRING NAME1,STRING NAME2);  
    QUEUE=Q;  
    RUN OBJECT/HIDRYER1;  
    FILE FILE1=#NAME1;  
    FILE FILE2=#NAME2;  
    STATION=MYSELF(SOURCESTATION);  
END JOB
```

To run the program the user enters

```
START HIDRYER1/JOB(Q,"NAME1","NAME2")
```

where Q is the queue number, NAME1 is HIDRYER1/PARAMS (or other data file conforming to the correct input syntax), and NAME2 is the name of the disk data file to which the output information is written and saved.

OBJECT/HIDRYER1 is obtained by compiling HIDRYER1 and saving the result. HIDRYER1 and its documentation are listed later in this appendix. About 20 seconds of processor time and 60 seconds of elapsed time are required for compilation of HIDRYER1.

HIDRYER1/PARAMS is a data file containing the following numerical information separated by commas:

TH,TB,BW,CSF,MRO,DTO,PMAX,RISTIM,IOPTP,IOPTU,METH,MITER

For example:

525.0,212.0,0.0420,650,1.500,1.37E-07,750.0,0.025,1,1,2,2

The input parameters are defined in the thesis and in the HIDRYER1/DOC section of this appendix. HIDRYER1 performs all calculations in English units, but the input and output may be given in either English or SI units.

#### HIDRYER1/DOC

HIDRYER1 is a FORTRAN implementation of the equations in this thesis. It mathematically performs a drying "experiment" based on the inputs from HIDRYER1/PARAMS and outputs the results to the printer and to a disk file named by the user.

The main part of the program is divided into four sections. The first section contains the file declarations, statements for inclusion of packaged subroutines, real variable declarations, values for constants, common statements, and preliminary input and output statements. The next three sections contain the equations for the heatup, transition, and linear drying regimes.

The main program is followed by a SUBROUTINE section containing 13 subroutines and a FUNCTION section containing 12 functions. The subroutine names and their purposes are:

CALLER: calls property subroutines

CNSTMN: determines constants for calculation of M and N

CNVRT1: converts from English to SI units

CNVRT2: converts from SI to English units

DLDTFN: calculates the compression of a saturated sheet

DUMFUN: calculates the Jacobian matrix for DLDTFN

PRESSR: calculates applied pressure and time derivative

PROP12: calculates and averages physical properties at T1 and T2

PROP23: calculates and averages physical properties at T2 and T3

PROP3B: calculates and averages physical properties at T3 and TB

PROPTB: calculates the physical properties at TB

WARNIN: corrects error conditions or prints warning messages

WRITER: writes output to printer and disk

Subroutine DLDTFN calls a set of subroutines from the International Mathematical and Statistical Library package for the solution of an initial value problem. More information on these subroutines may be found in the appropriate IMSL documentation.

The function names and their purposes are:

DELHD : calculates latent heat of vaporization increment

DPVDT : calculates derivative of vapor pressure with temperature

EVALM : calculates the M compression constant

EVALN : calculates the N compression constant

HFG : calculates the latent heat of vaporization

HYDRAL: calculates the hydraulic pressure

SPRES : calculates the specific filtration resistance

VF : calculates the liquid water specific volume  
VG : calculates the water vapor specific volume  
VISF : calculates the liquid water viscosity  
VISG : calculates the water vapor viscosity  
PV : calculates the vapor pressure

The main program variable names and definitions are:

A thermal diffusivity term  
Ax interface rate-of-advance terms  
ALF  $\Delta T_2 - \Delta T_1$   
ALFA  $\Delta T_3 - \Delta T_1$   
BET  $\Delta T_3 - \Delta T_2$   
BETA  $\Delta T_1 - \Delta T_3$   
BIDX product of Biot number and DX  
BW sheet basis weight  
BWx basis weight of zone x  
BWCORR basis weight correction factor  
BWSUM sum of corrected zone basis weights  
Cx dry fiber concentration of zone x  
COEFF coefficient in mechanical pressure calculations  
CONST C3/DFIBER  
CPF specific heat of cellulose  
CPW specific heat of water  
CSF Canadian Standard Freeness  
Dx rates of interface advance  
DBWxDT rate of change of basis weight of zone x  
DC product of density, specific heat and moisture ratio  
DELTAx position of interface x  
DELTAf position of grid point closest to outer interface  
DELTAI position of grid point closest to inner interface  
DELTAT sheet thickness  
DELTSI DELTAT in SI units  
DENOM denominator term used in various calculations  
DF reciprocal of DFIBER  
DFIBER density of cellulose  
DHx constants in DELHD  
DIFFF relative distance term  
DIFFFX relative distance term  
DIFFI relative distance term  
DIFFIX relative distance term  
DK product of MR, DFIBER, and KWATER  
DLDT rate of change of saturated sheet thickness  
DPDT rate of change of mechanical pressure  
DPDTxy vapor pressure with temperature derivative over x and y  
DPVDTB vapor pressure at TB  
DSTAR interface rate of advance  
DT time increment

DTx	calculated time increments
DTDZxy	temperature gradient over x and y
DTMAX	maximum time increment
DTO	default time increment (in hours)
DW	density of liquid water
DX	relative position increment
DXX	relative position increment
Ex	porosity of zone x
EMIN	minimum allowable porosity
ESTAR	interfiber porosity
ESx	constants for calculation of ESTAR
Fx	factors for temperature calculations
F3X	product of F3 and DX
FACTOR	factor for conversion of English units
FLAG	signal for absence of zone 3
GAMM	DELTAT - DELTA3
H	time increment
HC	contact coefficient
HCx	constants for calculation of HC
HCDRY	contact coefficient of dry cellulose
HCREF	HCDRY at PREF2
HCWET	contact coefficient of water
HFGx	latent heat of vaporization at interface x
HFGTB	latent heat of vaporization at TB
I	loop iteration counter
IDUMMY	subroutine work vector
IER	subroutine error indicator
IFINI	number of grid point closest to outer interface
IMAX	maximum iteration counter
INDEX	subroutine call parameter
INIT	number of grid point closest to inner interface
IOPTx	interface motion indicators
IOPTP	pressure pulse option (1=ramp, 2=sine)
IOPTU	units option (1=English, 2=SI)
IWK	subroutine work vector
J	print control variable
K	loop iteration counter
Kx	thermal conductivity of zone x
KABSx	absolute permeability of zone x
KAKV	product of KABS3 and KV
KAKW	product of KABS3 and KW
KFIBER	thermal conductivity of dry cellulose
KK	grid point counter
KMIN	initial number of grid points
KV	vapor relative permeability
KW	liquid relative permeability
KWATER	thermal conductivity of water
L	print control variable
LIQDEW	mass of liquid water removed
LMAX	print control variable
M	number of points for internal temperature calculations
Mx	compression constant for zone x
MC	moisture content
METH	subroutine parameter (1=Adams method, 2=Gear's method)

MFINAL	target final moisture content
MITER	subroutine parameter (0=iteration, 1=analytic, etc.)
MO	initial mass of water present
MR	moisture ratio
MREL	relative amount of moisture removed
MREM	amount of moisture remaining
MRO	initial moisture ratio
MRSTAR	intrafiber MR
N	print control variable
Nx	compression constant for zone x
NEXP	exponent in calculation of Nx
OHTC	overall heat transfer coefficient
OHTCSI	OHTC in SI units
P	structural pressure
Px	structural pressure in zone x
PDENOM	denominator in pressure calculation
PGAGSI	PGAUGE in SI units
PGAUGE	gage vapor pressure at T1
PHx	hydraulic pressure in zone x
PHI	thermal diffusivity term
PMAX	maximum mechanical pressure
PMID	pressure midway between PMAX and PREF1
PREFx	reference menchanical pressures
PR3LOG	natural log of PREF3
PSI	velocity term
PS3	structural pressure of saturated sheet
PVTB	vapor pressure at TB
PW	liquid pressure
Q	instantaneous heat flux
QINIT	heat supplied during heatup regime
QSI	Q in SI units
QTHEOR	theoretical heat requirement
QOTHERx	term in calculation of QTHEOR
QTOT	total heat input during drying
QTOTAL	heat supplied during transition and linear regimes
R	resistance factor
RATEx	rates of interface advance
RATIOx	DELTAx/DELTAT
REM	remainder in distance calculations
RISTIM	time required to attain PMAX (in seconds)
Sx	saturation of zone x
S3STAR	interfiber saturation
SDUMMY	subroutine work variable
SEC	time in seconds
SIGN	variable in LIQDEW calculation
STAR	variable in MRSTAR calculation
SUM12	sum of BW1 and BW2
SUM123	sum of SUM12 and BW3
Tx	temperature of interface x
TxSI	Tx in SI units
TB	boiling point temperature
TBARx	average temperature of zone x
TC	temperature at a fixed point in the sheet
TERMx	terms used in various calculations

TH	hot surface temperature
THICKx	thickness of zone x
TI	initial sheet temperature
TIME	time
TIMEND	time endpoint for initial value problem
TIMER	factor used in temperature calculations
TMID	temperature midway through the sheet basis weight
TMIDSI	TMID in SI units
TNEW	new temperature at a given grid point
TOL	subroutine convergence tolerance
TOLD	old temperature at a given grid point
TOx	old temperature at interface x
TS	sheet surface temperature
TSSI	TS in SI units
U	fractional basis weight
V	velocity term
VFxy	specific volume of liquid water over x and y
VFTB	specific volume of liquid water at TB
VGxy	specific volume of water vapor over x and y
VGTB	specific volume of water vapor at TB
VISFxy	viscosity of liquid water over x and y
VISFTB	viscosity of liquid water at TB
VISGxy	viscosity of water vapor over x and y
VISGTB	viscosity of water vapor at TB
W	product of MRSTAR and C2
WK	subroutine work variable
X	product of MR and C3
XX	grid point variable
Y	product of (MR-MRSTAR) and C3
YL	thickness of saturated sheet
Z	Y/X
ZTC	location of fixed points within the sheet

In the subroutines, the variables not linked to the main program by COMMON statements are:

CALLER

all variables in common with main program

CNSTMN

Ax	constants for calculation of CMx
Bx	constants for calculation of CMx
Cx	constants for calculation of CNx
CMx	constants for calculation of M compression constant



CNx        constants for calculation of N compression constant  
Dx        constants for calculation of CNx  
Ex        constants for calculation of TERM  
TERM      constant for calculation of CMx and CNx

CNVRT1

Ax        constants in unit conversions

CNVRT2

Ax        constants in unit conversions

DLDTFN

YPRIME    rate of change of saturated sheet thickness

DUMFUN

PD        partial derivative of YPRIME with respect to YL

PRESSR

Ax        constants in sine pressure pulse calculation

PI        numerical value 3.14159...

PROP12

all variables in common with main program

PROP23

all variables in common with main program

PROP3B

all variables in common with main program

PROPTB

all variables in common with main program

WARNIN

all variables in common with main program

WRITER

all variables in common with main program

In the functions, the variables not linked to the main program by COMMON statements are:

DELHD

all variables in common with main program

DPVDT

Ax constants used in property calculation

EVALM

A constant used in calculation of M compression constant

Ax constants used in calculation of A and B

B constant used in calculation of M compression constant

CMx constants in common with CNSTMN

CORRCT correction in calculation of M compression constant

EVALN

A constant used in calculation of N compression constant

Ax constants used in calculation of A and B

B constant used in calculation of N compression constant

C uncorrected value for N compression constant

CNx constants in common with CNSTMN

---

NDENOM denominator in correction of N compression constant  
NMID value of N at PMID  
NSAT value of N at PREF3  
PTERM pressure term in correction of N compression constant  
SIGN variable in correction of N compression constant

HFG

Ax constants used in property calculation

HYDRAL

all variables in common with main program

SPRES

Ax constants used in property calculation

RREF reference specific filtration resistance

X variable used in property calculation

VF

Ax constants used in property calculation

VG

Ax constants used in property calculation

VISF

Ax constants used in property calculation

VISG

Ax constants used in property calculation

PV

Ax constants used in property calculation

The following discussion of HIDRYER1 is divided into sections by program line numbers and headings. Refer to the program listing for the actual FORTRAN statements.

#### OPENING SECTION OF MAIN PROGRAM

1 : Format line.

Sets standard FORTRAN format.

5 - 23 : Headers

Program references and identification.

28 - 32 : File declarations.

File 1 is the parameter input file; file 2 is the disk output file;  
file 5 is the terminal; and file 6 is the line printer.

34 - 44 : Include statements.

Include the required subroutines from the IMSL package.

46 - 48 : Real variable declarations.

Sets variables ordinarily assumed to be integers to be real variables  
and dimensions some arrays.

50 : Dimension statement.

Sets dimension of an integer array.

52 : External statement.

Declares two subroutines external to the IMSL package.

55 - 64 : Fixed input assignment.

Assigns values to certain constants in the program.

67 - 85 : Subroutine common blocks.

Names common blocks for subroutines.

88 - 91 : Input statement.

Reads input parameters in free format from file 1.

94 - 101 : Write statements.

Write headings and repeat input parameters on line printer.

104 - 107 : Set print controls.

Set counters for frequency of printing output results.

110 - 114 : Set fixed internal points.

Set fixed fractions of basis weight at which temperatures are to be calculated. This is for direct comparison to experimental results.

117 - 120 : Compute properties at TB.

Convert to English units if necessary and compute vapor and liquid properties at TB for use later in the program.

#### HEATUP REGIME

129 - 168 : Initialize variables.

Set initial variable values for heatup regime and for use later in the main program.

171 - 223 : Calculate mechanical pressure and sheet properties.

Calculate mechanical pressure for nonsaturated or saturated sheets and determine sheet properties like thickness, porosity, etc.

226 - 232 : Calculate heat transfer parameters.

Determine contact coefficient, thermal conductivity and BIDX.

235 - 260 : Calculate interior temperatures.

Use finite difference methods to find internal temperatures for a non-saturated or saturated sheet undergoing compression.

263 - 275 : Calculate boundary temperatures.

Use finite difference methods to calculate boundary temperatures for nonsaturated or saturated sheets.

278 - 282 : Reset old temperature values.

Reset TOLD for next set of finite difference calculations.

285 - 291 : Compute temperatures at fixed locations.

Use linear interpolation to find temperatures at fixed basis weight fractions in the sheet.

294 - 314 : Increment quantities and write results.

Calculate quantities which must be calculated at every time increment and determine if the output should be printed on this iteration. If the output needs to be printed, then calculate additional output quantities that do not have to be determined at every time step.

317 - 320 : Increment print control variables.

Increase the values of the counters for print control.

323 - 327 : Determine exit criteria.

Check time and physical criteria for exit to transition regime or program termination.

330 - 345 : Write heatup regime final output.

Calculate final values for quantities and write output if it is not a duplication of the last printed output.

#### TRANSITION REGIME

354 - 356 : Write transition regime heading.

Write heading on printer to signal onset of transition regime.

359 - 404 : Initialize variables.

Set initial values for transition regime variables.

407 -417 : Compute required derivatives.

Calculate the rates of advance for the different interfaces which may be present in the sheet.

420 - 460 : Set maximum allowable time increment.

Examine rates of interface advance and determine the maximum allowable time increment which will not violate the interface position criteria. Determine if new interface position permits the use of usual finite difference formulations or requires use of unequally spaced points. Increment the time and include the factor TIMER to account for round-off or truncation errors in the determination of DT.

463 - 501 : Calculate new temperature distribution.

Use finite difference methods to determine internal and "boundary" (INIT and IFINI) temperatures in the transition zone and in zone 4, if it exists.

504 -519 : Calculate rates of basis weight change.

Select the dominant rate at each interface and determine any liquid dewatering that takes place.

522 -535 : Calculate mechanical and hydraulic pressure.

Calculate applied mechanical pressure based on time and IOPTP and calculate the hydraulic (vapor) pressure for each zone. Obtain the effective structural pressure for each zone by subtraction.

538 - 585 : Calculate basis weight, concentration, and thickness.

Calculate rates of basis weight change and new basis weights. Correct basis weights for slight calculation errors. Evaluate the compression constants, dry fiber concentration, and thickness of each zone.

588 - 623 : Calculate porosity and saturation.

Calculate porosity based on dry fiber concentration, and saturation based on dry fiber concentration and moisture ratio. Correct zone 3 saturation if greater than unity.

626 - 645 : Increment interface positions.

Calculate new interface positions, locations of INIT and IFINI, and position increments for finite difference calculations.

648 - 658 : Compute thermal conductivity and contact coefficient.

Find thermal conductivity of each zone and contact coefficient.

661 - 669 : Calculate permeability factors.

Calculate specific filtration resistance, absolute permeability for the zones and KAKW.

672 - 680 : Set relative interface positions.

Compute the RATIOx values and calculate the remaining moisture and relative moisture loss.

683 - 735 : Compute new interface temperatures.

Calculate new interface temperatures based on equations appropriate for types and locations of interfaces present.

738 - 761 : Recompute variables for derivative calculations.

Calculate temperature gradient terms for zones and multipliers for rate expressions.

764 - 879 : Handle special case of intrafiber water only.

If FLAG = 1, then this section handles all calculations for the transition regime. The calculations are based on those of the previous sections and modified for this special case. If FLAG = 0, then this section is bypassed.

882 - 889 : Reset temperature distribution and time options.

Reset TOLD values for next finite difference calculations and reset IOPT1 and IOPT2 for the next time increment.

892 - 912 : Compute temperatures at fixed locations.

Same strategy as for lines 285 - 291.



915 - 934 : Increment quantities and write results.

Same strategy as for lines 294 - 314.

937 - 940 : Increment print control variables.

Same strategy as for lines 317 - 320.

943 - 949 : Determine exit criteria.

Same strategy as for lines 323 - 327.

952 - 968 : Write transition regime final output.

Same strategy as for lines 330 - 345.

#### LINEAR REGIME

977 - 979 : Write linear regime heading.

Same strategy as for lines 354 - 356.

982 - 989 : Set FLAG and go to first temperature calculation.

Set the value for FLAG and go directly to interface temperature calculation right from the transition regime.

992 - 1005 : Compute required derivatives.

Same strategy as for lines 407 - 417, with additional calculations for other types of interfaces that may be present.

1008 - 1032 : Set maximum allowable time increment.

Same strategy as for lines 420 - 460, but no restriction on interface position relative to grid points.

1035 - 1053 : Calculate rates of basis weight change.

Same strategy as for lines 504 - 519.

1056 - 1070 : Calculate mechanical and hydraulic pressure.

Same strategy as for lines 522 - 535.

1073 - 1121 : Calculate basis weight, concentration, thickness.

Same strategy as for lines 538 - 585.

1124 - 1159 : Calculate porosity and saturation.

Same strategy as for lines 588 - 623.

1162 - 1169 : Increment interface positions.

Same strategy as for lines 626 - 645, but no finite difference grid spacings need to be calculated.

1172 - 1182 : Compute thermal conductivity, contact coefficient.

Same strategy as for lines 648 - 658.

1185 - 1194 : Calculate permeability factors.

Same strategy as for lines 661 - 669, with KAKV also determined.

1197 - 1204 : Set relative interface positions.

Same strategy as for lines 672 - 680.

1207 - 1286 : Compute new interface temperatures.

Same strategy as for lines 683 - 735, but with equations appropriate for linear regime (including vapor flow in zone 3).

1289 - 1317 : Recompute variables for derivative calculations.

Same strategy as for lines 738 - 761.

1320 - 1338 : Compute temperatures at fixed locations.

Same strategy as for lines 892 - 912.

1341 - 1357 : Increment quantities and write results.

Same strategy as for lines 915 - 934.

1360 - 1363 : Increment print control variables.

Same strategy as for lines 937 - 940.

1366 - 1369 : Determine exit criteria.

Same strategy as for lines 943 - 949, but time and moisture content are the only criteria for the linear regime.

1372 - 1385 : Write final output.

Calculate and write total values for cumulative variables.

1388 - 1410 : Format statements.

Statements for printer headings and output variable format.

1413 - 1416 : End main program.

STOP and END statements for main program.

The remainder of HIDRYER1 is composed of the SUBROUTINE and FUNCTION sections, which have been previously described.

HIDRYER1 (CS/21/85)

RESET FREE

```
*****
**      HIGH INTENSITY DRYING PROGRAM      **
**                                          **
**              HIDRYER1                  **
**                                          **
**      INSTITUTE OF PAPER CHEMISTRY      **
**                                          **
**              JOSEPH H POUNDER          **
**                                          **
**              MARCH 25, 1985            **
*****
```

```
*****
*      PROGRAM DOCUMENTATION IS IN THE HIDRYER1/DCC FILE      *
*                                                                *
* INSTRUCTIONS FOR RUNNING THE PROGRAM ARE IN THE HIDRYER1/USE FILE *
*****
```

```
FILE 1(KIND=DISK,NEWFILE=FALSE,FILETYPE=7,MYUSE=IN)
FILE 2(KIND=DISK,NEWFILE=TRUE,MAXRECSIZE=21,PROTECTION=SAVE,
* MYUSE=OUT)
FILE 5(KIND=REMOTE,MYUSE=IO)
FILE 6(KIND=PRINTER)
```

```
INCLUDE "IMSL/DERCS"
INCLUDE "IMSL/DGEAR"
INCLUDE "IMSL/DERIA"
INCLUDE "IMSL/DERPS"
INCLUDE "IMSL/DGRST"
INCLUDE "IMSL/LUCATF"
INCLUDE "IMSL/LUGELMF"
INCLUDE "IMSL/LECT18"
INCLUDE "IMSL/UEARTST"
INCLUDE "IMSL/UGETIO"
INCLUDE "IMSL/USPNC"
```

```
REAL KABS2,KABS3,KABS4,KAKV,KAKW,KFIBER,KV,KW,KWATER,K1,K2,K3,
K4,LIGDEW,MC,MFINAL,MO,MR,MREL,MREM,MRO,MRSTAR,M1,M2,M3,M4,NEXP,
N1,N2,N3,N4,TC(10),TREW(501),TOLD(501),WK(250),YL(2),ZTC(10)
```

DIMENSION IWK(1)

000001  
000002  
000003  
000004  
000005  
000006  
000007  
000008  
000009  
000010  
000011  
000012  
000013  
000014  
000015  
000016  
000017  
000018  
000019  
000020  
000021  
000022  
000023  
000024  
000025  
000026  
000027  
000028  
000029  
000030  
000031  
000032  
000033  
000034  
000035  
000036  
000037  
000038  
000039  
000040  
000041  
000042  
000043  
000044  
000045  
000046  
000047  
000048  
000049  
000050

```

C
EXTERNAL DLDTFN,DUMFUN
C
C
C*****FIXED INPUTS ARE:
C
DATA
*DH1,DH2/33.2815,-14.9522/, ES1,ES2/1.55,0.55/, IMAX/10/,
*KMIN/101/, M/3/, DFIBER,KFIBER,CPF/96.76,0.14,0.346/,
*RWATER,CFW/0.394,1.00/, FACTOR/1.6679002E+07/, LMAX/25/,
*STAR/C.005684/, MFINAL/0.06/, TIMER/0.95/, TI/75.0/, J/ 25/,
*HCREP,HCRET/100.,1000./, PREF1,PREF2,PREF3/0.10,1.,1000./,
*HC1,HC2,HC3/1.45159,0.33333333,0.479354/, TOL/1.0E-05/,
*INDEX/1/, NEXP/3.0/
C
C
C*****SUBROUTINE COMMON BLOCKS ARE:
C
COMMON /GEAR/ DUMMY(48),SDUMMY(4),IDLMHY(38)
COMMON /LABEL1/ TB,PVTE,DFVCTB,VFTB,VGTB,HFGTB,VISGTB,VISFTB
COMMON /LABEL2/ TH,T1,T2,T3,TI,IMID
COMMON /LABEL3/ DPDT12,VF12,VG12,VISG12
COMMON /LABEL4/ DPDT23,VF23,VISF23,VG23,VISG23
COMMON /LABEL5/ DPDT38,VG38,VISG38
COMMON /LABEL6/ DXX,DIFFIX,CIFFFX,EMIN
COMMON /LABEL7/ PREF1,PMAX,RISTIM,P,IOPTP,DPDT
COMMON /LABEL8/ M1,M2,M3,M4,N1,N2,N3,N4
COMMON /LABEL9/ DLDT,FACTOR,BW,DW,DFIBER,COEFF,PS3
COMMON /LABEL10/ CSF
COMMON /LABEL11/ SEC,MREL,TS,RATIO1,RATIO2,RATIO3,DELTA1,0,OHTC,
* PGAGE
COMMON /LABEL12/ TSSI,T1SI,T2SI,T3SI,DELTSI,QSI,OHTCSEI,PGAGSEI,
* THICSEI
COMMON /LABEL13/ DH1,DH2,MR,MSTAR
COMMON /LABEL14/ NEXP,PF3LOG,PREF3,PMID,PDENOM,DF
C
C
C*****READ INPUT FROM DATA FILE
C
READ(1,/) TH,TB,BW,CSF,MRO,DIO,PMAX,RISTIM,IOPTP,IOPTU,
* METH,MITER
C
C
C*****WRITE HEADINGS AND STARTING PARAMETERS
C
WRITE(6,900)
WRITE(6,905)
WRITE(6,910) TH,TB,BW,CSF,MRO,PMAX,RISTIM
WRITE(6,915)
WRITE(6,920) DIO,IOPTP,IOPTU,METH,MITER
WRITE(6,925)
C
C
C*****SET VARIABLES FOR PRINTING OF RESULTS

```

000051  
000052  
000053  
000054  
000055  
000056  
000057  
000058  
000059  
000060  
000061  
000062  
000063  
000064  
000065  
000066  
000067  
000068  
000069  
000070  
000071  
000072  
000073  
000074  
000075  
000076  
000077  
000078  
000079  
000080  
000081  
000082  
000083  
000084  
000085  
000086  
000087  
000088  
000089  
000090  
000091  
000092  
000093  
000094  
000095  
000096  
000097  
000098  
000099  
000100  
000101  
000102  
000103  
000104

N=J	000105
L=1	000106
*****SET POSITIONS FOR FIXED-POINT TEMPERATURE CALCULATIONS	000107
DO 10 I=1,M	000108
ZTC(I)=I/(M+1.)	000109
10 CONTINUE	000110
*****COMPUTE PROPERTIES AT SATURATION TEMPERATURE	000111
IF(ICPTU.EQ.2) CALL CNVRT1	000112
CALL PROPT6	000113
*****	000114
***** THE HEATUP REGIME *****	000115
*****	000116
*****INITIALIZE VARIABLES	000117
DN=1./VF(TI)	000118
VF23=1./DN	000119
CF=1./DFIBER	000120
FR3LOG=ALOG(PREF3)	000121
PDENOM=(PREF3-PREF1)/2.	000122
FMID=(PREF3+PREF1)/2.	000123
MRSTAR=STAR*DN	000124
IF(MRSTAR.GT.MRO) MRSTAR=MRO	000125
IF(MRSTAR.EQ.MRO) FLAG=1	000126
PG=MRO*Eh	000127
EMIN=ES2/ES1	000128
CALL CNSTMN(CSF)	000129
N=KMIN	000130
XX=(N-1)/(N+1)	000131
CX=1./(N-1)	000132
DO 20 I=1,N	000133
TOLC(I)=TI	000134
20 CONTINUE	000135
IF(FLAG.EQ.1) RATIO2=1.	000136
RATIO3=1.	000137
PR=MRO	000138
P1=EVALP(O.,TB)	000139
P2=EVALP(MRSTAR,TB)	000140
	000141
	000142
	000143
	000144
	000145
	000146
	000147
	000148
	000149
	000150
	000151
	000152
	000153
	000154
	000155
	000156
	000157
	000158
	000159

C	M4=M1	000160
	N1=EVALN(1,C,0.)	000161
	N2=EVALN(1,MRSTAR,0.)	000162
	N4=N1	000163
C	CC=DFIBER*(CPF+MR*CPH)	000164
	CK=MR*DFIBER*KWATER	000165
	A=(KFIBER+CK/DK)/DC	000166
C		000167
C		000168
C		000169
C	*****CALCULATE MECHANICAL PRESSURE AND SHEET PROPERTIES	000170
C		000171
	3C IF(S3.EQ.1.) GO TO 40	000172
	CALL PRESSR(TIME)	000173
	TBAR1=(TOLD(1)+TOLD(K))/2.	000174
	M3=EVALM(MR,TBAR1)	000175
	N3=EVALN(2,M3,F)	000176
	DELTA1=BK/(M3*P**N3)	000177
	PSI=A/DELTA1**2	000178
	DT=TIMER*DX**2/(2.*PSI)	000179
	Fk=PVIB	000180
	TIME=TIME+DT	000181
	GO TO 50	000182
C		000183
	4C YL(1)=DELTA1	000184
	MR=Ck*(YL(1)/BK-1./DFIBER)	000185
	TBAR1=(TOLD(1)+TOLD(K))/2.	000186
	M3=EVALM(MR,TBAR1)	000187
	N3=EVALN(2,M3,F)	000188
	CC=DFIBER*(CPF+MR*CPH)	000189
	CK=MR*DFIBER*KWATER	000190
	A=(KFIBER+CK/DK)/DC	000191
C		000192
	PHI=-CK*CPH*DLDT*DFIBER/(CC*BK)	000193
	PSI=A/(YL(1)**2)	000194
C		000195
	DT=TIMER*DX/(2.*PSI/DX+ABS(PHI)/2.)	000196
	F2=PSI*DT/(DX**2)	000197
	F3=PHI*DT/DX	000198
	TERM1=PHI*DT/3.	000199
	TERM2=2.*F2/9.	000200
C		000201
	h=DT/100.	000202
	TIMEND=TIME+DT	000203
	CALL DGEAR(1,DLDTFN,DUMFUN,TIME,H,YL,TIMEND,TOL,METH,MITER,	000204
	* INDEX,IHM,MN,IER)	000205
	IF(IER.GT.128) WRITE(6,/) ICL,YL(1),TIMEND,H,TIME,METH,MITER,	000206
	* INDEX	000207
	P=(BK/(YL(1)*M3))**(1./N3)	000208
	Fk=PVIB+1.5*DLDT/CGEFF	000209
	TIME=TIMEND	000210
C		000211
	5C C3=M3*P**N3	000212
	Y=(MR-MRSTAR)*C3	000213
		000214

```

DELTA T=EW/C3
CONST=C3/DFIBER
E3=1.-CONST
IF(E3.LT.EMIN) CALL WARNIN(2,3,E3)
IF(E3.LT.EMIN) GO TO 9999
ESTAR=ES1*E3-ES2
S3=MR*C3/(E3*DW)
IF(S3.GT.1.) S3=1.
S3STAR=Y/(ESTAR*CW)

```

000215  
000216  
000217  
000218  
000219  
000220  
000221  
000222  
000223

#### \*\*\*\*\*CALCULATE HEAT TRANSFER PARAMETERS

```

HCDRY=HCREP*(HC1*(P/PREF2)**HC2-HC3)
HC=(HCDRY+MR*DFIBER*HCHET/DW)*CONST
M1=MFIBER*CONST
K3=K1+DK*CONST/DW
BIDX=HC*DELTA T*DX/M3

```

000224  
000225  
000226  
000227  
000228  
000229  
000230  
000231  
000232

#### .....CALCULATE INTERIOR TEMPERATURES

```

IF(S3.EG.1.) GO TO 70
GO 60 I=2,K-1
TNEW(I)=TIMER*(TOLD(I+1)+TOLD(I-1))/2.+(1.-TIMER)*TOLD(I)
60 CONTINUE
GO TO 110

70 IF(PHI.LT.0.) GO TO 90
GO 80 I=3,K-1
F3X=F3*(I-1)*DX
TNEW(I)=(F2-F3X/3)*TOLD(I+1)+(1.-2.*F2-F3X/2.)*TOLD(I)+
* (F2+F3X)*TOLD(I-1)-(F3X/6)*TOLD(I-2)
80 CONTINUE
TNEW(2)=(F2-F3*DX/2.)*TOLD(3)+(1.-2.*F2)*TOLD(2)+(F2+F3*DX/2.)*
* TOLD(1)
GO TO 120

90 GO 100 I=2,K-2
F3X=F3*(I-1)*DX
TNEW(I)=(F2-F3X)*TOLD(I+1)+(1.-2.*F2+F3X/2.)*TOLD(I)+
* (F2+F3X/3)*TOLD(I-1)+(F3X/6)*TOLD(I+2)
100 CONTINUE
TNEW(K-1)=(F2-F3*(K-2)*DX/2.)*TOLD(K)+(1.-2.*F2)*TOLD(K-1)+
* (F2+F3*(K-2)*DX/2.)*TOLD(K-2)
GO TO 120

```

000233  
000234  
000235  
000236  
000237  
000238  
000239  
000240  
000241  
000242  
000243  
000244  
000245  
000246  
000247  
000248  
000249  
000250  
000251  
000252  
000253  
000254  
000255  
000256  
000257  
000258  
000259

#### .....CALCULATE BOUNDARY TEMPERATURES

```

110 TNEW(1)=TOLD(1)-(TNEW(2)-TOLD(2))/3.+(TIMER/9.)*(6.*BIDX*(TH-
* TOLD(1))-2.*TOLD(1)-3.*TOLD(2)+6.*TOLD(3)-TOLD(4))
TNEW(K)=TOLD(K)-(TNEW(K-1)-TOLD(K-1))/3.-(TIMER/9.)*(2.*TOLD(K)+
* 3.*TOLD(K-1)-6.*TOLD(K-2)+TOLD(K-3))
GO TO 130

```

000260  
000261  
000262  
000263  
000264  
000265  
000266  
000267  
000268  
000269



C		000270
	12C TNEW(1)=TOLD(1)-(TNEW(2)-TOLD(2))/3.+TERM1*BIDX*(TH-TOLD(1))+	000271
	* TERM2*(6.*BIDX*(TH-TOLD(1))-2.*TOLD(1)-3.*TOLD(2)+6.*TOLD(3)-	000272
	* TOLD(4))	000273
	TNEW(K)=TOLD(K)-(TNEW(K-1)-TOLD(K-1))/3.-TERM2*(2.*TOLD(K)+	000274
	* 3.*TOLD(K-1)-6.*TOLD(K-2)+TOLD(K-3))	000275
C		000276
C		000277
C	.....RESET OLD TEMPERATURE VALUES	000278
C		000279
	13C GO 140 I=1,N	000280
	TOLD(I)=TNEW(I)	000281
	14C CONTINUE	000282
C		000283
C		000284
C	*****COMPUTE TEMPERATURES AT FIXED-POINT LOCATIONS	000285
C		000286
	GO 150 I=1,N	000287
	KK=I*XX	000288
	REM=I*XX-KK	000289
	TC(I)=TNEW(1+KK)-REM*(TNEW(1+KK)-TNEW(2+KK))	000290
	150 CONTINUE	000291
C		000292
C		000293
C	*****INCREMENT QUANTITIES AND WRITE RESULTS	000294
C		000295
	TS=TNEW(1)	000296
	QINIT=QINIT+(Q+HC*(TH-TS))*DT/2.	000297
	G=HC*(TH-TS)	000298
	IF(N.LT.J.AND.L.GT.LMAX.AND.TNEW(1)-LT.TB) GO TO 160	000299
C		000300
	T1=TS	000301
	T2=T1	000302
	FGAUGE=Fh-PVTB	000303
	IF(PGAUGE.LT.0.) PGAUGE=0.	000304
	SEC=TIME*3600.	000305
	THIC=TC(1+N/2)	000306
	CHTC=Q/(TH-THIC)	000307
	PREM=PR*BM	000308
	PREL=1.-PREM/MC	000309
C		000310
	T3=TNEW(K)	000311
	CALL WRITER(IOPTU)	000312
	A=1	000313
	GO TO 170	000314
C		000315
C		000316
C	*****INCREMENT PRINT CONTROL VARIABLES	000317
C		000318
	16C A=N+1	000319
	17C L=L+1	000320
C		000321
C		000322
C	*****DETERMINE EXIT CRITERIA	000323
C		000324

```

IF(1800*TIME.GE.RISTIM.ANC.IOPTP.EQ.2) GO TO 9999
IF((FLAG.EQ.1.AND.TNEW(K).LT.TB).OR.
* PV(TNEW(1)).LT.PW.OR.FV(TNEW(1)).LT.PVTB) GO TO 30

*****WRITE HEATUF REGIME FINAL OUTPUT

I1=TS
I2=I1
FGAUGE=PW-PVTB
IF(PGAUGE.LT.0.) PGAUGE=0.
SEC=TIME*3600.
THIC=TC(1+M/2)
CHIC=G/(TH-THIC)
PREM=MR*BW
PREL=1.-PREP/MG

I3=TNEW(K)
IF(K.NE.1) CALL WRITER(IOPTU)
WRITE(6,930)
WRITE(6,935) (I,TNEW(I),I=1,K)
*****

*****
***** THE TRANSITION REGIME *****
*****

*****WRITE TRANSITION REGIME HEADING

WRITE(6,940)

*****INITIALIZE VARIABLES

L=1
IF(FLAG.EQ.1) DELTA2=DELTA1
DELTA3=DELTA1
THICK2=DELTA2
THICK3=DELTA3
IF(FLAG.EQ.1.) THICK3=0.

RATIO2=DELTA2/DELTA1
RATIO3=DELTA3/DELTA1
LIQDEW=MG-E3*S3*DW*DELTA1

F=SPRES(F)/FACIOR
NAKW=S3STAR**4/(CR*C3)
EW3=BW
IF(FLAG.EQ.1) EW3=0.
IF(FLAG.EQ.1) EW2=BW
C1=M1*P**N1
C2=M2*P**N2

```

000325  
000326  
000327  
000328  
000329  
000330  
000331  
000332  
000333  
000334  
000335  
000336  
000337  
000338  
000339  
000340  
000341  
000342  
000343  
000344  
000345  
000346  
000347  
000348  
000349  
000350  
000351  
000352  
000353  
000354  
000355  
000356  
000357  
000358  
000359  
000360  
000361  
000362  
000363  
000364  
000365  
000366  
000367  
000368  
000369  
000370  
000371  
000372  
000373  
000374  
000375  
000376  
000377  
000378

	C4=M4*P**N4	000379
	M=MRSTAR*C2	000380
	X=MR*C3	000381
C		000382
	T3=TB	000383
	Z=1.-MRSTAR/MR	000384
	CXX=DX	000385
	CIFFIX=DXX	000386
	CIFFI=DX	000387
	CIFFFX=DXX	000388
	CIFFF=DX	000389
	DELTA1=CIFFIX*THICK3	000390
	DELTA2=DELTA1-CIFFF*THICK3	000391
C		000392
	INIT=2	000393
	IFINI=K-1	000394
C		000395
	IF(FLAG.EQ.1) GO TO 350	000396
C		000397
	CTDZ23=(T2-T3)/DELTA1	000398
C		000399
	CALL PROP23(1)	000400
	A2=KAKW*CPDT23/(VISF23*VF23*Y)	000401
	V=A2*Y*CPW*CTDZ23/((1.-E3)*DC)	000402
	FSI=A/DELTA1**2	000403
	FHI=V/DELTA1	000404
C		000405
C		000406
C	*****COMPUTE REQUIRED DERIVATIVES	000407
C		000408
	180 C2=A2*CTDZ23	000409
	C4=A4*CTDZ12	000410
	C5=D2-A5*CTDZ12	000411
	C6=-A6*CTDZ38	000412
	IF(RATIO3.EQ.1..AND.TNEW(K).GE.TB) D6=K3*(TNEW(K)-TNEW(K-1))/	000413
	* (CHF6(T3)+DELHD(3))*CXX*THICK3*X)	000414
	C7=D2*C2	000415
C		000416
	DENOM=D6+C7	000417
C		000418
C		000419
C	*****SET MAXIMUM ALLOWABLE TIME INCREMENT	000420
C		000421
	CTMAX=TIMER*CX/(2.*PSI/DX+PHI/2.)	000422
C		000423
	CT1=CTMAX	000424
	CT2=CTMAX	000425
	CT3=CTMAX	000426
	CT4=CTMAX	000427
	CT5=CTMAX	000428
C		000429
	IF(DELTA1.NE.DELTA2) GO TO 190	000430
	IF(D2.NE.DENOM) DT1=(DELTA3-DELTA2)/(D2-DENOM)	000431

```

CT=AMIN1(DT1,DTMAX)                                000432
IF((C2*DT).GE.CIFFIX*THICK3) IOPT1=1                000433
GO TO 200                                              000434
190 IF(D4.NE.D5) DT1=(DELTA2-DELTA1)/(D4-D5)         000435
IF(DT1.LT.0.) DT1=DTMAX                              000436
IF(D5.NE.DENOM) DT2=(DELTA3-DELTA2)/(D5-DENOM)       000437
IF(DT2.LT.0.) DT2=DTMAX                              000438
CT=AMIN1(DT1,DT2,DTMAX)                             000439
IF((C5*DT).GE.CIFFIX*THICK3) IOPT1=1                000440
200 IF((-DENOM*CT).GE.DIFFFX*THICK3) IOPT2=1          000441
IF(10PT1.EQ.1.AND.10PT2.EQ.1) GO TO 210             000442
IF(10PT1.EQ.0) DT3=DIFFI*DX/(2.*PSI)                 000443
IF(DENOM.LE.0.) DT4=DIFF*DX/(2.*PSI)                 000444
IF(DENOM.GT.0..AND.RATIO3.NE.1.) DT5=(DXX-DIFFX)*THICK3/DENOM 000445
IF(DT5.EQ.0.) DT5=DXX*THICK3/DENOM                  000446
CT=AMIN1(DT1,DT2,DT3,DT4,DT5,DTMAX)                  000447
IF(DELTA1.EQ.DELTA2.AND.D2*DT.GE.DIFFIX*THICK3) IOPT1=1 000448
IF(DELTA1.EQ.DELTA2.AND.D2*DT.LT.DIFFIX*THICK3) IOPT1=0 000449
IF(DELTA1.NE.DELTA2.AND.D5*DT.GE.CIFFIX*THICK3) IOPT1=1 000450
IF(DELTA1.NE.DELTA2.AND.D5*DT.LT.CIFFIX*THICK3) IOPT1=0 000451
IF((-DENOM*CT).GE.DIFFFX*THICK3) IOPT2=1             000452
IF((-DENOM*CT).LT.DIFFFX*THICK3) IOPT2=0             000453
CT=TIMER*DT                                            000454
210 TIME=TIME+DT                                       000455
*****CALCULATE NEW TEMPERATURE DISTRIBUTION          000456
LC=DFIBER*(CPF*MR*CPH)                                000457
CK=MR*DFIBER*KWATER                                    000458
A=(KFIBER+CK*VF23)/DC                                 000459
V=D2*V*CPH/((1.-E3)*DC)                              000460
FSI=A*(C3/8h)**2                                       000461
PHI=V*C3/8h                                           000462
F2=PSI*DT/DX**2                                       000463
F3=PHI*DT/DX                                          000464
TERM2=2.*F2/9.                                        000465
GO 220 I=INIT,INIT+1                                  000466
TNEW(I)=(F2-F3/2)*TOLD(I+1)+(1-2*F2)*TOLD(I)+(F2+F3/2)*TOLD(I-1) 000467
220 CONTINUE                                           000468
GO 230 I=INIT+2,IFINI                                  000469
TNEW(I)=(F2-F3/3)*TOLD(I+1)+(1-2*F2-F3/2)*TOLD(I)+(F2+F3)* 000470
* TOLD(I-1)-(F3/6)*TOLD(I-2)                          000471
230 CONTINUE                                           000472
IF(10PT1.EQ.0) TNEW(INIT)=TOLD(INIT)-PHI*DT*((TOLD(INIT+1)-T2)/ 000473
* (DX+CIFFI))+2.*PSI*DT*(TOLD(INIT+1)/(DX*(DIFFI+DX))-TOLD(INIT) 000474
000475
000476
000477
000478
000479
000480
000481
000482
000483
000484
000485

```

	* /(DIFFI*DX)+T2/(DIFFI*(DIFFI+DX)))	000486
C	IF(IGPT2.EQ.0.AND.RATIO3.NE.1.) TNEW(IFINI)=TOLD(IFINI)-PHI*DT*	000487
	* ((T3-TOLD(IFINI-1))/(DX+DIFFF))+2.*PSI*DT*(T3/(DIFFF*	000488
	* (DX+DIFFF))-TOLD(IFINI)/(DX+DIFFF)+TOLD(IFINI-1)/(DX*(DX+	000489
	* DIFFF)))	000490
C	TNEW(K)=TOLD(K)-(TNEW(K-1)-TOLD(K-1))/3.-TERM2*(2.*TOLD(K)+	000491
	* 3.*TOLD(K-1)-6.*TOLD(K-2)+TOLD(K-3))	000492
	IF(TNEW(K).GT.TNEW(K-1)) TNEW(K)=TNEW(K-1)	000493
	IF(TNEW(K).GE.18) TNEW(K)=18	000494
	IF(RATIO3.EQ.1.) GO TO 240	000495
C	DO 240 I=IFINI+1,K	000496
	TNEW(I)=TB	000497
	240 CONTINUE	000498
C		000499
C	*****CALCULATE RATES OF BASIS HEIGHT CHANGE	000500
C	RATE1=0.	000501
	IF(DELTA1.NE.DELTA2) RATE1=D4	000502
C		000503
	RATE2=D2	000504
	IF(DELTA1.NE.DELTA2) RATE2=D5	000505
C		000506
	RATE3=DENOM	000507
C		000508
	IF(FLAG.EQ.1) RATE3=0.	000509
C		000510
	SIGN=0.	000511
	IF(D6.EQ.0.) SIGN=1.	000512
	IF(RATIO3.EQ.1.) LIQDEN=SIGN*MREL*MO*(1.-SIGN)*	000513
	*(LIQDEN+RATE3)*DT)	000514
C		000515
C		000516
C	*****CALCULATE MECHANICAL AND HYDRAULIC PRESSURE	000517
C	CALL PRESSR(TIME)	000518
C		000519
	PH1=HYDRAL(T1,T1)	000520
	PH2=HYDRAL(T1,T2)	000521
	PH3=HYDRAL(T2,T3)	000522
	PH4=HYDRAL(T3,TB)	000523
C		000524
	F1=P-PH1	000525
	IF(P1.LE.0.) P1=PREF1	000526
	F2=P-PH2	000527
	F3=P-PH3	000528
	F4=P-PH4	000529
C		000530
C		000531
C	*****CALCULATE BASIS WEIGHT, CONCENTRATION AND THICKNESS	000532
C		000533
		000534
		000535
		000536
		000537
		000538
		000539

CBW1DT=C2*RATE1	000540
CBW2DT=C3*RATE2-DBW1DT	000541
CBW3DT=C3*(RATE3-RATE2)	000542
IF(RATIO3.EQ.1..AND..RATE3.EQ.0.) DBW3DT=-C3*RATE2	000543
CBW4DT=-C3*RATE3	000544
	000545
EW1=BW1+CBW1DT*DT	000546
EW2=EW2+DBW2DT*DT	000547
EW3=BW3+CBW3DT*DT	000548
IF(FLAG.EQ.1) EW3=0.	000549
EW4=BW4+DBW4DT*DT	000550
	000551
IF(EW1.LT.0.) BW1=0.	000552
IF(BW2.LT.0.) BW2=0.	000553
IF(BW3.LT.0..OR..FLAG.EQ.1) BW3=0.	000554
IF(EW4.LT.0.) BW4=0.	000555
	000556
EWSUM=BW1+BW2+EW3+BW4	000557
BWCORR=BW/BSUM	000558
	000559
EW1=EW1*BWCORR	000560
EW2=EW2*BWCORR	000561
EW3=EW3*BWCORR	000562
EW4=EW4*BWCORR	000563
	000564
TBAR1=(T5+T1)/2.	000565
TBAR2=(T1+T2)/2.	000566
TBAR3=(T2+TNEW(IFINI))/2.	000567
TBAR4=(TNEW(IFINI)+TNEW(K))/2.	000568
	000569
P1=EVALM(0.,TBAR1)	000570
P2=EVALM(MRSTAR,TBAR2)	000571
P3=EVALM(MR,TBAR3)	000572
P4=EVALM(0.,TBAR4)	000573
	000574
A3=EVALN(2,PR,P3)	000575
	000576
C1=M1*P1**N1	000577
C2=M2*P2**N2	000578
C3=M3*P3**N3	000579
C4=M4*P4**N4	000580
	000581
THICK1=BW1/C1	000582
THICK2=BW2/C2	000583
THICK3=BW3/C3	000584
THICK4=BW4/C4	000585
	000586
	000587
CALCULATE POROSITY AND SATURATION	000588
	000589
E1=1.-C1/DFIBER	000590
E2=1.-C2/DFIBER	000591
E3=1.-C3/DFIBER	000592
ESTAR=E51+E3-E52	000593

E4=1.-C4/DFIBER	000594
IF(C1.GT.DFIBER) CALL WARNIN(1,1,C1)	000595
IF(E2.LT.EMIN) CALL WARNIN(2,2,E2)	000596
IF(E3.LT.EMIN) CALL WARNIN(2,3,E3)	000597
IF(C4.GT.DFIBER) CALL WARNIN(1,4,C4)	000598
IF(C1.GT.DFIBER.OR.E2.LT.EMIN.OR.E3.LT.EMIN.OR.C4.GT.DFIBER)	000599
* GO TO 9999	000600
C	000601
CALL CALLER(4)	000602
W=MRSTAR*C2	000603
X=MR*C3	000604
Y=(MR-MRSTAR)*C3	000605
Z=Y/X	000606
C	000607
S2=W*VF12/E2	000608
S3=X*VF23/E3	000609
S3STAR=Y*VF23/ESTAR	000610
IF(S3.LE.1.) GO TO 270	000611
IF(BW4.NE.0.) GO TO 260	000612
S3=1.	000613
S3STAR=1.	000614
MR=E3/(VF23*C3)	000615
X=E3/VF23	000616
Y=(MR-MRSTAR)*C3	000617
Z=Y/X	000618
GO TO 270	000619
260 BW4=BW4-(S3-1.)*BW3	000620
IF(BW4.LT.0.) BW4=0.	000621
BW3=BW-BW1-BW2-BW4	000622
GO TO 250	000623
C	000624
C	000625
C*****INCREMENT INTERFACE POSITIONS	000626
C	000627
270 DELTA1=THICK1	000628
DELTA2=DELTA1+THICK2	000629
DELTA3=DELTA2+THICK3	000630
DELTA4=DELTA3+THICK4	000631
IF(THICK3.EC.0.) DELTA3=DELTA4	000632
C	000633
IF(D5.GT.0.) INIT=((BW1+BW2)/BW)*(K-1)+2	000634
IFINI=(K-1)-(K-1)*BW4/BW	000635
IF(IFINI.LE.INIT) GO TO 450	000636
CXX=DX*BW/BW3	000637
CIFFFX=DXX-BW4/BW	000638
CIFFIX=1.-DIFFFX-(IFINI-INIT)*DXX	000639
IF(CIFFIX.GT.0XX) CALL WARNIN(3,1,0.)	000640
IF(DIFFFX.GT.0XX) CALL WARNIN(4,1,0.)	000641
DELTA1=DELTA2+CIFFIX*THICK3	000642
DELTA4=DELTA3-CIFFFX*THICK3	000643
CIFF1=DIFFIX*BW3/BW	000644
CIFFF=DIFFFX*BW3/BW	000645
C	000646
C	000647
C*****CALCULATE THERMAL CONDUCTIVITY AND CONTACT COEFFICIENT	000648

```

K1=KFIBER*(1.-E1)
K2=KFIBER*(1.-E2)+KWATER*E2*S2
K3=KFIBER*(1.-E3)+KWATER*E3*S3
K4=KFIBER*(1.-E4)

HCDRY=HCREP*(HC1*(P1/PREF2)+HC2-HC3)
PC=HCDRY*(1.-E1)
IF(DELTA1.EQ.0.) HC=HCDRY*(1.-E2)+E2*S2*HCNET
IF(DELTA2.EQ.0.) HC=HCDRY*(1.-E3)+E3*S3*HCNET

```

\*\*\*\*\*CALCULATE PERMEABILITY FACTORS

```

R=SPRES(F)/FACTOR

```

```

KABS2=1./(R*C2)
KABS3=1./(R*C3)
KABS4=1./(R*C4)

```

```

KAK=KABS3*S3STAR**4

```

\*\*\*\*\*SET RELATIVE INTERFACE POSITIONS AND REMAINING MOISTURE

```

RATIO1=DELTA1/DELTA1
RATIO2=DELTA2/DELTA1
RATIO3=DELTA3/DELTA1

PREM=MR*Bh3+MRSTAR*Bh2
PREL=1.-PREP/MC
IF(RATIO2.EQ.1.) GO TO 390

```

\*\*\*\*\*COMPUTE NEW VALUES FOR T1, T2 AND T3

```

IF(DELTA1.NE.DELTA2) GO TO 280
ALFA=DELTA3-DELTA1
TERM1=(1./HC*DELTA1/K1)*K3/(DELTA1-DELTA1)
T1=(TH+TERM1*TNEH(INIT))/(1.+TERM1)
T2=T1
GO TO 290

```

```

280 GO 250 I=1,IMAX

```

```

T01=T1
T02=T2

CALL PROPT2
HFG1=HFG(T1)+DELHD(1)
HFG2=HFG(T2)+DELHD(2)

ALF=DELTA2-DELTA1

```

000649  
000650  
000651  
000652  
000653  
000654  
000655  
000656  
000657  
000658  
000659  
000660  
000661  
000662  
000663  
000664  
000665  
000666  
000667  
000668  
000669  
000670  
000671  
000672  
000673  
000674  
000675  
000676  
000677  
000678  
000679  
000680  
000681  
000682  
000683  
000684  
000685  
000686  
000687  
000688  
000689  
000690  
000691  
000692  
000693  
000694  
000695  
000696  
000697  
000698  
000699  
000700  
000701



	EET=DELTA3-DELTA2	000702
C		000703
	TERM1=(1./HC*DELTA1/K1)*(1./ALF)*(HFG1*KABS2*DPDT12/	000704
	* (VG12*VISG12)*K2)	000705
	TERM2=(KABS2*DPDT12*HFG2/(K3*VG12*VISG12)*K2/K3)*	000706
	* (DELTA1-DELTA2)/ALF	000707
	DENOM=1.+TERM1+TERM2	000708
C		000709
	T1=((1.+TERM2)*TH+TERM1*TNEW(INIT))/DENOM	000710
	T1=(T01+T1)/2.	000711
	T2=(TERM2*TH+(1.+TERM1)*TNEW(INIT))/DENOM	000712
	T2=(T02+T2)/2.	000713
290	CONTINUE	000714
C		000715
	IF(RATIO3.EQ.1.) GO TO 310	000716
C		000717
	CALL PROF3E	000718
	HFG3=HFG(T3)+DELHD(3)	000719
C		000720
	DO 300 I=1,IMAX	000721
C		000722
	T03=T3	000723
C		000724
	TERM1=(KABS4*HFG3*DPDT3B/(K3*VISG3B*VG3B))*(DELTA3-DELTA4)	000725
	* /(DELTA7-DELTA3)	000726
C		000727
	T3=(TNEW(IFINI)+TERM1*TB)/(1.+TERM1)	000728
	T3=(T03+T3)/2.	000729
300	CONTINUE	000730
	GO TO 320	000731
C		000732
	310 T3=TB	000733
C		000734
	320 IF((TNEW(IFINI)-T3)/DIFFFX.EQ.(T2-T3)) GO TO 450	000735
C		000736
C		000737
C	*****RECOMPUTE VARIABLES FOR DERIVATIVE CALCULATIONS	000738
C		000739
	IF(DELTA1.NE.DELTA2) GO TO 330	000740
	DTDZ12=0.	000741
	DTDZ23=(T2-T3)/ALFA	000742
	IF(T2.LE.TB) DTDZ23=0.	000743
	GO TO 340	000744
C		000745
	330 DTDZ12=(T1-T2)/ALF	000746
	IF(T2.LE.TB) DTDZ12=(T1-TB)/ALF	000747
	IF(T1.LE.TB) DTDZ12=0.	000748
	DTDZ23=(T2-T3)/BET	000749
	IF(T2.LE.TB) DTDZ23=0.	000750
C		000751
	340 DTDZ3B=0.	000752
	IF(RATIO3.NE.1.) DTDZ3E=(T3-TB)/(DELTA7-DELTA3)	000753
C		000754
	CALL CALLER(1)	000755

```

A2=KAKH*DPOT23/(VISF23*VF23*Y)
A4=KABS2*DPCT12/(VISG12*VG12*W)
A5=A4*W/Y
A6=KABS4*DPCT3E/(VG3B*VISG3B*X)
GO TO 400

```

000756  
000757  
000758  
000759  
000760  
000761  
000762  
000763  
000764  
000765  
000766  
000767  
000768  
000769  
000770  
000771  
000772  
000773  
000774  
000775  
000776  
000777  
000778  
000779  
000780  
000781  
000782  
000783  
000784  
000785  
000786  
000787  
000788  
000789  
000790  
000791  
000792  
000793  
000794  
000795  
000796  
000797  
000798  
000799  
000800  
000801  
000802  
000803  
000804  
000805  
000806  
000807  
000808  
000809

\*\*\*\*\*HANDLE SPECIAL CASE OF INTRA-FIBER WATER

```

35C CTMA)=TIMER*CX**2/(2.*PSI)
   CIFFFX=CXX
   I1=TNEW(1)
   I2=TNEW(K)
   HFG2=HFG(I2)+DELHD(1)
   C7=0.
   X=MR*C2

36C C6=M3*(I2-TNEW(IFINI))/(HFG2+DXX*THICK2*X)

   CT1=CTMAX
   CT2=CTMAX
   CT1=(DELTA2-DELTA1)/(-D6)
   CT=AMIN1(CT1,CTMAX)
   IF((-C6*DT).GE.DIFFFX*THICK2) ICPT2=1
   IF(ICPT2.EQ.1) GO TO 37C
   CT2=DX*CIFFF/(2.*PSI)
   CT=AMIN1(CT1,CT2,CTMAX)
   CT=TIMER*DT

37C TIME=TIME+DT

   A=(KFIBER+DX*VF12)/DC
   PSI=A*(C2/BH)**2
   F2=PSI*DT/DX**2

   GO 380 I=INI1,IFINI
   TNEW(I)=F2*(TOLD(I+1)+TOLD(I-1))/2.+(1.-2.*F2)*TOLD(I)

38C CONTINUE

   TNEW(1)=TOLD(1)-(TNEW(2)-TOLD(2))/3.+(2.*F2/9.)*(6.*BIDX*(TH-
* TOLD(1))-2.*TOLD(1)-3.*TOLD(2)+6.*TOLD(3)-TOLD(4))
   I1=TNEW(1)
   TOLD(1)=TNEW(1)

   IF(ICPT2.EQ.0) TNEW(IFINI)=TOLD(IFINI)+2.*PSI*DT*(I2/(DIFFF*
* (DIFFF+DX))-TOLD(IFINI)/(C)*DIFFF)+TOLD(IFINI-1)/(DX*(DX+
* CIFFF)))

   FATE2=D6
   CALL PRESSR(TIME)
   PH2=HYDRAL(I1,I2)
   PH4=HYDRAL(I2,I1)
   F2=F-PH2
   F4=F-PH4

```

C	CEW2DT=C2*RA1E2	000810
	CEW4DT=-DBW2DT	000811
C		000812
	EW2=BW2*DBW2DT*DT	000813
	EW4=EW4*DBW4DT*DT	000814
C		000815
	BWSUM=BW2+BW4	000816
	EWCORR=EW/BWSUM	000817
	EW2=EW2*EWCORR	000818
	EW4=EW4*EWCORR	000819
	TBAR2=(T1+T2)/2.	000820
	TBAR4=(T2+T8)/2.	000821
	P2=EVALM(MRSTAR,TBAR2)	000822
	M4=EVALM(0.,TBAR4)	000823
	C2=M2*P2**N2	000824
	C4=M4*P4**N4	000825
C		000826
	THICK2=EW2/C2	000827
	THICK4=EW4/C4	000828
C		000829
	E2=1.-C2/DFIBER	000830
	E4=1.-C4/DFIBER	000831
	IF(E2.LT.EMIN) CALL WARNIN(2,2,E2)	000832
	IF(C4.GT.DFIBER) CALL WARNIN(1,4,C4)	000833
	IF(E2.LT.EMIN.OR.C4.GT.DFIBER) GO TO 9999	000834
C		000835
	CALL PRCP12	000836
	X=MR*C2	000837
	Z=C.	000838
	S2=X*VF12/E2	000839
C		000840
	DELTA2=THICK2	000841
	DELTA4=DELTA2*THICK4	000842
	IFINI=(K-1)-(K-1)*BW4/BW	000843
	DXX=DX*BW/BW2	000844
	DIFFFX=DXX-BW4/BW	000845
	IF(DIFFFX.GT.0)X) CALL WARNIN(4,1,0.)	000846
	DELTA4=DELTA2-DIFFFX*THICK2	000847
	K2=KFIBER*(1.-E2)+KWATER*E2*S2	000848
	M4=KFIBER*(1.-E4)	000849
	HCDRY=HCREP*(HC1*(P2/PREF2)**HC2-HC3)	000850
	PC=HCDRY*(1.-E2)+E2*S2*HCDRY	000851
	EIDX=HC*BW*DX/(K2*C2)	000852
C		000853
	R=SPRES(P)/FACTOR	000854
	MABS2=1./(R*C2)	000855
	MABS4=1./(R*C4)	000856
C		000857
	FATIG1=0.	000858
	FATIG2=DELTA2/DELTA4	000859
	FATIG3=1.	000860
C		000861
	PREP=MRSTAR*EW2	000862
	PREL=1.-PREP/PC	000863
C		000864
		000865

```

CALL PROF23(2)
HFG2=HFG(T2)*DELHD(1)

IF(RATIO2.EQ.1.) GO TO 390
DO 390 I=1,IMA
  T2=T1
  TERM1=(KAES4*HFG2*CPDT23/(K3*VISG23*VG23))*(DELTA2-DELTA1)/
  * (DELTA1-DELTA2)
  T2=(TNEW(IFINI)+TERM1*TB)/(1.+TERM1)
  T2=(T2+T1)/2.
390 CONTINUE

IF(RATIO2.EQ.1.) T2=TB
IF((TNEW(IFINI)-T2)/DIFFF).EQ.(T1-T2) GO TO 450

*****RESET TEMPERATURE DISTRIBUTION AND TIME OPTIONS

400 DO 410 I=INIT,K
  TOLD(I)=TNEW(I)
410 CONTINUE

  ICPT1=0
  ICPT2=0

*****COMPUTE TEMPERATURES AT FIXED-POINT LOCATIONS

  SUM12=BW1+B*2
  SUM123=SUM12+B*3
  DO 420 I=1,M
    L=ZTC(I)*BW
    KK=I*XX
    REM=I*XX-KK
    IF(U.LT.BW1.AND.BW1.NE.0.) TC(I)=TS-(TS-T1)*(U/BW1)
    IF(U.GT.BW1.AND.U.LT.SUM12.AND.BW2.NE.0.) TC(I)=T1-(T1-T2)*
  * (L-BW1)/BW2
    IF(U.GT.SUM12.AND.U.LT.SUM123.AND.BW3.NE.0.) TC(I)=TNEW(1+KK)-
  * REM*(TNEW(1+KK)-TNEW(2+KK))
    IF(U.GT.SUM123.AND.U.LT.B*4.AND.BW4.NE.0.) TC(I)=T3-(T3-TB)*
  * (U-SUM123)/BW4

    IF(U.EQ.BW1) TC(I)=T1
    IF(U.EQ.SUM12) TC(I)=T2
    IF(U.EQ.SUM123) TC(I)=T3
    IF(U.EQ.BW) TC(I)=TB
420 CONTINUE

*****INCREMENT QUANTITIES AND WRITE RESULTS

PC=PREM/(MREM*BW)
TS=(TH*HC*DELTA1/K1+T1)/(1.+HC*DELTA1/K1)

```

000866  
 000867  
 000868  
 000869  
 000870  
 000871  
 000872  
 000873  
 000874  
 000875  
 000876  
 000877  
 000878  
 000879  
 000880  
 000881  
 000882  
 000883  
 000884  
 000885  
 000886  
 000887  
 000888  
 000889  
 000890  
 000891  
 000892  
 000893  
 000894  
 000895  
 000896  
 000897  
 000898  
 000899  
 000900  
 000901  
 000902  
 000903  
 000904  
 000905  
 000906  
 000907  
 000908  
 000909  
 000910  
 000911  
 000912  
 000913  
 000914  
 000915  
 000916  
 000917  
 000918

```

C      CTOTAL=CTOTAL+(Q+MC*(TH-TS))*DT/2.                                000919
C      C=MC*(TH-TS)                                                         000920
C      IF(N.LT.J.AND.L.GT.LMAX.AND.MC.GT.MFINAL) GO TO 430                000921
C                                                                              000922
C      PGAUGE=PV(T1)-FVTB                                                    000923
C      IF(PGAUGE.LT.0.) PGAUGE=0.                                           000924
C      SEC=TIME*3600.                                                         000925
C      TMID=TC(1+M/2)                                                        000926
C      CHTC=G/(TH-TMID)                                                       000927
C                                                                              000928
C      IF(RATIO3.EQ.1.) T3=INEN(K)                                          000929
C      IF(FLAG.EQ.1) T3=TE                                                    000930
C      CALL WRITER(10PTU)                                                     000931
C      T3=TE                                                                  000932
C      A=1                                                                    000933
C      GO TO 440                                                              000934
C                                                                              000935
C                                                                              000936
C      C*****INCREMENT PRINT CONTROL VARIABLES                            000937
C                                                                              000938
C      43C A=N+1                                                              000939
C      44C L=L+1                                                              000940
C                                                                              000941
C                                                                              000942
C                                                                              000943
C      C*****DETERMINE EXIT CRITERIA                                       000944
C                                                                              000945
C      IF(1800*TIME.GE.RISTIN.AND.10PTP.EQ.2) GO TO 9999                  000946
C      IF(MC.LT.MFINAL) GO TO 9999                                           000947
C      IF(RATIO2.EQ.1.) GO TO 450                                            000948
C      IF(FLAG.NE.1.AND.MC.GT.MFINAL) GO TO 180                            000949
C      IF(FLAG.EQ.1.AND.MC.GT.MFINAL) GO TO 360                            000950
C                                                                              000951
C                                                                              000952
C      C*****WRITE TRANSITION REGIME FINAL OUTPUT                         000953
C                                                                              000954
C      45C PC=MREP/(MREM+EM)                                                  000955
C      TS=(TH+MC*DELTA1/K1+T1)/(1+MC*DELTA1/K1)                            000956
C      CTOTAL=CTOTAL+(Q+MC*(TH-TS))*DT/2.                                    000957
C      C=MC*(TH-TS)                                                         000958
C      PGAUGE=PV(T1)-FVTB                                                    000959
C      IF(PGAUGE.LT.0.) PGAUGE=0.                                           000960
C      SEC=TIME*3600.                                                         000961
C      TMID=TC(1+M/2)                                                        000962
C      CHTC=G/(TH-TMID)                                                       000963
C                                                                              000964
C      IF(RATIO3.EQ.1.) T3=INEN(K)                                          000965
C      IF(FLAG.EQ.1) T3=TE                                                    000966
C      IF(N.NE.1) CALL WRITER(10PTU)                                         000967
C      WRITE(6,930)                                                           000968
C      IF(IFINI.LE.K) WRITE(6,935) (I,TNEW(I),I=INIT,IFINI)                000969
C      C*****                                                                000970
C                                                                              000971
C                                                                              000972
C      ***** THE LINEAR REGIME *****                                    000973

```

\*\*\*\*\*

000974

000975

000976

000977

000978

000979

000980

000981

000982

000983

000984

000985

000986

000987

000988

000989

000990

000991

000992

000993

000994

000995

000996

000997

000998

000999

001000

001001

001002

001003

001004

001005

001006

001007

001008

001009

001010

001011

001012

001013

001014

001015

001016

001017

001018

001019

001020

001021

001022

001023

001024

001025

001026

001027

001028

\*\*\*\*\*WRITE LINEAR REGIME HEADING

WRITE(6,945)

\*\*\*\*\*SET FLAG AND GO TO FIRST TEMPERATURE CALCULATION

L=1

T3=TE

NAKV=KABS3\*(1.-S3STAR)\*\*3\*(1.+3.\*S3STAR)

IF(RATIO2.EQ.1.) FLAG=1

DTMAX=DT0

GO TO 550

\*\*\*\*\*COMPUTE REQUIRED DERIVATIVES

460 D1=A1\*DTDZ23

D2=A2\*DTDZ23

D3=A3\*DTDZ23

D4=A4\*DTDZ12

D5=A5\*DTDZ23

D6=-K3\*DTDZ23/(HFG3\*X)

D7=D2\*Z

D8=A8\*DTDZ12

IF(DELTA1.EQ.DELTA2.AND.D1.GE.D2) D7=0.

IF(DELTA1.NE.DELTA2.AND.D5.GE.D2) D7=0.

DENOM=D6+D7

\*\*\*\*\*SET MAXIMUM ALLOWABLE TIME INCREMENT

DT1=DTMAX

DT2=DTMAX

IF(DELTA1.NE.DELTA2) GO TO 470

IF(D1.GE.D2.AND.D1.NE.D6) DT1=(DELTA3-DELTA1)/(D1-D6)

IF(D1.LT.D2.AND.D2.NE.DENOM) DT1=(DELTA3-DELTA2)/(D2-DENOM)

GO TO 490

470 IF(FLAG.EQ.1) GO TO 480

DSTAR=AMAX1(D2,D5)

IF(DSTAR.NE.DENOM) DT1=(DELTA3-DELTA2)/(DSTAR-DENOM)

IF(D4.GT.DSTAR) DT2=(DELTA2-DELTA1)/(D4-DSTAR)

GO TO 490

480 DSTAR=0.

IF(D4.NE.D8) DT1=(DELTA2-DELTA1)/(D4-D8)

490 IF(DT1.LE.0.) DT1=DTMAX

IF(DT2.LE.0.) DT2=DTMAX

C	CT=AMIN1(DT1,DT2,DTMAX)	001029
C	CT=TIMER*CT	001030
C	TIME=TIME+DT	001031
C		001032
C		001033
C		001034
C	*****CALCULATE RATES OF BASIS WEIGHT CHANGE	001035
C		001036
C	IF(DELTA1.NE.DELTA2) GO TO 500	001037
C	IF(D1.GE.D2) RATE1=D1	001038
C	RATE2=RATE1	001039
C	IF(D1.LT.D2) RATE2=D2	001040
C	IF(D1.LT.D2.ANC.D3.GE.D2) RATE1=RATE2	001041
C	IF(D1.LT.D2.ANC.D3.LT.D2) RATE1=D3	001042
C	GO TO 510	001043
C		001044
C	500 RATE1=D4	001045
C	RATE2=DSTAR	001046
C	IF(FLAG.EQ.1) RATE2=D8	001047
C		001048
C	510 RATE3=DENGM	001049
C	IF(FLAG.EQ.1) EW3=0.	001050
C	IF(FLAG.EQ.1) RATE3=0.	001051
C		001052
C	IF(BW4.EQ.0.) LIQDEN=LIQDEN+RATE3*X*DT	001053
C		001054
C		001055
C	*****CALCULATE MECHANICAL AND HYDRAULIC PRESSURE	001056
C		001057
C	CALL PRESSR(TIME)	001058
C		001059
C	PH1=HYDRAL(T1,T1)	001060
C	PH2=HYDRAL(T1,T2)	001061
C	PH3=HYDRAL(T2,T3)	001062
C	PH4=HYDRAL(T3,TB)	001063
C	IF(FLAG.EQ.1) PH4=PH3	001064
C		001065
C	F1=F-PH1	001066
C	IF(P1.LE.0.) P1=PREF1	001067
C	F2=P-PH2	001068
C	F3=P-PH3	001069
C	F4=F-PH4	001070
C		001071
C		001072
C	*****CALCULATE BASIS WEIGHT, CONCENTRATION AND THICKNESS	001073
C		001074
C		001075
C	CBW1DT=C2*RATE1	001076
C	CBW2DT=C3*RATE2-CBW1DT	001077
C	IF(FLAG.EQ.1) CBW2DT=C2*(RATE2-RATE1)	001078
C	CBW3DT=C3*(RATE3-RATE2)	001079
C	IF(RATIO3.EQ.1..AND.RATE3.GT.0.) CBW3DT=-C3*RATE2	001080
C	CBW4DT=-C3*RATE3	001081
C	IF(FLAG.EQ.1) CBW4DT=-C2*RATE2	001082

E <sub>h</sub> 1=B <sub>h</sub> 1+CBW1DT*DT	001083
E <sub>h</sub> 2=B <sub>h</sub> 2+CBW2DT*DT	001084
E <sub>h</sub> 3=B <sub>h</sub> 3+CBW3DT*DT	001085
E <sub>h</sub> 4=B <sub>h</sub> 4+CBW4DT*DT	001086
	001087
	001088
IF(B <sub>h</sub> 1.LT.0.) BW1=0.	001089
IF(B <sub>h</sub> 2.LT.0.) BW2=0.	001090
IF(B <sub>h</sub> 3.LT.0..OR.FLAG.EQ.1) BW3=0.	001091
IF(B <sub>h</sub> 4.LT.0.) BW4=0.	001092
	001093
520 BWSUM=BW1+BW2+BW3+BW4	001094
BWCCRR=B <sub>h</sub> /BWSUM	001095
	001096
E <sub>h</sub> 1=BW1*BWCCRR	001097
E <sub>h</sub> 2=BW2*BWCCRR	001098
E <sub>h</sub> 3=BW3*BWCCRR	001099
E <sub>h</sub> 4=BW4*BWCCRR	001100
	001101
TBAR1=(TS+T1)/2.	001102
TBAR2=(T1+T2)/2.	001103
TBAR3=(T2+T3)/2.	001104
TBAR4=(T3+TE)/2.	001105
	001106
P1=EVALM(0.,TBAR1)	001107
P2=EVALM(HRSTAR,TBAR2)	001108
P3=EVALM(HR,TBAR3)	001109
P4=EVALM(0.,TBAR4)	001110
IF(FLAG.EQ.1) P4=EVALM(0.,TEAR3)	001111
	001112
C1=M1*P1**N1	001113
C2=M2*P2**N2	001114
C3=M3*P3**N3	001115
C4=M4*P4**N4	001116
	001117
THICK1=E <sub>h</sub> 1/C1	001118
THICK2=E <sub>h</sub> 2/C2	001119
THICK3=E <sub>h</sub> 3/C3	001120
THICK4=E <sub>h</sub> 4/C4	001121
	001122
	001123
*****CALCULATE POROSITY AND SATURATION	001124
	001125
E1=1.-C1/DFIBER	001126
E2=1.-C2/DFIBER	001127
E3=1.-C3/DFIBER	001128
ESTAR=E3-E2	001129
E4=1.-C4/DFIBER	001130
IF(C1.GT.DFIBER) CALL WARNIN(1,1,C1)	001131
IF(E2.LT.EMIN) CALL WARNIN(2,2,E2)	001132
IF(E3.LT.EMIN) CALL WARNIN(2,3,E3)	001133
IF(C4.GT.DFIBER) CALL WARNIN(1,4,C4)	001134
IF(C1.GT.DFIBER.OR.E2.LT.EMIN.OR.E3.LT.EMIN.OR.C4.GT.DFIBER)	001135
* GO TO 9999	001136
	001137



CALL CALLER(4)	001138
D=MRSTAR*C2	001139
X=MR*C3	001140
Y=(MR-MRSTAR)*C3	001141
Z=Y/X	001142
C	001143
S2=W*VF12/E2	001144
S3=X*VF23/E3	001145
S3STAR=Y*VF23/ESTAR	001146
IF(S3.LE.1..OR.FLAG.EQ.1) GO TO 540	001147
IF(BW4.NE.0.) GO TO 530	001148
S3=1.	001149
S3STAR=1.	001150
MR=E3/(VF23*C3)	001151
X=E3/VF23	001152
Y=(MR-MRSTAR)*C3	001153
Z=Y/X	001154
GO TO 540	001155
530 BW4=BW4-(S3-1.)*BW3	001156
IF(BW4.L1.0.) BW4=0.	001157
BW3=BW-BW1-BW2-BW4	001158
GO TO 520	001159
C	001160
C	001161
C*****INCREMENT INTERFACE POSITIONS	001162
C	001163
540 DELTA1=THICK1	001164
DELTA2=DELTA1+THICK2	001165
DELTA3=DELTA2+THICK3	001166
DELTA4=DELTA3+THICK4	001167
IF(THICK3.EQ.0.) FLAG=1	001168
IF(THICK3.EQ.C.) DELTA3=DELTA4	001169
C	001170
C	001171
C*****CALCULATE THERMAL CONDUCTIVITY AND CONTACT COEFFICIENT	001172
C	001173
K1=KFIBER*(1.-E1)	001174
K2=KFIBER*(1.-E2)*KWATER*E2*S2	001175
K3=KFIBER*(1.-E3)*KWATER*E3*S3	001176
K4=KFIBER*(1.-E4)	001177
C	001178
HCDRY=HCREP*(HC1*(P1/PREF2)**HC2-HC3)	001179
HC=HCDRY*(1.-E1)	001180
IF(DELTA1.EQ.0.) HC=HCDRY*(1.-E2)*E2*S2*HCWET	001181
IF(DELTA2.EQ.0.) HC=HCDRY*(1.-E3)*E3*S3*HCWET	001182
C	001183
C	001184
C*****CALCULATE PERMEABILITY FACTORS	001185
C	001186
R=SPRES(P)/FACTOR	001187
C	001188
KABS2=1./(R*C2)	001189
KABS3=1./(R*C3)	001190
KABS4=1./(R*C4)	001191

KAKV=KABS3\*(1.-S3STAR)\*\*3\*(1.+3.\*S3STAR)  
KAKH=KABS3\*S3STAR\*\*4

\*\*\*\*\*SET RELATIVE INTERFACE POSITIONS AND REMAINING MOISTURE

RATIO1=DELTA1/DELTAT  
RATIO2=DELTA2/DELTAT  
RATIO3=DELTA3/DELTAT

MREM=MR\*BM3+MRSTAR\*BM2  
MREL=1.-MREM/MC

\*\*\*\*\*COMPUTE NEW VALUES FOR T1, T2 AND T3

550 IF(DELTA1.NE.DELTA2) GO TO 570

DO 560 I=1,IMAX

T2=T2  
T3=T3

CALL CALLER(2)

HFG2=HFG(T2)+DELHD(3)  
HFG3=HFG(T3)+DELHD(3)

ALFA=DELTA3-DELTA2  
BETA=DELTA7-DELTA3

TERM1=(1./HC+DELTA1/K1)\*(1./ALFA)\*(HFG2+KAKV\*DPDT23/  
\* (VG23+VISG23)+K3)  
TERM3=(BETA\*(KAKV\*DPDT23/(VG23+VISG23)+K3/HFG3))/  
\* (ALFA+KABS4\*DPDT3B/(VG3B+VISG3B))  
DENOM=1.+TERM1+TERM3

T2=(TH\*(1.+TERM3)+TB\*TERM1)/DENOM  
T2=(T2+T2)/2.  
T3=(TH\*TERM3+TB\*(1.+TERM1))/DENOM  
T3=(T3+T3)/2.

560 CONTINUE

T1=T2  
GO TO 590

570 DO 590 I=1,IMAX

T1=T1  
T2=T2  
T3=T3

CALL CALLER(3)

001192  
001193  
001194  
001195  
001196  
001197  
001198  
001199  
001200  
001201  
001202  
001203  
001204  
001205  
001206  
001207  
001208  
001209  
001210  
001211  
001212  
001213  
001214  
001215  
001216  
001217  
001218  
001219  
001220  
001221  
001222  
001223  
001224  
001225  
001226  
001227  
001228  
001229  
001230  
001231  
001232  
001233  
001234  
001235  
001236  
001237  
001238  
001239  
001240  
001241  
001242  
001243  
001244  
001245  
001246

HFG1=HFG(T1)+DELHD(1)	001247
HFG2=HFG(T2)+DELHD(2)	001248
IF(FLAG.EQ.1) HFG2=HFG(T2)+DELHD(1)	001249
HFG3=HFG(T3)+DELHD(3)	001250
C	001251
ALF=DELTA2-DELTA1	001252
BET=DELTA3-DELTA2	001253
GAMM=DELTA1-DELTA3	001254
IF(BET.EQ.0.) FLAG=1	001255
IF(FLAG.EQ.1) GO TO 580	001256
C	001257
TERM1=(1./HC+DELTA1/K1)*(1./ALF)*(HFG1*KABS2*DPDT12/	001258
* (VG12*VISG12)+K2)	001259
TERM2=(BET*(KABS2*DPDT12/(VG12*VISG12)+K2/HFG2))/	001260
* (ALF*(KAKV*DPDT23/(VG23*VISG23)+K3/HFG2))	001261
TERM3=(GAMM*(KAKV*DPDT23/(VG23*VISG23)+K3/HFG3))/	001262
* (BET*KABS4*DPDT38/(VG38*VISG38))	001263
TERM4=TERM2*(1.+TERM3)	001264
DENOM=1.+TERM1+TERM4	001265
C	001266
T1=(TH*(1.+TERM4)+TB*TERM1)/DENOM	001267
T1=(T01+T1)/2.	001268
T2=(TH*TERM4+TB*(1.+TERM1))/DENOM	001269
T2=(T02+T2)/2.	001270
T3=(TH*TERM2+TERM3+TB*(1.+TERM1+TERM2))/DENOM	001271
T3=(T03+T3)/2.	001272
GO TO 590	001273
C	001274
580 TERM1=(1./HC+DELTA1/K1)*(1./ALF)*(HFG1*KABS2*DPDT12/	001275
* (VG12*VISG12)+K2)	001276
TERM2=(BET*(KABS2*DPDT12/(VG12*VISG12)+K2/HFG2))/	001277
* (ALF*KABS4*DPDT23/(VG23*VISG23))	001278
DENOM=1.+TERM1+TERM2	001279
C	001280
T1=(TH*(1.+TERM2)+TB*TERM1)/DENOM	001281
T1=(T01+T1)/2.	001282
T2=(TH*TERM2+TB*(1.+TERM1))/DENOM	001283
T2=(T02+T2)/2.	001284
T3=TB	001285
590 CONTINUE	001286
C	001287
C	001288
C*****RECOMPUTE VARIABLES FOR DERIVATIVE CALCULATIONS	001289
C	001290
IF(DELTA1.NE.DELTA2) GO TO 600	001291
CTD212=0.	001292
CTD223=(T2-T3)/ALFA	001293
GO TO 610	001294
C	001295
600 CTD212=(T1-T2)/ALF	001296
CTD223=0.	001297
IF(FLAG.EQ.0) CTD223=(T2-T3)/BET	001298
C	001299

610 CALL CALLER(4)	001300
HFG2=HFG(T2)+DELHD(1)	001301
	001302
	001303
IF(FLAG.EQ.1) GO TO 620	001304
A1=KAKV*DPDT23/(VISG23*VG23*X)	001305
A2=KAKW*CPDT23/(VISF23*VF23*Y)	001306
A3=KAKV*CPDT23/(VISG23*VG23*W)	001307
A4=KABS2*DPDT12/(VISG12*VE12*W)	001308
A5=KAKV*CPDT23/(VISG23*VG23*Y)	001309
GO TO 630	001310
	001311
620 A1=0.	001312
A2=0.	001313
A3=0.	001314
A4=KABS2*DPDT12/(VISG12*VE12*W)	001315
A5=0.	001316
AB=-K2/(HFG2*W)	001317
	001318
	001319
*****COMPUTE TEMPERATURES AT FIXED-POINT LOCATIONS	001320
	001321
630 SUM12=BW1+BW2	001322
SUM123=SUM12+BW3	001323
CG 640 I=1,M	001324
L=2TC(I)*BW	001325
IF(U.LT.BW1.AND.BW1.NE.0.) TC(I)=TS-(TS-T1)*(U/BW1)	001326
IF(U.GT.BW1.AND.U.LT.SUM12.AND.BW2.NE.0.) TC(I)=T1-(T1-T2)*	001327
* (U-BW1)/BW2	001328
IF(U.GT.SUM12.AND.U.LT.SUM123.AND.BW3.NE.0.) TC(I)=T2-(T2-T3)*	001329
* (U-SUM12)/BW3	001330
IF(U.GT.SUM123.AND.U.LT.BW4.AND.BW4.NE.0.) TC(I)=T3-(T3-TB)*	001331
* (U-SUM123)/BW4	001332
	001333
IF(U.EQ.BW1) TC(I)=T1	001334
IF(U.EQ.SUM12) TC(I)=T2	001335
IF(U.EQ.SUM123) TC(I)=T3	001336
IF(U.EQ.BW4) TC(I)=TB	001337
640 CONTINUE	001338
	001339
	001340
*****INCREMENT QUANTITIES AND WRITE RESULTS	001341
	001342
PC=MREM/(MREM+BW)	001343
TS=(TH*HC*DELTA1/K1+T1)/(1+HC*DELTA1/K1)	001344
CTOTAL=CTOTAL+(Q+HC*(TH-TS))*DT/2.	001345
G=HC*(TH-TS)	001346
IF(N.LT.J.AND.L.GT.LMAX.AND.MC.GT.MFINAL) GO TO 650	001347
	001348
FGAUGE=FV(T1)-FVTB	001349
SEC=TIME*3600.	001350
TMID=TC(1+M/2)	001351
CHTC=G/(TH-TMID)	001352
	001353

IF(L.NE.1) CALL WRITER(IOPTU)	001354
WRITE(6,/) MREL, LIQDEN, S3, MR, RATE1, RATE2, RATE3, X, D7, DT	001355
N=1	001356
GO TO 660	001357
C	001358
C	001359
C*****INCREMENT PRINT CONTROL VARIABLES	001360
C	001361
650 N=N+1	001362
660 L=L+1	001363
C	001364
C	001365
C*****DETERMINE EXIT CRITERIA	001366
C	001367
IF(1800*TIME.GE.RISTIM.AND.IOPTP.EQ.2) GO TO 9999	001368
IF(MC.GT.MFINAL) GO TO 460	001369
C	001370
C	001371
C*****WRITE FINAL OUTPUT	001372
C	001373
IF(N.NE.1) CALL WRITER(IOPTU)	001374
WRITE(6,950) QINIT	001375
WRITE(6,955) QTOTAL	001376
QTOT=QINIT+QIC1AL	001377
WRITE(6,960) QTOT	001378
GTHERR1=(BW*CPF+MC*CPW)*(TB-TI)	001379
GTHERR2=MC*HFGTE	001380
GTHEOR=GTHERR1+GTHERR2	001381
IF(TB.LT.TI) GTHEOR=GTHERR2	001382
WRITE(6,965) GTHEOR	001383
LIQDEN=LIQDEN*100./MO	001384
WRITE(6,970) LIQDEN	001385
C	001386
C	001387
C*****FORMAT STATEMENTS	001388
C	001389
500 FORMAT(" ***** HIDRYER1 PROGRAM OUTPUT *****")	001390
505 FORMAT(1H0," TH TS BW CSF MRG"	001391
" PMAX RISTIM")	001392
510 FORMAT(2F9.2,F11.5,I8,F9.2,F10.2,F9.3)	001393
515 FORMAT(1H0," DTQ IOPTP IOPTU"	001394
" METH MITER")	001395
520 FORMAT(E13.5,2I8,2I11)	001396
525 FORMAT(1H0," SEC MREL TS T1 T2"	001397
" I3 RATIO1 RATIO2 RATIO3 DELTAT 0"	001398
" QHTC PGALGE SEC")	001399
530 FORMAT(1H0)	001400
535 FORMAT(10(I5,F8.3))	001401
540 FORMAT(1H0," START OF TRANSITION REGIME")	001402
545 FORMAT(1H0," START OF LINEAR REGIME")	001403
550 FORMAT(1H0,1X,F6.2," BTU/F12 REQUIRED TO HEAT THE SHEET")	001404
555 FORMAT(1H0,1X,F6.2," BTU/F12 REQUIRED FOR DOWATERING THE SHEET")	001405
560 FORMAT(1H0,1X,F6.2," BTU/F12 TOTAL THERMAL ENERGY INPUT")	001406
565 FORMAT(1H0,1X,F6.2," BTU/F12 THEORETICALLY REQUIRED FOR HEATUP")	001407

```

      * AND EVAPORATION OF ALL LIQUID AT SATURATION TEMPERATURE")
57C FORMAT(1H0,1X,F6.2," PERCENT OF THE MOISTURE IS REMOVED IN"
      * LIQUID FORM")
001408
001409
001410
001411
001412
001413
001414
001415
001416
001417
001418
001419
001420
001421
001422
001423
001424
001425
001426
001427
001428
001429
001430
001431
001432
001433
001434
001435
001436
001437
001438
001439
001440
001441
001442
001443
001444
001445
001446
001447
001448
001449
001450
001451
001452
001453
001454
001455
001456
001457
001458
001459
001460
001461
001462

*****END MAIN PROGRAM

9595 STOP
END
*****

***** THE SUBROUTINES *****

*****SUBROUTINE TO CONVERT FROM ENGLISH TO SI UNITS

SUBROUTINE CAVRT1

DATA A1,A2,A3,A4,A5/9,5,32,4.8224,6.8948/

COMMON /LABEL1/ TB,PVTB,DFVDTB,VFTB,VGTB,HFGTB,VISGTB,VISFTB
COMMON /LABEL2/ TH,T1,T2,T3,TI,TMID
COMMON /LABEL7/ FREF1,FMAX,FISTIM,P,IOPTP,DPDT
COMMON /LABEL9/ DLOT,FACTCR,BW,CN,DFIBER,COEFF,PS3

TH=A1*TH/A2+A3
TB=A1*TB/A2+A3
EW=BW/A4
FMAX=PMAX/A5

RETURN
END
*****

*****SUBROUTINE TO DETERMINE THE CONSTANTS FOR CALCULATION OF M AND N

SUBROUTINE CNSTMN(X)

DATA
*A1,A2,A3,A4,A5,A6/2.9613453E+00,-2.8919415E-01,5.7420518E+01,
*
*-3.3796161E+01,4.411387E+00,1.2974508E+00/,
001453
001454
001455
001456
001457
001458
001459
001460
001461
001462

```

COMMON /LABEL15/ CM1,CM2,CM3,CM4,CM5,CM6	001463
COMMON /LABEL16/ CN1,CN2,CN3,CN4,CN5,CN6	001464
C	001465
TERM=((X-E1)/E2)**2	001466
IF(X.LT.0.) TERM=0.	001467
CM1=A1+B1*TERM	001468
CM2=A2+E2*TERM	001469
CM3=A3+B3*TERM	001470
CM4=A4+B4*TERM	001471
CM5=A5+E5*TERM	001472
CM6=A6+B6*TERM	001473
C	001474
CN1=C1+D1*TERM	001475
CN2=C2+D2*TERM	001476
CN3=C3+D3*TERM	001477
CN4=C4+D4*TERM	001478
CN5=C5+D5*TERM	001479
CN6=C6+D6*TERM	001480
C	001481
RETURN	001482
END	001483
C*****	001484
C	001485
C	001486
C*****SUBROUTINE TO CALCULATE PROPERTIES AT TB	001487
C	001488
SUBROUTINE PROPTB	001489
C	001490
COMMON /LABEL1/ TB,PVTB,DPVDTB,VFTB,VGTB,HFGTB,VISGTB,VISFTB	001491
C	001492
PVTB=PV(TB)	001493
DPVDTB=DPVDT(TB)	001494
VFTB=VF(TB)	001495
VGTB=VG(TB)	001496
HFGTB=HFG(TB)	001497
VISGTB=VISG(TB)	001498
VISFTB=VISF(TB)	001499
C	001500
RETURN	001501
END	001502
C*****	001503
C	001504
C	001505
C*****SUBROUTINE TO CALL PROPERTY SUBROUTINES	001506
C	001507
SUBROUTINE CALLER(I)	001508
C	001509
COMMON /LABEL2/ TH,T1,T2,T3,TI,THID	001510
C	001511
IF(I.EQ.4) GO TO 10	001512
C	001513
CALL PROP3B	001514
IF(I.EQ.2) GO TO 20	001515
C	001516
1C CALL PROP12	001517

1F(I.EQ.3) GO TO 20

CALL PROP23(1)  
GO TO 30

20 CALL PROP23(2)

30 RETURN  
END

\*\*\*\*\*

\*\*\*\*\*SUBROUTINE TO CALCULATE T1-T2 AVERAGE PROPERTIES

SUBROUTINE PROP12

COMMON /LABEL2/ TH,T1,T2,T3,TI,TMID  
COMMON /LABEL3/ DPDT12,VF12,VG12,VISG12

DPDT12=(DPVD1(T1)+DPVD1(T2))/2.  
VF12=(VF(T1)+VF(T2))/2.  
VG12=(VG(T1)+VG(T2))/2.  
VISG12=(VISE(T1)+VISG(T2))/2.

RETURN  
END

\*\*\*\*\*

\*\*\*\*\*SUBROUTINE TO CALCULATE T2-T3 AVERAGE PROPERTIES

SUBROUTINE PROP23(1)

COMMON /LABEL2/ TH,T1,T2,T3,TI,TMID  
COMMON /LABEL4/ DPDT23,VF23,VISF23,VG23,VISG23

GO TO (10,20) I

10 VF23=(VF(T2)+VF(T3))/2.  
VISF23=(VISF(T2)+VISF(T3))/2.  
GO TO 30

20 VG23=(VG(T2)+VG(T3))/2.  
VISG23=(VISE(T2)+VISG(T3))/2.

30 DPDT23=(DPVD1(T2)+DPVD1(T3))/2.

RETURN  
END

\*\*\*\*\*

\*\*\*\*\*SUBROUTINE TO CALCULATE T3-T8 AVERAGE PROPERTIES

001518  
001519  
001520  
001521  
001522  
001523  
001524  
001525  
001526  
001527  
001528  
001529  
001530  
001531  
001532  
001533  
001534  
001535  
001536  
001537  
001538  
001539  
001540  
001541  
001542  
001543  
001544  
001545  
001546  
001547  
001548  
001549  
001550  
001551  
001552  
001553  
001554  
001555  
001556  
001557  
001558  
001559  
001560  
001561  
001562  
001563  
001564  
001565  
001566  
001567  
001568  
001569  
001570  
001571



	SUBROUTINE PROP3B	001572
C	COMMON /LABEL1/ TB,PVTB,DPVDTB,VFTB,VGTB,HFGTB,VISGTB,VISFTB	001573
	COMMON /LABEL2/ TH,T1,T2,T3,TI,TMID	001574
	COMMON /LABEL5/ DPDT3B,VG3B,VISG3B	001575
C	DPDT3B=(DPVDT(T3)+DPVDTB)/2.	001576
	VG3B=(VG(T3)+VGTB)/2.	001577
	VISG3B=(VISE(T3)+VISGTB)/2.	001578
C	RETURN	001579
	END	001580
C	*****	001581
C		001582
C		001583
C	*****SUBROUTINE TO CALCULATE APPLIED PRESSURE AND ITS DERIVATIVE	001584
C	SUBROUTINE PRESSR(A)	001585
		001586
C	DATA PI,A2/3.1415927,4.712389/	001587
C	COMMON /LABEL7/ PREF1,PMAX,RISTIM,P,IOFTP,DPDT	001588
C	GO TO (10,20) IOFTP	001589
C	10 DPDT=PMAX*3600./RISTIM	001590
	F=PREF1+A*DPDT	001591
	IF(P.GT.PMAX) F=PMAX	001592
	IF(F.GE.PMAX) DPDT=0.	001593
	GO TO 30	001594
C	20 A1=PI*3600./RISTIM	001595
	F=PREF1+PMAX*(1.+SIN(A1*A+A2))/2.	001596
	DPDT=A1*PMAX*COS(A1*A+A2)/2.	001597
	IF(1800.*A.GE.RISTIM) P=PREF1	001598
	IF(1800.*A.GE.RISTIM) CLDT=C.	001599
C	30 RETURN	001600
	END	001601
C	*****	001602
C		001603
C		001604
C	*****SUBROUTINE TO CALCULATE THE THICKNESS OF A SATURATED MEDIUM	001605
C	SUBROUTINE CLDTFN(N,TIME,YL,YPRIME)	001606
		001607
C	REAL YL(N),YPRIME(N),TIME	001608
C	COMMON /LABEL1/ TB,PVTB,DPVDTB,VFTB,VGTB,HFGTB,VISGTB,VISFTB	001609
	COMMON /LABEL7/ PREF1,PMAX,RISTIM,F,IOFTP,DPDT	001610
	COMMON /LABEL8/ M1,M2,M3,M4,N1,N2,N3,N4	001611
	COMMON /LABEL9/ CLDT,FACTGR,BW,DW,DFIBER,COEFF,PS3	001612
C	CALL PRESSR(TIME)	001613
	FS3=(BW/(YL(1)*M3))**(1./N3)	001614
		001615
		001616
		001617
		001618
		001619
		001620
		001621
		001622
		001623
		001624
		001625
		001626

```

R=SPRES(P)/FACTOR
COEFF=3./(VISF18*BW*R)
YPRIME(1)=(PS3-P)*COEFF
CLOT=YPRIME(1)

```

```

RETURN
END

```

001627  
001628  
001629  
001630  
001631  
001632  
001633

\*\*\*\*\*SUBROUTINE TO CALCULATE THE JACOBIAN FOR A SATURATED MEDIUM

```

SUBROUTINE DUMFUN(N,TIME,YL,PD)

```

```

REAL TIME,YL(N),PD(1,1)

```

```

COMMON /LABEL8/ M1,M2,M3,M4,N1,N2,N3,N4
COMMON /LABEL9/ CLOT,FACTOR,BW,Dh,DFIBER,COEFF,PS3

```

```

PD(1,1)=-COEFF*PS3/(N3*YL(1))

```

```

RETURN
END

```

001634  
001635  
001636  
001637  
001638  
001639  
001640  
001641  
001642  
001643  
001644  
001645  
001646  
001647  
001648  
001649

\*\*\*\*\*SUBROUTINE TO WRITE OUTPUT

```

SUBROUTINE WRITER(I)

```

```

COMMON /LABEL2/ TH,T1,T2,T3,TI,TMID
COMMON /LABEL11/ SEC,MREL,TS,RATIO1,RATIO2,RATIO3,DELTAT,Q,QHTC,
* PGALGE
COMMON /LABEL12/ TSSI,T1SI,T2SI,T3SI,DELTSI,QSI,QHTCSI,PGAGSI,
* TMIDSI

```

```

IF(I.EQ.2) GO TO 10

```

```

WRITE(6,20) SEC,MREL,TS,T1,T2,T3,RATIO1,RATIO2,RATIO3,DELTAT,Q,
* QHTC,PGALGE,SEC
WRITE(2,20) SEC,MREL,TS,T1,T2,T3,RATIO1,RATIO2,RATIO3,DELTAT,Q,
* QHTC,PGALGE,TMID
GO TO 30

```

```

10 CALL CNVRT2

```

```

WRITE(6,20) SEC,MREL,TSSI,T1SI,T2SI,T3SI,RATIO1,RATIO2,RATIO3,
* DELTSI,QSI,QHTCSI,PGAGSI,SEC
WRITE(2,20) SEC,MREL,TSSI,T1SI,T2SI,T3SI,RATIO1,RATIO2,RATIO3,
* DELTSI,QSI,QHTCSI,PGAGSI,TMIDSI

```

```

20 FORMAT(1X,F8.5,F8.4,4F9.3,3F8.4,F10.6,F11.1,F8.2,F8.3,F10.5)

```

```

30 RETURN

```

001650  
001651  
001652  
001653  
001654  
001655  
001656  
001657  
001658  
001659  
001660  
001661  
001662  
001663  
001664  
001665  
001666  
001667  
001668  
001669  
001670  
001671  
001672  
001673  
001674  
001675  
001676  
001677  
001678  
001679  
001680

```

      END
C*****
C
C
C*****SUBROUTINE TO CONVERT FROM ENGLISH TO SI UNITS
C
      SUBROUTINE CNVRT2
C
      DATA A1,A2,A3,A4,A5,A6,A7/5,32,9,0.3048,3.1546,5.6783,6.8948/
C
      COMMON /LABEL2/ TH,T1,T2,T3,TI,TMID
      COMMON /LABEL11/ SEC,MREL,TS,RATIO1,RATIO2,RATIO3,DELTA1,Q,QHTC,
* PGAGE
      COMMON /LABEL12/ TSSI,T1SI,T2SI,T3SI,DELTSI,QSI,QHTCSI,PGAGSI,
* TMIDSI
C
      TSSI=A1*(TS-A2)/A3
      T1SI=A1*(T1-A2)/A3
      T2SI=A1*(T2-A2)/A3
      T3SI=A1*(T3-A2)/A3
      TMIDSI=A1*(TMID-A2)/A3
      DELTSI=DELTA1*A4
      QSI=Q*A5
      QHTCSI=QHTC*A6
      PGAGSI=PGAGE*A7
C
      RETURN
      END
C*****
C
C
C*****SUBROUTINE TO CORRECT ERROR CONDITION OR PRINT WARNING MESSAGE
C
      SUBROUTINE WARNIN(I,J,X)
C
      COMMON /LABEL6/ DX,DIFFIX,DIFFFX,EMIN
      COMMON /LABEL9/ CLDT,FACTCR,BW,CW,DFIBER,COEFF,PS3
C
      GO TO (10,20,30,40) I
C
      10 WRITE(6,50) J,X,DFIBER
      GO TO 70
C
      20 WRITE(6,60) J,X,EMIN
      GO TO 70
C
      30 DIFFIX=DX
      GO TO 70
C
      40 DIFFFX=DX
C
      50 FORMAT('*** ZONE ',I2,' DENSITY ',E16.10,' IS GREATER THAN THE'
* ' MAXIMUM ALLOWABLE DENSITY ',E16.10,' *** COMPUTATION')

```

001681  
 001682  
 001683  
 001684  
 001685  
 001686  
 001687  
 001688  
 001689  
 001690  
 001691  
 001692  
 001693  
 001694  
 001695  
 001696  
 001697  
 001698  
 001699  
 001700  
 001701  
 001702  
 001703  
 001704  
 001705  
 001706  
 001707  
 001708  
 001709  
 001710  
 001711  
 001712  
 001713  
 001714  
 001715  
 001716  
 001717  
 001718  
 001719  
 001720  
 001721  
 001722  
 001723  
 001724  
 001725  
 001726  
 001727  
 001728  
 001729  
 001730  
 001731  
 001732  
 001733

\*" TERMINATED")

```
60 FORMAT('*** ZONE ',I2,' POROSITY ',E16.10,' IS LESS THAN THE'
  * ' MINIMUM ALLOWABLE POROSITY ',E16.10,' *** COMPUTATION'
  * ' TERMINATED')
```

7C RETURN  
END

\*\*\*\*\*  
 \*\*\*\*\* THE FUNCTIONS \*\*\*\*\*  
 \*\*\*\*\*

### \*\*\*\*\*VAPOR PRESSURE FUNCTION

FUNCTION PV(T)

```
DATA
* A1,A2,A3,A4,A5/1.5284E+00,-6.42281E-02,9.7657E-04,-5.85595E-06,
* 1.91309E-08/
```

$$FV = A1 + T * (A2 + T * (A3 + T * (A4 + T * A5)))$$

RETURN  
END

### \*\*\*\*\*VAPOR PRESSURE DERIVATIVE FUNCTION

FUNCTION DPYCT(T)

```
DATA
*A1,A2,A3,A4/-6.42281E-02,9.7657E-04,-5.85595E-06,1.91309E-08/
```

```
CPVDI=A1+I*(2.*A2+I*(3.*A3+4.*A4*I))
```

RETURN  
END

### \*\*\*\*\*LIQUID SPECIFIC VOLUME FUNCTION

FUNCTION VF(1)

```
DATA
* A1,A2,A3,A4,A5/1.60571E-02,-2.35188E-06,3.69301E-08,-6.94068E-11,
* 8.C4005E-14/
```

$$VF = A1 + T * (A2 + T * (A3 + T * (A4 + T * A5)))$$

```

C                                001788
      RETURN                                001789
      END                                001790
C*****                                001791
C                                001792
C                                001793
C*****VAPOR SPECIFIC VOLUME FUNCTION 001794
C                                001795
      FUNCTION VG(T)                    001796
C                                001797
      DATA                            001798
      *A1,A2,A3,A4,A5/9.40601E+00,-4.37418E-02,9.59205E-05,-1.41015E-07, 001799
      * 9.35084E-11/                  001800
C                                001801
      VG=EXP(A1+T*(A2+T*(A3+T*(A4+T*A5)))) 001802
C                                001803
      RETURN                            001804
      END                                001805
C*****                                001806
C                                001807
C                                001808
C*****LATENT HEAT FUNCTION          001809
C                                001810
      FUNCTION HFG(T)                  001811
C                                001812
      DATA                            001813
      *A1,A2,A3,A4,A5/1.09351E+03,-5.6626E-01,8.20598E-05,-5.70484E-07, 001814
      * -6.91038E-10/                 001815
C                                001816
      HFG=A1+T*(A2+T*(A3+T*(A4+T*A5))) 001817
C                                001818
      RETURN                            001819
      END                                001820
C*****                                001821
C                                001822
C                                001823
C*****LIQUID VISCOSITY FUNCTION     001824
C                                001825
      FUNCTION VISF(T)                 001826
C                                001827
      DATA                            001828
      *A1,A2,A3,A4/-1.3917E-04,1.85E-07,6.4841E-02,-7.0869E-01/ 001829
C                                001830
      VISF=A1+T*A2+A3/T+A4/T**2      001831
C                                001832
      RETURN                            001833
      END                                001834
C*****                                001835
C                                001836
C                                001837
C*****VAPOR VISCOSITY FUNCTION      001838
C                                001839
      FUNCTION VISG(T)                 001840
C                                001841

```

DATA	001842
*A1,A2/5.499E-06,1.3908E-08/	001843
	001844
VISG=A1+T*A2	001845
	001846
RETURN	001847
END	001848
*****	001849
	001850
***** EVALUATION FUNCTION	001851
	001852
FUNCTION EVALM(X,T)	001853
	001854
DATA A1,A2,A3/1.5,1.,0.25/	001855
	001856
	001857
COMMON /LABEL2/ TH,T1,T2,T3,TI,TMID	001858
COMMON /LABEL15/ CM1,CM2,CM3,CM4,CM5,CM6	001859
	001860
A=X+A1	001861
E=X+A2	001862
CORRCT=(T/TI)**A3	001863
EVALM=(CM1+CM2*X+CM3/A+CM4/A**2+CM5/B+CM6/B**2)*CORRCT	001864
	001865
RETURN	001866
END	001867
*****	001868
	001869
***** EVALUATION FUNCTION	001870
	001871
FUNCTION EVALN(I,X,Y)	001872
	001873
REAL NDENOM,NMID,NSAT	001874
	001875
	001876
DATA A1,A2/1.5,1./	001877
	001878
COMMON /LABEL4/ DPDT23,VF23,VISF23,VG23,VISG23	001879
COMMON /LABEL7/ PREF1,PMAX,RISTIN,P,IOPTP,DPDT	001880
COMMON /LABEL16/ CN1,CN2,CN3,CN4,CN5,CN6	001881
COMMON /LABEL8/ M1,M2,M3,M4,N1,N2,N3,N4	001882
COMMON /LABEL13/ CH1,DH2,MR,MRSTAR	001883
COMMON /LABEL14/ NEXP,PR3LOG,PREF3,PMID,PDENOM,DF	001884
	001885
A=X+A1	001886
E=X+A2	001887
C=CN1+CN2*X+CN3/A+CN4/A**2+CN5/B+CN6/B**2	001888
EVALN=C	001889
IF(I.EQ.1) GO TO 10	001890
IF(X.LE.MRSTAR) GO TO 10	001891
	001892
NSAT=ALOG(1./(M3*(X*VF23+DF)))/PR3LOG	001893
NMID=(NSAT+C)/2.	001894
NDENOM=NSAT-NMID	001895
FTEMP=ABS(Y-PMID)/PDENOM	001896

C		001897
	SIGN=1.	001898
	IF(Y.LT.PMID) SIGN=-1.	001899
	IF(Y.EQ.PMID) SIGN=0.	001900
	EVALN=NMID+SIGN*NDENOM*PTERM**((1./NEXP)	001901
	IF(Y.LT.PREF1) EVALN=C	001902
	IF(Y.GT.PREF3) EVALN=NSAT	001903
C	WRITE(5,/) I,X,Y,C,NSAT,NFIC,NDENOM,PTERM,PMID,PDENOM,EVALN	001904
C		001905
	10 RETURN	001906
	END	001907
C	*****	001908
C		001909
C		001910
C	*****SPECIFIC FILTRATION RESISTANCE FUNCTION	001911
C		001912
	FUNCTION SPRES(P)	001913
C		001914
	DATA A1,A2,A3,A4,A5,A6/7.C27,2.013E-05,0.142,0.464,0.187,0.344/	001915
C		001916
	COMMON /LABL10/ CSF	001917
C		001918
	RREF=((A1-ALOG(CSF))/A2)**2	
	X=P/A3	001920
	SPRES=RREF*(A4+A5*X+A6*SQRT(X))	001921
C		001922
	RETURN	001923
	END	001924
C	*****	001925
C		001926
C		001927
C	*****HYDRAULIC PRESSURE FUNCTION	001928
C		001929
	FUNCTION HYDRAL(A,B)	001930
C		001931
	COMMON /LABEL1/ TB,PVIB,DFVCTB,VFTB,VGTB,HFGTB,VISGTB,VISFTB	001932
C		001933
	HYDRAL=(FV(A)+FV(B))/2.-PVIB	001934
C		001935
	RETURN	001936
	END	001937
C	*****	001938
C		001939
C		001940
C	*****LATENT HEAT INCREMENT FUNCTION	001941
C		001942
	FUNCTION DELHD(I)	001943
C		001944
	COMMON /LABL13/ DH1,DH2,MR,MRSTAR	001945
C		001946
	GO TO (10,20,30) I	001947
C		001948
	10 DELHD=DH1*(1.-EXP(DH2*MRSTAR))/MRSTAR	001949
	GO TO 40	001950

2C DELHD=DE1*(EXP(DH2*MRSTAR)-EXP(DH2*MR))/(MR-MRSTAR)	001951
GC TC 4C	001952
	001953
3C DELHC=DE1*(1.-EXP(DH2*MR))/MR	001954
	001955
	001956
4C RETURN	001957
END	001958
*****	001959



The programs for the various stages of model development and the data files used to generate the graphs for this thesis are stored on magnetic tape in the Institute computer center.

The model equations, supplementary relationships, and data file information and names are in Institute research notebooks 3578 and 3711.